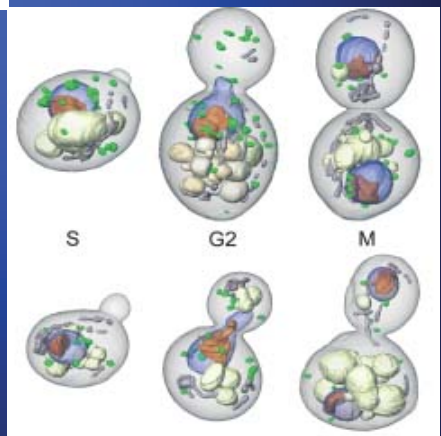
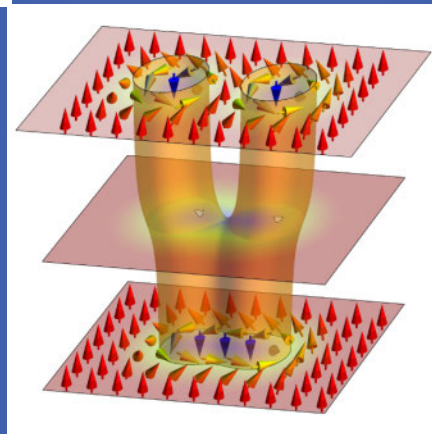
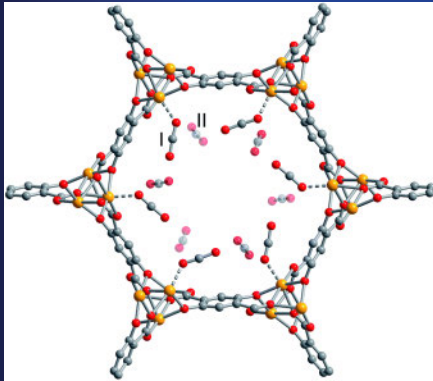
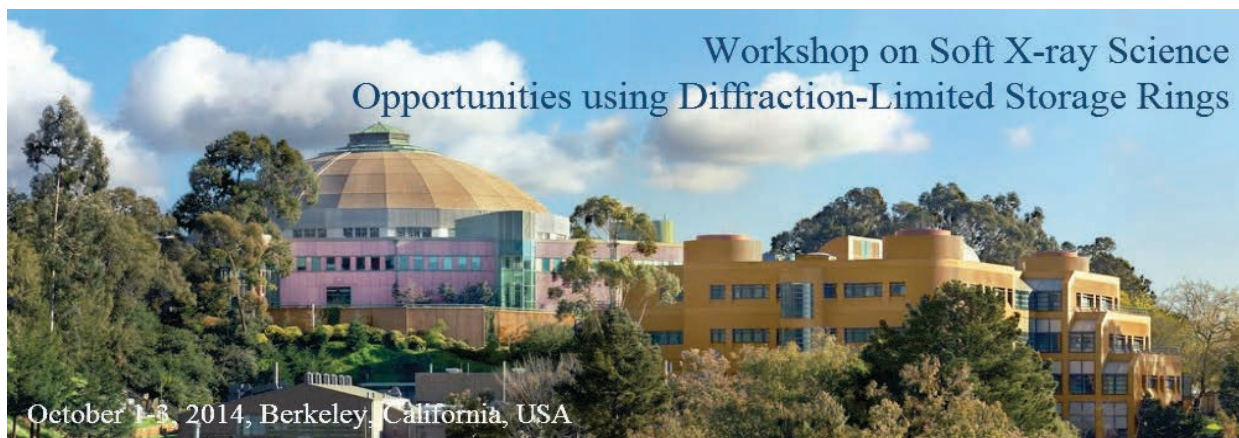


Soft X-ray Science Opportunities Using Diffraction-Limited Storage Rings

Enabling control of nanoscale landscapes



October 1-3, 2014
Advanced Light Source
Berkeley, California



Executive Summary

An important goal in many science and engineering disciplines is to design and build chemical, biological, and material structures that offer functionality to address the world's pressing energy and environmental challenges. Examples include photoelectrochemical cells developed to achieve efficient artificial photosynthesis, material devices able to store and process information with ultralow power input, prokaryotic cells engineered to produce useful chemicals from low value starting materials, chemical micro-reactors designed to achieve efficient and selective multistep chemical syntheses, and nanoporous membranes optimized to purify water with high selectivity and efficiency. Successful development of any of these capabilities - and many others - would have enormous social and economic impact around the world.

These functional structures will be designed using concepts from the basic physical, life, and environmental sciences and assembled using the nanoscience toolbox. To optimize how the structures function - how various nanostructures are positioned and interconnected and how their collective operation is regulated - will require the ability to image where molecules, ions, and electrons are located and to measure how they move around and interact to support efficient function. Importantly, this will need to be done with nanometer sensitivity, with broad temporal resolution, and with high chemical selectivity. Emerging diffraction limited soft X-ray sources will provide these combined sensitivities and in this way will revolutionize our ability to measure and to optimize functional devices and materials.

Cover images: A focal point of the workshop was to develop soft X-ray tools to image chemical, magnetic, electronic, and structural landscapes and also to measure the motion of mass, charge, and spin on these landscape. The images on the cover present three examples: Top: Functionalized metal-organic framework structure designed for efficient and selective capture of CO₂. (Queen, *et. al.*, DOI:10.1039/C4SC02064B) Middle: Schematic of the interaction between two skyrmions, swirling topological spin structures proposed for low power information processing (Melde, *et. al.*, DOI: 10.1126/science.1234657). Right: Tomographic images of yeast cells demonstrating the existence of internal structure in these eucariotic cells that might be developed for efficient biomanufacturing of solar fuels (Uchida, *et. al.*, DOI: 10.1002/yea.1834).

With these thoughts in mind, a workshop entitled *Soft X-ray Science Opportunities Using Diffraction-Limited Storage Rings* was organized and held at the Advanced Light Source at Lawrence Berkeley National Laboratory on October 1-3, 2014. A key stimulus for the workshop is a revolutionary new accelerator technology that will produce diffraction limited beams of soft X-rays. “Diffraction limited” means that the wave fronts will be smooth or “coherent”, across the entire beam, something like a laser beam. The charge of the workshop was to evaluate how this unprecedented phase coherence and stability can be leveraged to address the challenges to design and optimize functional structures.

Why do coherent soft X-ray wave fronts matter? Paradoxically, a *coherent* wave front provides the ability to probe systems that are highly *incoherent*, that is, systems that are heterogeneous and undergoing random thermal motion. An easy way to appreciate this is to consider that scattering a coherent wave front off an incoherent sample encodes the instantaneous sample heterogeneity onto the scattered wave fronts, which can then be detected and analyzed to understand the underlying heterogeneity and its temporal evolution. Moreover, soft X-rays, at wavelengths between ~0.5 and 10 nm, offer excellent sensitivity to chemical and magnetic structure with nanometer sensitivity. This is a very powerful combination that directly addresses the sensitivities required to measure and optimize functional structures.

This workshop report is divided into four sections. The first provides an introduction to the problems of interest at a slightly deeper level than described above, a brief description of the revolutionary accelerator technology that enables diffraction limited storage rings, and longer discussion of the coherent soft X-ray tool box illustrated with six “killer applications” that will be enabled by these sources. Like the examples of functional systems mentioned in the first paragraph above, the killer applications lie at the forefront of a broad range of basic scientific disciplines – chemistry, biology, physics, earth sciences – yet all would enable technologies having major societal impact. The next three sections of the report contain a total of 10 chapters that provide more depth about the ideas mentioned above. Each of these sections provides a 1-2 page introduction that is accessible to the non-expert and which further highlights the opportunities enabled by these revolutionary sources.

We very much look forward to the exciting opportunities provided by this new generation of X-ray sources, and look forward to working with the community to make them a reality and to develop the tools needed to understand functional structures.

Roger Falcone, Director
Advanced Light Source

Steve Kevan, Deputy for Science
Advanced Light Source

Soft X-ray Science Opportunities Using Diffraction-Limited Storage Rings

Table of Contents

Executive Summary	i
Table of Contents	iv
I. Introduction	1
I.1 Emerging Ultrahigh Brightness X-ray Sources	5
I.2 Six 'Killer Applications' Enabled by the Emerging Soft X-ray Toolbox	9
References: Section I	28
II. Enabling Directed Chemistry at the Nanoscale	29
II.1 Bridging Scales in Chemical Kinetics and Dynamics	31
II.2 Enabling Designed Catalysts	39
II.3 Optimizing Functional Energy Materials	45
II.4 Measuring and Understanding Earth Processes at the Molecular Scale	54
II.5 Heterogeneous Aerosol Chemistry	66
References: Section II	70
III. Controlling and Deploying Emergent Electronic and Magnetic Phases	74
III.1 Magnetism and Spin Structures	76
III.2 Quantum Materials	86
III.3 Enabling Transformative Information Processing Technologies	93
References: Section III	101
IV. Understanding Soft Systems at their Natural Energy and Time Scales	103
IV.1 Biosciences Using Diffraction Limited Light Sources	105
IV.2 Spatiotemporal Scales in Soft Condensed Matter	117
References: Section IV	125
Appendices	
A.1 Workshop Charge and Agenda	127
A.2 List of Acronyms	130
A.3 List of Attendees	131

I. Introduction

Steve Kevan and Eli Rotenberg

The portfolio of synchrotron radiation research has evolved continuously over the past 50 years from a few specialized tools used primarily by physical scientists to an essential suite of capabilities accessed by materials scientists, bioscientists, chemists, geologists, archeologists, and many more. Worldwide the number of users annually is now measured in 10s of thousands. It is difficult to find any modern technology that has not been impacted either directly or indirectly by synchrotron radiation research. The penetrating power and spectral/spatial sensitivity and of X-rays drives this diversity of applications. There are now over 100,000 entries in the protein databank, most of them determined by synchrotron X-ray diffraction, most industrial catalysts have been studied and optimized using synchrotron X-ray spectroscopy, and nearly all modern electronic components have been impacted by synchrotron X-ray analysis.

Facilitated by advances in accelerator technology, development of new applications of synchrotron radiation has remained robust for decades. Initially the primary metric driving these applications was the X-ray spectral flux, which determines the throughput of many X-ray spectroscopy and diffraction experiments. More recently, the X-ray spectral brightness, or brightness for short, has become a favored metric since it determines the throughput of combined spectroscopy/microscopy experiments and therefore measures our ability to probe systems that are spatially, temporally, and spectrally heterogeneous. Since 1960, the source brightness of storage rings has increased by 14 orders of magnitude, which has spawned new applications from the infrared through the hard X-ray regimes of the electromagnetic spectrum.

Within the next two years the first of a new class of accelerators will be commissioned that will increase the source brightness by another 2-3 orders of magnitude.¹ More importantly, these new sources will produce X-ray beams that are diffraction limited or nearly so. "Diffraction limited" means that the light source is so small and so well-collimated that we cannot distinguish it from a point source, and the resulting wavefronts are smooth or coherent. Coherence has already started to generate new X-ray techniques that will revolutionize our ability to probe diverse forms of matter. The new sources will take these emerging applications from heroic to routine and thereby will greatly expand their impact. The new sources will also enable entirely new techniques that control and utilize the phase of x-ray beams to study diverse classes of materials in unprecedented detail simultaneously in the spatial, temporal, and spectral domains.

These revolutionary capabilities motivated a workshop entitled *Soft X-ray Science Opportunities using Diffraction-Limited Storage Rings*, held at the Advanced Light Source (ALS) at Lawrence Berkeley National Laboratory on Oct. 1-3, 2014. 94 participants attended the workshop from around the world, about half from X-ray user facilities and the rest with focused expertise in chemical, material, biological, and earth science disciplines. Attendees were charged (Appendix 1) to focus on transformational tools that will enable transformational science opportunities at emerging highly coherent soft X-ray (SXR) sources. The chapters in this workshop report were drafted by participants and constitute an initial consensus concerning the opportunities offered by these emerging sources. The primary finding is that coherent SXR

beams offer an unmatched combination of chemical and material spectral contrast, nanometer spatial sensitivity, and high coherent flux that will be crucial to analyze and help perfect the next generation of functional materials and devices.

Beyond Reductionism in Science and Technology

Through most of human history a dominant paradigm in science and technology has been reductionism, that is, the process of understanding and optimizing the behavior of a material or device in terms of the properties of its sub-components. An early example that spans many civilizations is adobe brick, which combines the durability and lifetime of dried clay with the tensile strength of plant fiber to produce a composite building material that sometimes lasts for millennia. Reductionism was a crucial ingredient of the industrial revolution and has led to the dazzling array of contrivances, from cars to computers, which are essential ingredients of a modern standard of living.

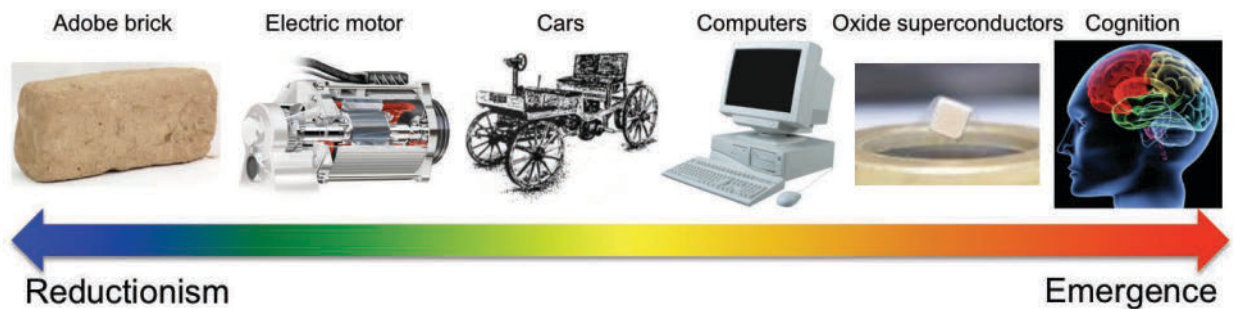


Figure I.1.1: The properties of an adobe brick (left end) are determined by both the durability of hardened clay and the tensile strength of the embedded plant fiber, thereby providing a classic example of reductionism. The human brain (right end) is composed of just a few elements arranged in a complex hierarchical structure that supports cognition, a paradigm emergent behavior. Between those limits the classification can become ill-defined: a classic car is reductionist, but new models are being endowed with increasing intelligence and might some day exhibit the emergent behavior of a robot that might use a neuromorphological processor. Reductionism tends to deploy components with macroscopic structure, the properties of which endow the composite system with hybrid properties. Emergent behaviors often develop from strongly interacting degrees of freedom in nanostructured materials, and phenomena like high temperature superconductivity (second from right) can emerge.

Increasingly, many areas of science focus on systems that cannot be understood within a reductionist framework (Figure I.1.1). We struggle to understand how a combination of few light elements with small concentrations of heavier elements produces living, cognitive systems. The discovery of high temperature superconductivity in nominally insulating copper oxide compounds was revolutionary, but nearly 30 years later the mechanism by which strongly coupled nanoscale interactions produce emergent superconductivity in close proximity to an insulating phase remains incompletely understood. While the basis of modern computers is largely reductionist, a closer look provides examples of material combinations that function in ways that are not simply related to the properties of the sub-components. We can also look forward to neuromorphological processors that begin to mimic emergent cognition in biological systems. Emergent phenomena are often difficult to understand, predict and control; by comparison, reductionism is conceptually easy.

Nature is rife with examples like this, where useful chemical, electronic, or mechanical function emerges in ways that are hard to predict for structures composed of well-understood subunits (Figure I.1.1). Even with the availability of extensive databases that catalog the structure and properties of small molecules, polymers, biopolymers, and hard materials, we still are not able to make batteries with stored energy density comparable to carbon-based fuels, to form carbon-carbon bonds efficiently, to catalyze artificial photosynthesis for efficient conversion of sunlight to fuels, or to separate contaminants from ground water with high fidelity and at the thermodynamic efficiency limit. Solving these problems and many others will involve deploying novel materials that function cooperatively in heterogeneous structures and environments, where interfaces and interphases are designed and controlled with high precision. Developing predictive power for such mesoscale systems will remain a primary focus of basic chemical, materials, environmental, and biological research for decades to come. How do we rationally design, build, and understand chemical, material, and biological structures, and, in particular, systems that combine aspects of all these components to achieve a desired function? How do we create adaptive material and chemical structures with integrated feedback, regulation and self-repair, which are essential ingredients of environmental and living systems, so that they maintain their desired functions with high fidelity and efficiency over long periods of time?

Emergence and the Future of Soft X-ray Science

Composite materials and devices designed within the reductionist paradigm – adobe bricks and cars, for example – tend to combine macroscopic components whose properties are clearly evident in the composite. By contrast, unexpected properties emerge when with degrees of freedom interact strongly – electronically, chemically, magnetically, etc. – on a scale ranging from an atom to several nanometers. Emergence is also closely related to function and thereby to the microscopic modes of a system. Soft condensed matter and biological systems, for example, exhibit diverse emergent phenomena, and these are driven by many interacting, low energy degrees of freedom that are simultaneously thermally activated. The oxide insulators SrTiO_3 and LiAlO_3 are wide band gap hard materials with no strongly interacting low energy degrees of freedom. Such materials are now well understood, and reductionism would posit that putting them together would not produce any unusual properties. But a heterojunction between these two is a ferromagnetic metal that is superconducting at low temperature.² The interface is one layer thick and has interacting, low energy degrees of freedom that produce an emergent metallic ground state.³⁻⁵ *To understand emergence we need tools that relate structure at the nanoscale to motion at the kT energy scale.*

As explained in more detail in the following chapters, the spatial, spectral, and temporal sensitivities of coherent SXR beams on diffraction limited storage rings are perfectly matched to probe emergent materials and structures. Firstly, SXR spectroscopies offer excellent chemical, electronic, magnetic, and structural sensitivity. One can, for example, probe the titanium or aluminum centers in a SrTiO_3 / LiAlO_3 heterojunction with core level spectroscopies or probe the 2D electron gas at the interface with angle-resolved photoelectron spectroscopy. Secondly, the length scale set by the SXR wavelength provides nanometer sensitivity in scattering and microscopy experiments, and in many cases SXR spectroscopy provides atomic-scale

sensitivity. For example, Fe L-edge spectroscopy probes the local structure around an iron center, while at the same time allowing the iron oxidation state in submicron Li_xFePO_4 battery cathode particles to be mapped. SXRs are inherently multi-scale and multimodal. Finally, as explained in the rest of the document, high brightness and coherent flux can be leveraged to achieve $h/k_B T$ temporal or $k_B T$ energy resolution characteristic of functioning systems.

The power of these sensitivities to address issues in emergent phenomena can be illustrated by a few aspirational challenges that were discussed in the workshop:

- **Connecting scales in space and time:** How do sub-picosecond, atomic-scale interactions and excitations build up into slower, macroscopic phenomena, for example, phase behaviors, chemical reactions, and magnetic switching?
- **Achieving kinetic control in a thermal environment:** How do we mimic the function of biological systems by designing structures that achieve a specific synthetic result using an incoherent thermal stimulus – in an environment dominated by thermal noise?
- **Managing our energy future:** How do we control energy conversion, flow, and storage with high efficiency and at low cost - especially low density forms of energy like heat and sunlight?

The final two chapters in this introductory section of the report discuss in cursory detail the approaching revolution in storage-ring-based X-ray sources and how high brightness will augment the spectral, spatial, and temporal sensitivities of existing and emerging SXR tools. The following sections and chapters outline in more detail how these tools will accomplish transformational research across a diverse range of disciplines.

1.1 Emerging Ultrahigh Brightness X-ray Sources

The advances in X-ray science and technology developed primarily at storage-ring-based synchrotron radiation facilities in recent decades have dramatically embellished the traditional strengths of X-ray tools and have rendered them essential to address questions like those posed in the introduction. In particular, X-ray techniques that combine *in situ* spectroscopic, spatial, and temporal sensitivities continue to be developed in order to enable optimization of functioning, heterogeneous mesoscale materials and devices. These developments will have increasing impact in the future and will particularly benefit from emerging ultrahigh brightness SXR sources that motivated this workshop.

The focus of the workshop was on research opportunities using ultrahigh brightness storage ring sources. While there was no specific emphasis on the revolutionary capabilities of emerging free electron laser (FEL) sources, the complementarity between pulsed FEL and nearly CW storage ring sources was a reoccurring topic and is mentioned on multiple occasions throughout this document (notably in section I.2.B and II.1). The capabilities of proposed energy recovery linac (ERL) sources overlap those storage rings and FELs, so many of the ideas discussed here are also relevant to ERLs.

How is ultrahigh source brightness connected to the research problems discussed in the introduction? Source brightness is defined as the flux of photons, which sets the temporal resolution of an experiment, normalized by the transverse phase space area, which sets the spatial resolution, and the source bandwidth, which sets the spectral resolution. Therefore, brightness is the metric that determines the available temporal, spatial, and spectral resolution of a particular X-ray experiment. It is directly related to our ability to address nanoscale (i.e., spatial) material and chemical (i.e., spectral) kinetic (i.e., temporal) processes that often lie at the heart of how emergent systems like those discussed in the previous paragraphs actually function. Very small source transverse dimension leads to very high brightness and to diffraction-limited photon beams that have full transverse or spatial coherence down to a particular wavelength. The resulting wave fronts will be coherent, that is, smooth, across the entire beam. This source coherence can be leveraged to probe spatially heterogeneous structures and temporally incoherent mesoscale processes. The application of ultrahigh brightness X-ray sources to such structures and processes motivated the workshop and is the primary focus of the remainder of this document.

Over the past several decades, the brightness of each generation of storage ring technology has increased by about a factor of 100 (Figure I.2), largely through improved accelerator lattice design. In 2000, the design of storage rings was considered to be mature, with no major brightness enhancements anticipated. The data point in Figure I.1.1 labeled 4th Generation/ DLSR (diffraction limited storage ring) indicates this has changed with the realization and international consensus that multibend achromat (MBA) accelerator lattices can provide large increases in source brightness.⁶ These advanced lattices will not be discussed in detail here, other than to say that, as the name suggests, MBA lattices place several soft bend magnets in each storage ring sector, rather than the two or three hard bend magnets common in third generation sources. The softer bends in an MBA lattice lead to a smaller horizontal beam

dispersion, and are interspersed with strong focusing magnets that correct this dispersion. Instead of an elliptical profile characteristic of current-generation lattices, MBA lattices will produce compact and nearly circular profiles (Figure I.1.1), with the horizontal spatial and angular widths of the source both decreased by about a factor of 10 relative to existing sources.

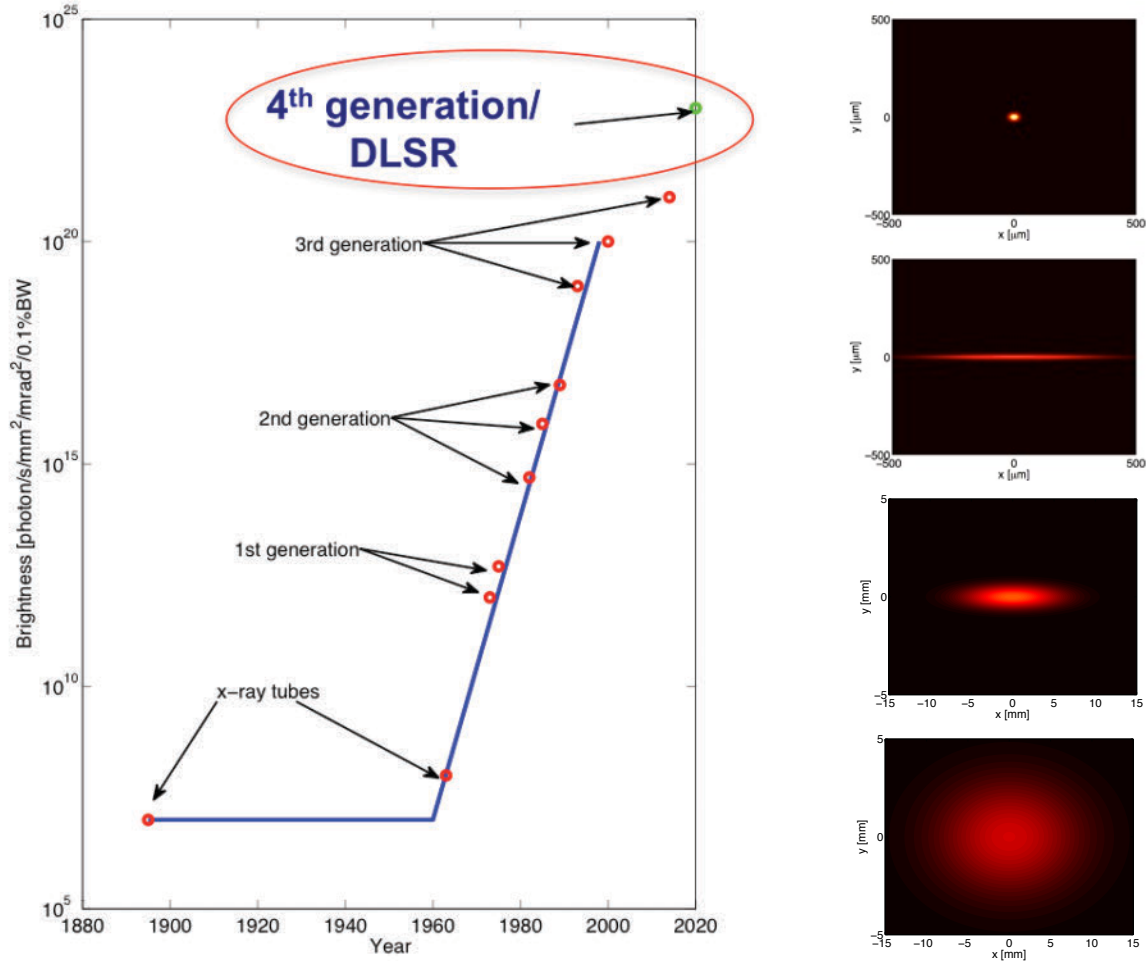


Figure I.1.1: Evolution of storage ring brightness (left) and schematic of the electron source profiles (right) over four generations of storage ring technology. The total flux does not markedly increase from generation to generation, but smaller source size and divergence increases the source brightness by typically a factor of 100 between generations.

Figure I.1.2 shows the predicted brightness and coherent flux for a few MBA lattices under construction or proposed around the world, compared to the same performance parameters available at existing third generation facilities. The first facilities based on the MBA lattice concept will be commissioned over the next few years at MAX IV in Sweden and, shortly thereafter, at SIRIUS in Brazil. Both of these facilities were well represented at the workshop. Several other facility upgrades have been proposed at facilities around the world and some are presently in the design and engineering phase. Other recently commissioned facilities, e.g., PETRA III at DESY in Hamburg and NSLS-II at Brookhaven National Laboratory, will achieve

higher brightness than existing sources, though not as high as the emerging MBA sources. Increased source brightness is a high priority goal at facilities around the world.

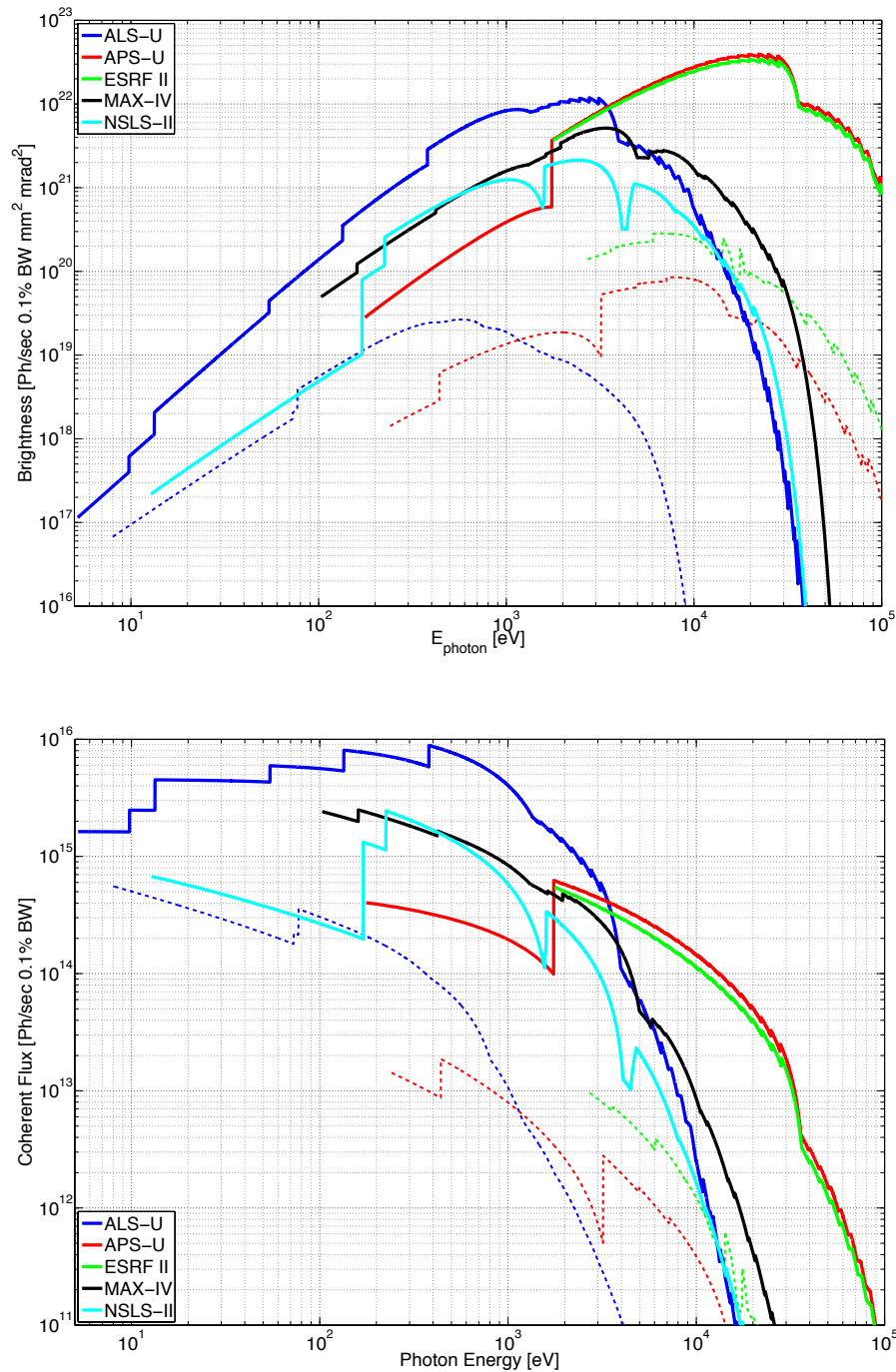


Figure I.1.2: Top: Brightness curves for a few existing 3rd generation sources (dashed curves) and for emerging or proposed upgraded 4th generation sources based on MBA lattice concepts. Bottom: Corresponding coherent flux of x-ray photons provided by existing and emerging/planned facilities.

As shown in Figure I.1.2, near the nominal photon energy at which a facility is optimized, an MBA lattice will increase the source brightness relative to 3rd generation facilities by a factor of 100-1000, enabling corresponding increases in spatial, temporal, and spectral dynamic range of experiments. Since the coherent flux scales as the brightness times the square of the wavelength, this metric emphasizes the benefit of the longer wavelength vacuum ultraviolet (VUV)/SXR regime. For example, the design of the proposed ALS upgrade (ALS-U) focuses on the SXR regime and is among the most aggressive proposed to date. It is therefore predicted to provide the highest possible coherent flux of any proposed new or upgraded storage ring facility at any photon energy.

We emphasize that high brightness implies the ability to achieve high spatial, temporal, and spectral resolution, but it does not imply higher total X-ray flux. Indeed, the total flux from emerging MBA sources will be comparable to that of existing sources. The higher brightness simply reflects the smaller source size and divergence. The terms “high brightness”, “full transverse coherence”, and “diffraction limited” are used interchangeably, though the connotations can be slightly different.

I.2 Six ‘Killer Applications’ Enabled by the Emerging Soft X-ray Toolbox

In this chapter we discuss SXR techniques that received significant discussion during the workshop. They offer the sensitivities needed to address the science issues as discussed in the introduction and will benefit greatly from emerging 4th generation high brightness sources. We make no attempt at a comprehensive discussion of all SXR techniques, and we emphasize that techniques that do not require high brightness and coherence will certainly still be possible and often improved using DLSR sources. Our main goal in this chapter is to provide background for the following chapters, which will further elaborate these tools as needed and describe how they will be applied to current and future research problems.

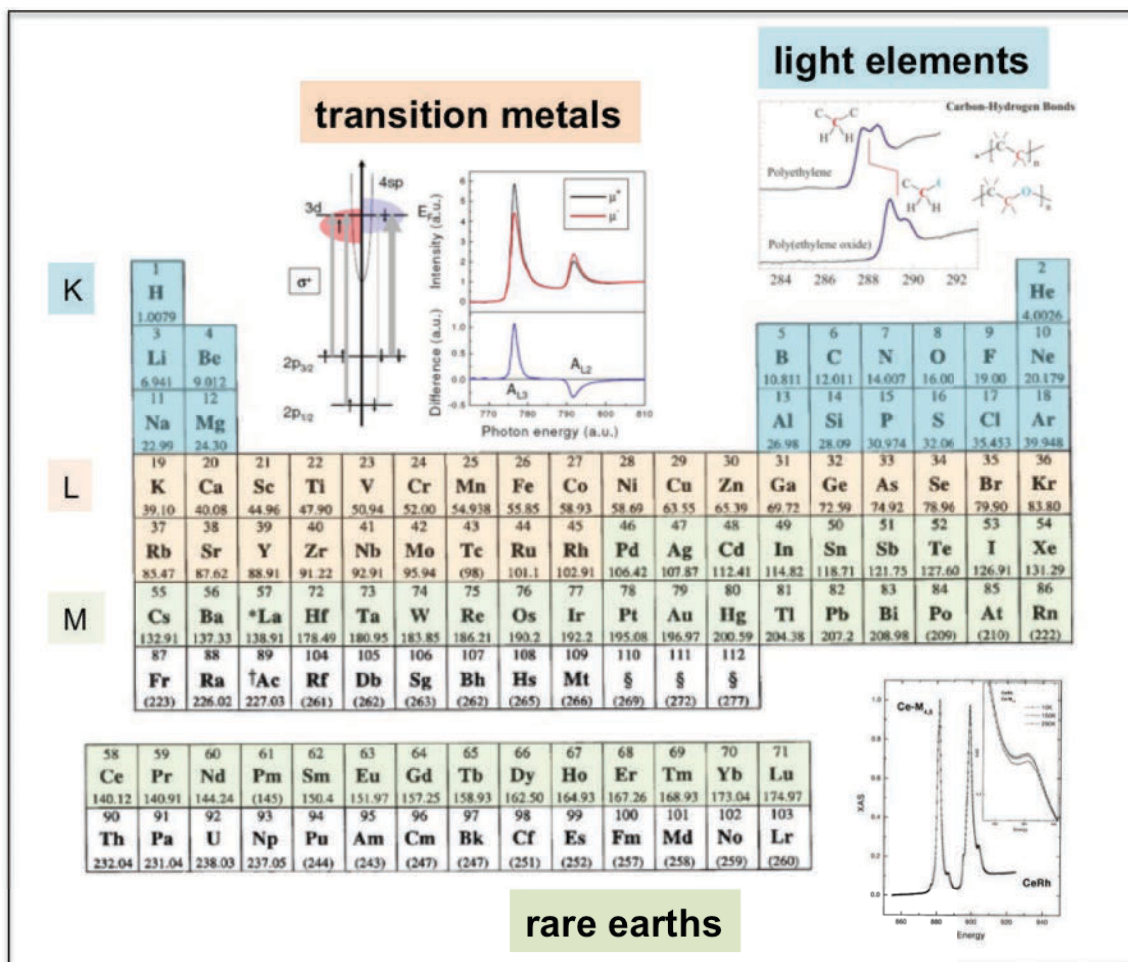


Figure I.2.1: Elements with K, L, and M X-ray absorption edges located in the SXR regime, with exemplary near-edge absorption spectra that demonstrate the chemical and magnetic sensitivity available. The SXR regime includes the narrowest core levels for all elements – those that are closest in energy to the valence levels responsible for chemical bonding, magnetism, superconductivity, mixed valence, and other material properties. The valence levels can often be accessed through SXR dipole transitions to provide spectroscopic and scattering contrast reflecting electronic properties.

Hard X-ray (HXR) techniques, notably the many variants of X-ray scattering and X-ray absorption, have long played a dominant role in determining the atomic structure of diverse classes of materials. The focus in this document is on SXR tools. The SXR energy regime, defined here to comprise photon energies between a few 10s of eV and a few keV, encompasses the binding energies of the narrowest core levels of most elements in the periodic chart (Figure I.2.1). These sharp core levels access the valence states relevant to chemical bonding, superconductivity, and magnetism via direct, dipole allowed (real or virtual) transitions. For this reason SXR spectroscopies provide the crucial contrast needed to probe diverse functioning systems, as indicated in the simple near-edge X-ray absorption (XAS) results in the insets in Figure I.2.1. For example, the K-edges of the important first row elements lie between 50 and 1000 eV. The inset in the upper right shows X-ray absorption spectra collected near the carbon $1s \rightarrow 2p$ threshold in polyethylene and polyethylene oxide and indicates that these two polymers can be easily distinguished without labeling. Moreover, the corresponding SXR wavelength range of ~ 0.6 nm to ~ 25 nm (~ 50 eV to 2 keV) readily accesses length scales relevant to the mesoscopic realm where unusual textures and properties like those discussed above emerge. HXR science often focuses on questions of structure, like “Where are the atoms?” and “What is the lattice strain in this material?”. SXR science focuses more on questions of function like “Where are the electrons?” and “How do they impact chemical bonding, kinetics, magnetism, superconductivity, etc?”. There is, of course, overlap between these sensitivities: SXR spectroscopies often provide atomic scale information, and X-ray scattering and microscopy are regularly applied to probe material textures as well.

An interesting development that becomes prominent throughout this chapter is that high brightness X-ray sources will accelerate the ongoing trend of blurring the boundaries between conventional X-ray spectroscopy, scattering, and imaging techniques. A very good example of this is coherent diffractive imaging (CDI) discussed below. In execution this is a scattering technique, but the goal of CDI is to phase a diffraction pattern to produce real-space amplitude and phase images of a heterogeneous material, and increasingly this is done at a resonant energy near an X-ray absorption edge so as to provide, for example, chemical or magnetic contrast, as suggested by Figure I.2.1. So, CDI is a combined scattering, imaging, and spectroscopy technique. To connect the techniques more directly to the research areas described in the rest of this document, we have split our discussion into two sections and offer a few examples of what is possible on current sources and what will be possible on emerging high brightness sources. We first focus on SXR microscopy techniques, which study the structure of materials with nanoscale resolution and high chemical, orbital, structural, or magnetic contrast, and then turn our attention to techniques that probe kinetic and dynamical phenomena relevant to how materials function over broad length and time scales.

To help address a confusing barrage of acronyms, we provide a table of techniques and their acronyms, with a few words of description and the advantage of high brightness, in Appendix 2.

A. High Coherent Flux and Soft X-ray Microscopy

Perhaps no class of techniques has had a larger impact on our understanding of the world around us than microscopy. Over the past few centuries, optical microscopy of biological systems, for example, has progressed from van Leeuwenhoek's first microscopic images of biological tissues and cells to the development of super-resolution fluorescence microscopy to map microtubules with ~10 nm resolution. Every step along that path has had a huge impact on both science and society. More recent development of electron, ion, X-ray, and scanned probe microscopies have continued the trend of probing the atomic and nanoworld with ever higher resolution and, as importantly, with diverse contrast mechanisms. These tools provide a crucial step in determining how a material works, whether it is a sub-cellular biostructure, a catalytic nanoparticle, or a magnetic bit.

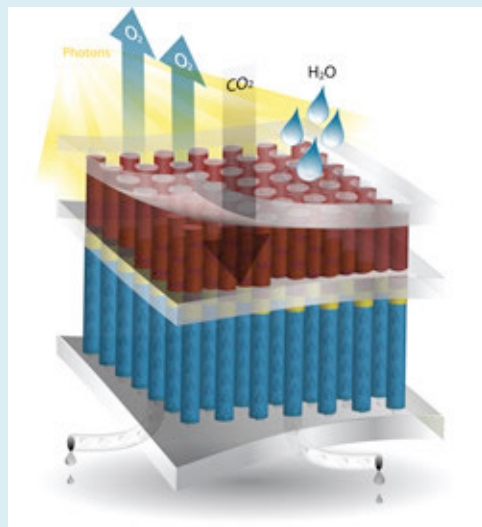
The trend toward ever more-powerful microscopy techniques shows no sign of abating, and the emergence of diffraction limited SXR sources is the next big enabling technology in X-ray microscopy. X-ray microscopy (excluding radiography) was basically not possible on 1st generation storage ring sources (Figure I.1.1), and it was a heroic experiment on 2nd generation sources. X-ray microscopy has become more routine on 3rd generation sources. X-ray microscopes with ~30 nm resolution are now commercially available and are being applied to a growing number of problems in diverse sample environments. Achieving better resolution than 20-30 nm, when possible, remains a heroic experiment. While such resolution is useful in many systems, a major impact of nanoscience, for example, is driven by the rapid increase in interface area as nanostructure size decreases. Consequently, the role of X-ray microscopy on mainstream nanoscience will be rather limited without routinely achieving ~10x better resolution.

In electron and X-ray microscopy, the resolution scales slowly – as the inverse cubic or quartic root - with the dose delivered to a single resolution element in the image.⁷ This dose is directly related to source brightness, so a 100-1000x increase in brightness at emerging diffraction-limited storage ring sources is essential to achieve the desired improvement in resolution. Coincidentally, the development and commercial deployment of 'super-tips' as field emission cathodes in transmission electron microscopes 10-15 years ago provided 200-300x increased source brightness and was a key enabling technology for atomic scale imaging.

X-ray microscopy will benefit enormously from the high coherent flux of emerging SXR DLSRs in two different ways. An obvious optical advantage of diffraction-limited photon beams, and one that was actively discussed at the workshop, is that it allows the beam to be focused into the smallest possible spot with the highest possible fidelity. Such a small spot can be readily combined with powerful SXR spectroscopies to enable spatially resolved measurements with high spectral contrast. We distinguish such measurements here as 'nanoscale spectroscopy', since the focal spots are typically a few 10s of nm at present. Alternatively, interference-based full-field microscopy techniques like holography and CDI will also benefit enormously from DLSR sources. An emerging combination of scanning and full field modalities called

#1: Optimizing catalytic correlations in space and time

Enzyme structures are exquisitely tuned to achieve highly selective biological function. An important goal in chemical catalysis is to mimic this biocatalytic precision by designing spatial and temporal correlations between catalytic centers. We know this is possible, by analogy to biological systems and through serendipitous discovery of high catalytic activity of some nanostructures. However, we lack the tools to probe these correlations at the relevant length and time scales to close the structure-function loop. As described in Chapter II.3, soft x-ray DLSR sources will enable tomographic studies of catalytic landscapes with nanometer spatial and microsecond temporal resolution combined with valuable chemical contrast. Faster kinetic processes will be probed with soft x-ray correlation spectroscopy and quasielastic scattering. This will help optimize the efficiency, for example, of artificial photosynthesis cells (right).



Conceptual drawing of an artificial photosynthetic system that uses only light, water, and carbon dioxide as inputs, and produces clean, renewable fuel.

ptychography is poised to revolutionize the whole field. To distinguish these techniques from the scanning approaches, we refer to them below as ‘spectroscopic imaging’.

Soft X-ray Nanoscale Spectroscopy

The conceptually simplest nanoscale spectroscopy is nano-X-ray absorption spectroscopy, commonly called scanning transmission X-ray microscopy (STXM). As suggested by the panels in Figure I.2.1, tuning the photon energy near core level resonances allows such a STXM measurement to map local chemical or magnetic structure at a resolution set by the focal spot size. Figure I.2.2 offers an example application to iron oxide catalytic nanoparticles supported on silica in an operating Fischer-Tropsch reactor.⁸ In this case, operating near the Fe L₃ edge, the authors were able quantify the iron oxide phases present during the reaction.

STXM and other scanned nanoscale spectroscopies benefit from a coherent focusing modality and the signal level varies in direct proportion to source brightness. A primary benefit of 4th generation facilities will therefore be throughput. On existing sources, acquiring an image like the one in Figure I.2.2 requires an acquisition of approximately a minute to collect. With ~100x higher brightness the same image will be collected in less than a second. This increased data rate could be used for serial imaging, e.g., to produce movies that characterize catalytic kinetics in real time, to employ higher spectral resolution and thus higher sensitivity, or to take multiple images at different orientation to produce 3D nanoscale tomographic reconstructions with full

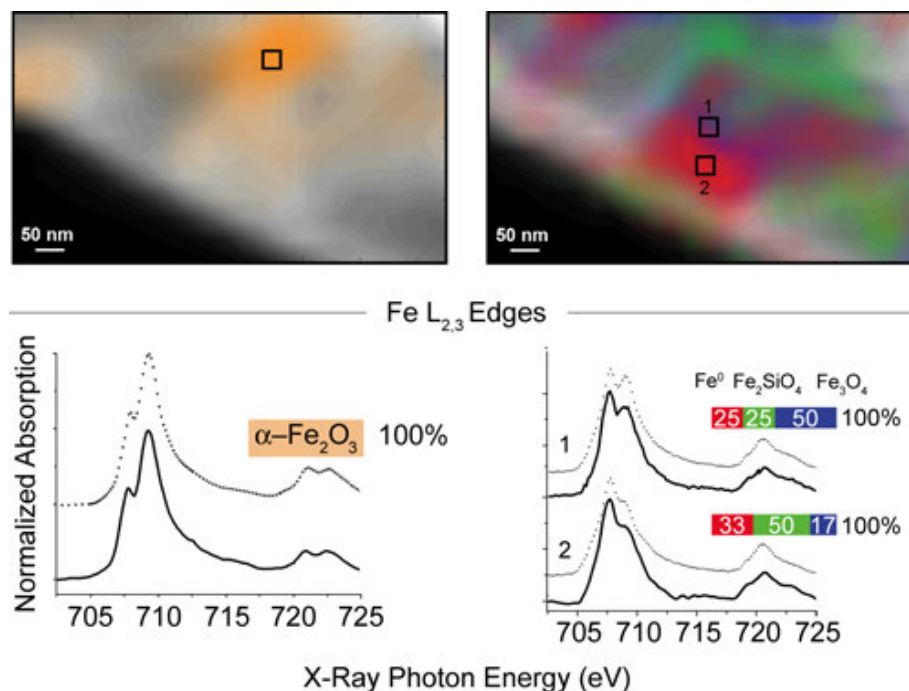


Figure I.2.2: Scanning transmission X-ray microscopy study of supported iron oxide nanoparticles during the Fischer-Tropsch catalytic synthesis of hydrocarbons from CO and H₂. Bottom: Fe L_{2,3} near edge X-ray absorption spectra showing the sensitivity to oxide phase before (left) and during (right) the reaction. Top: Corresponding chemical maps of iron oxide phases before and during the reaction.⁸

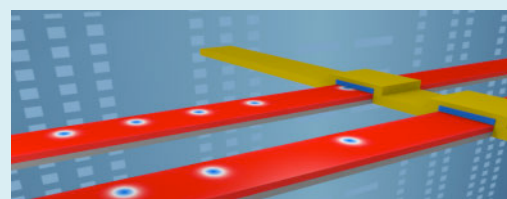
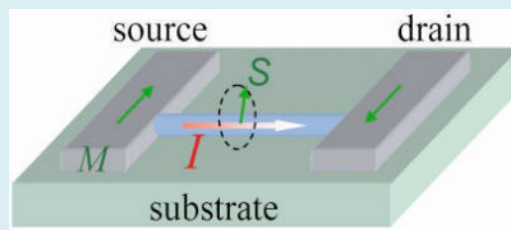
spectral contrast. Radiation damage and sample heating will often limit the total X-ray dose and thus the resolution that can be achieved, particularly in imaging soft/organic/biological materials. Evolutionary improvements in techniques and detectors, and imaging static frozen samples, is expected to enable imaging to ~10 nm resolution in these radiation sensitive systems.⁷

Scanning SXR microscopes will have difficulty achieving few-nanometer resolution, both due to the difficulty of producing the required X-ray optical elements and the high flux density and consequent sample heating and radiation damage inside the focal spot. With higher brightness sources and further development of Fresnel zone plate lenses, down to 5 nm resolution could be achieved in the future on damage-resistant materials and would enable some of the important applications discussed in this document.

Many SXR spectroscopies are being developed into nanoscale spectroscopies using a scanning modality. For example, X-ray magnetic circular and linear dichroism (XMCD/XMLD) are variants of X-ray absorption spectroscopy and provide element- and oxidation-state-resolved magnetometry results from ferromagnetic, ferrimagnetic, and antiferromagnetic samples. Nano-XMCD/XMLD will achieve this performance with nanoscale resolution. Combining full tomographic reconstructions with complete polarization control will allow mapping the vector magnetization in magnetic nanostructures. A competitive technique is Lorentz Transmission

#2: Imaging motion of topological spin states and spin textures

Creating and controlling currents of spins and spin textures (e.g. skyrmions) are common ingredients in proposed technologies for low power classical and quantum computing. Topological insulators were first observed using soft x-ray ARPES and are now proposed as internal spin sources, spin field effect transistors, and other spintronic devices (top figure). The magnetic contrast of soft x-ray imaging and scattering techniques has recently been applied to study topological skyrmions, which are proposed for low power information storage and processing (bottom figure). As discussed in Section III, high brightness DLSR sources will revolutionize studies of charge and motion and interactions in such structures, through the advent of nanoARPES with spin resolution and the use of coherence in correlation spectroscopy, quasielastic scattering, and interferometric detection and imaging.



Using topological spin states to achieve low dissipation. Top: FET based on the intrinsic high mobility of a topological insulator. Bottom: Race track memory based on low power needed to move topological skyrmions.

Electron Microscopy (LTEM), which measures stray transverse fields around inhomogeneous textures rather than the magnetization directly. Magnetic STXM will be able to probe thicker structures in more diverse environments than LTEM.

STXM and other scanned nanoscale spectroscopies benefit from a coherent focusing modality and the signal level varies in direct proportion to source brightness. A primary benefit of 4th generation facilities will therefore be throughput. On existing sources, acquiring an image like the one in Figure I.2.2 requires an acquisition of approximately a minute to collect. With ~100x higher brightness the same image will be collected in less than a second. This increased data rate could be used for serial imaging, e.g., to produce movies that characterize catalytic kinetics in real time, to employ higher spectral resolution and thus higher sensitivity, or to take multiple images at different orientation to produce 3D nanoscale tomographic reconstructions with full spectral contrast. Radiation damage and sample heating will often limit the total X-ray dose and thus the resolution that can be achieved, particularly in imaging soft/organic/biological materials. Evolutionary improvements in techniques and detectors, and imaging static frozen samples, is expected to enable imaging to ~10 nm resolution in these radiation sensitive systems.⁷

Similar developments using small spots are underway for photoelectron and secondary photon emission spectroscopies. This includes important probes of electronic and chemical structure: nanoARPES (nano-angle-resolved photoelectron spectroscopy, Figure I.2.3),⁹ nanoAPXPS (nano-ambient pressure X-ray photoelectron spectroscopy), and nanoXES (nano-SXR emission

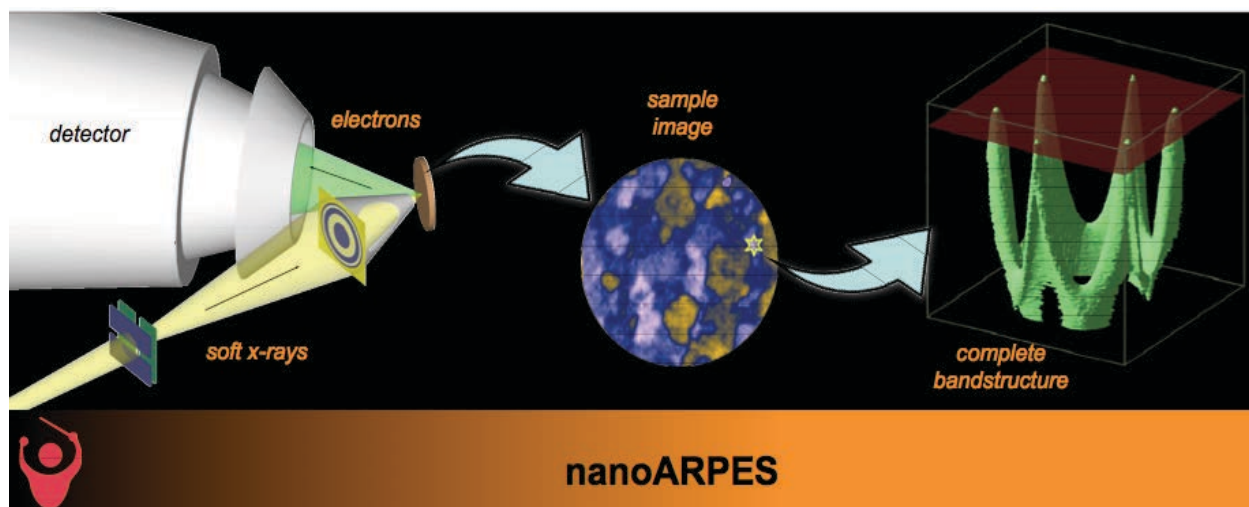


Figure I.2.3: Schematic of a “nanoARPES” experiment. In this case the transversely coherent fraction of an X-ray beam is focused into spot 10’s of nanometers in size and is used to study electronic inhomogeneities in diverse materials [from Eli Rotenberg, ALS].⁹

spectroscopy). Applications of all of these will be discussed further in other chapters.

Soft X-ray Full Field Spectroscopic Imaging

Just as SXR spectroscopies are evolving into nanoscale spectroscopies, SXR microscopies are similarly evolving to achieve spectroscopic imaging. An important goal that was actively discussed at the workshop is to achieve few-nanometer resolution with full spectroscopic contrast and robust operation in diverse environments. Nanostructures and nanoscale

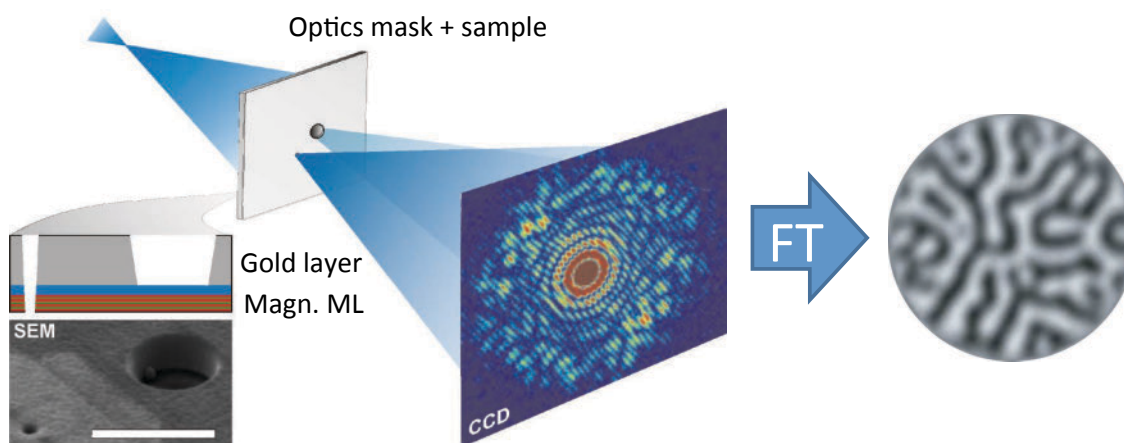
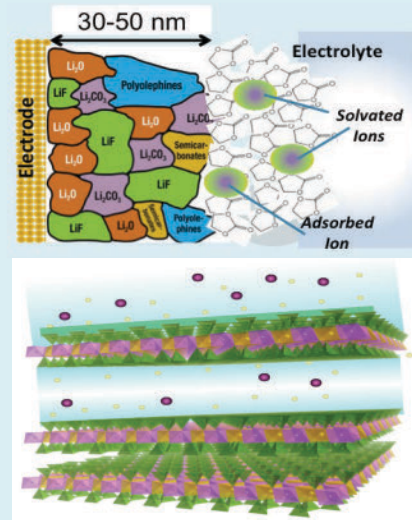


Figure I.2.4: Schematic setup for inline X-ray holography, hologram, and reconstructed image.¹⁰ A transversely coherent SXR beam illuminates a sample and nearby pinhole. A reference wave diffracted off the pinhole interferes with an object wave scattered off the sample, which in this case was wormlike magnetic domains. The resulting hologram can be reconstructed by simple Fourier transformation.

#3: Imaging ion drift and diffusion in batteries, clays, memristors. . .

Ion transport on complex nanostructured landscapes governs many important processes, ranging from charging and discharging batteries to CO₂ sequestration in clay minerals to switching electronic memristors. Battery lifetime and charging rate is determined by transport across the solid-electrolyte interphase (right). Transport of CO₂ and radio-nuclides in shales is governed by the motion of brine in and around layers of aluminosilicates. But the underlying drift and diffusion processes in these are often modeled with poorly validated models. As discussed in sections II.3 and II.4, high brightness DLSR soft x-ray sources will revolutionize studies of ion transport nanometer length and sec – ps time scales through development of advanced tomographic imaging techniques with nanoscale resolution coupled to x-ray photon correlation spectroscopy and quasielastic soft x-ray scattering.



Ion motion on nanoscale landscapes is a key feature in many systems, including batteries (above), clay minerals (below), and even emerging electronic devices called memristors.

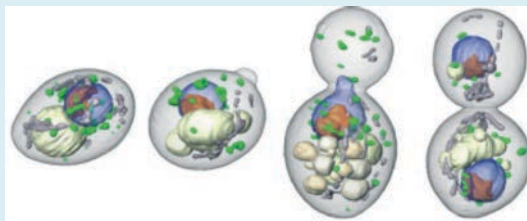
interphase regions, in 2D and 3D, could then be imaged *in situ* with high fidelity. Accomplishing this will require combining the high coherent flux from DLSR facilities with rapidly developing CDI techniques, as explained below and elaborated elsewhere in this report. Acknowledging the above discussion about radiation damage, a more precise statement of this goal is full spectral imaging at a resolution down to the radiation damage limit, which depends strongly on material class, sample environment, and experimental protocol.

Various X-ray microscopy techniques, notably those based on full field and scanning modalities, have complementary strengths that are not discussed in detail here. Full-field transmission X-ray microscopes (TXMs) are now commercially available and are installed at many facilities. They function in a fashion analogous to a light microscope with condensing and projective optics and regularly achieve a spatial resolution of ~30 nm using diffractive Fresnel zone plate lenses. TXMs normally use an incoherent imaging modality and do not benefit from high brightness and coherent flux; indeed, coherence produces speckles in XRM images that must be dealt with. The resolution of TXMs is limited by optics, and might eventually achieve <10 nm resolution on a regular basis.

In principle the optics-limited resolution of a TXM can be addressed by scattering techniques, which measure in Fourier space with large numerical aperture, and either encode the phase holographically or recover phase computationally to transform a scattering pattern into a real-space image. For example, X-ray holography techniques continue to be developed and

#4: High throughput cellular tomography with 10 nm resolution

While long-established for eukaryotes, in the past decade the importance of subcellular organization in the functioning of prokaryotic cells has become evident. Accordingly, the ability to visualize the mesoscale organization and dynamics of subcellular metabolism will play a transformative role in engineering microbial cell factories for biofuels and green chemicals. This will provide an entirely new means of phenotyping engineered biological systems. As discussed in chapter IV.1, DLSR sources will enable high throughput tomographic diffractive imaging at the expected damage limited resolution of ~10 nm in just 10s of seconds, thereby allowing subcellular positioning of macromolecular assemblies to be a design parameter in bioengineering.



Tomographic images of frozen yeast cells through cell division collected with full-field soft x-ray microscope (Carolyn Larabell, ALS; DOI: 10.1002/yea.1834). Sub-cellular organization is readily apparent at the optics-limited resolution of 50 nm. Damage limited resolution of ~10 nm will be achieved using diffractive imaging on a soft x-ray DLSR source.

were actively discussed at the workshop. These coherently illuminate both a thin sample and reference pinhole (Figure I.2.4) to produce a hologram with high NA, which is then simply Fourier transformed to produce a real-space image.¹¹ The technique is simple and the results are easy to analyze, though the resolution is limited by the finite size of the pinhole used to produce the reference wave. 3D tomographic holographic imaging using this approach is more problematic. The resolution can be improved by using the holographic result as input to a coherent diffractive imaging (CDI) phase retrieval and reconstruction algorithm. The advent of high coherence beams at the emerging DLSR facilities will be of major benefit to X-ray holography, and there remains strong interest in further developing and applying holographic techniques.

CDI (Figure I.2.5) is similar in execution to the in-line holography experiment, but there is no reference pinhole and so no holographic encoding. Instead, an image is produced directly from the speckle-diffraction pattern on a computer using iterative phase retrieval algorithms, which have been developing rapidly over the past decade.¹²⁻¹⁴ The algorithms require a strong source constraint and for this reason CDI by itself is most successfully applied to spatially limited structures.

Ptychography is a hybrid of STXM and CDI that has been developing rapidly in the past few years.¹⁵ It received much attention at the workshop since it can be more easily applied to extended objects than CDI while maintaining the resolution advantage over STXM. The object is illuminated and speckle-diffraction patterns are collected from overlapping regions on the sample. The overlapping regions provide a strong real-space constraint for iterative phase

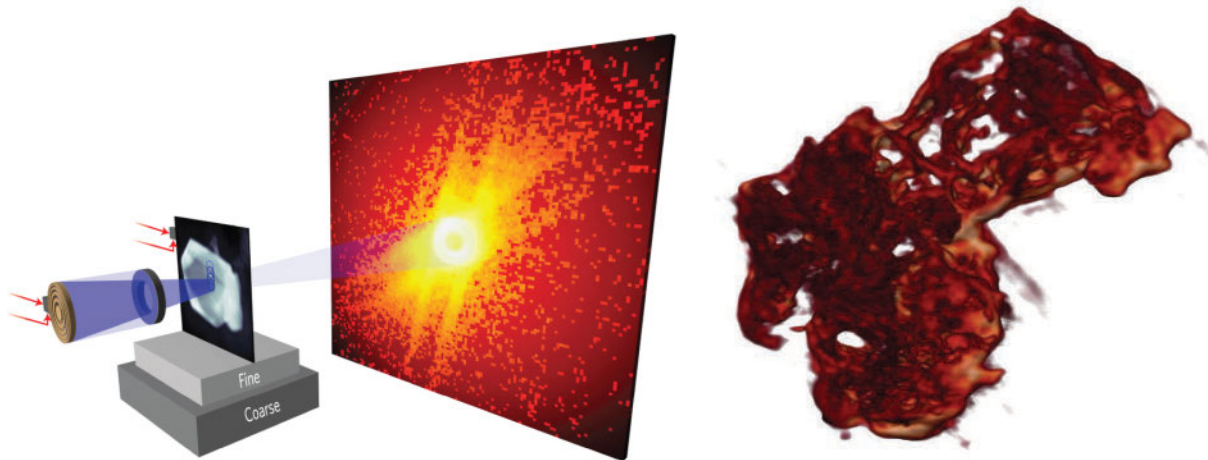


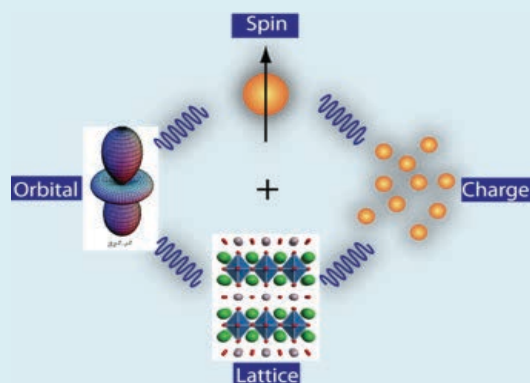
Figure I.2.5: Left: Schematic of a coherent diffraction imaging experiment. A coherent beam is focused onto a sample using a Fresnel lens, and a speckle-diffraction pattern is produced, often in transmission. If the pattern is sufficiently oversampled and if the object is of finite extent, a real space image of the exit wave field, containing amplitude and phase information, can be recovered computationally. A ptychography experiment is closely related: a series of overlapping exposures is collected; the overlap is used as a constraint to help the inversion to real space converge quickly and accurately. Right: 3D image of a soot particle collected using ptychography, collected at 700 eV and with ~ 20 nm resolution in all three dimensions (from David Shapiro, ALS).¹⁶

retrieval and lead to high fidelity images on spatially extended objects. A 100-fold brightness increase is essential to reduce the ~ 20 nm resolution of the image in Figure I.2.5 to 2-3 nm.¹⁶

A final emerging coherence-based imaging technique that received discussion at the workshop was fluctuation X-ray scattering (FXS) (see chapter IV.1).¹⁷ The name is mildly deceiving, since the system to be studied is not intended to be fluctuating. FXS is proposed to image biopolymer molecules and complexes in solution, though applications in other areas are possible as well. A small number of such particles is illuminated coherently with a single X-ray pulse that is short enough to eliminate rotational diffusion effects in the recorded speckle pattern. Recording many “time frozen” speckle patterns with different molecular orientations (i.e., due to rotational fluctuations from image to image) and subsequent alignment and binning on a computer provides results similar to small angle X-ray scattering (SAXS) patterns but with significantly increased information content due to the reduced angular averaging. To date the technique has been applied exclusively using X-ray pulses from FELs. The high coherent flux from a DLSR will enable FXS measurements with the added benefits of high stability and repetition rate. FXS will be described and some preliminary results will be provided in the chapter on bioscience.

#5: Energy and lifetime of coupled excitations in complex oxides

Diverse emergent properties exhibited by transition metal oxides result from a complex coupling between low energy excitations – spin, charge, orbital, lattice. To understand these properties and to learn how to control and optimize them will require that we understand how these excitations are coupled and modified by external fields and nanoscale structuring. The ‘smoking gun’ for the mechanism of high temperature superconductivity, for example, will likely come from measuring how these excitations evolve through the cuprate phase diagram. As discussed in chapters III.1 and III.2, DLSR soft x-ray sources will enable revolutionary approaches to understand the subtle textures observed in oxides and the energy, coupling and decay of associated excitations.



Coupling between low energy degrees of freedom produce many unusual properties in transition metal oxides and beyond.

B. Collective Excitations, Fluctuations, and Dynamics

While the static image of a material structure or device is a key starting point to understand its function, determining its temporal behavior is at least equally important since this relates directly to function. Breakout sessions on excitations, fluctuations, and dynamics in chemical and materials systems were focused on how coherent SXR beams will enable bridging scales from ultrafast local excitations to mesoscale kinetic transformations. This idea cuts across many of the science themes discussed at the workshop; for example, it provides a valuable connection between atomic physics, chemical dynamics, and chemical catalysis, and between spin flips, domain wall motion, and magnetization switching. We discuss these concepts here in the form of a few examples relevant to the coherent SXR tool box, and will refer back to these ideas repeatedly throughout this document.

A wide-ranging scientific challenge is to understand how individual, atomic-scale excitations build up into macroscopic phenomena such as phase transitions and chemical reactions:

- How is a specific unimolecular reaction channel, no matter how efficient on the single molecule scale, relevant to the success of a catalytic assembly?
- When, where, and at what frequency does a spin flip have to occur to initiate the phase transition of entire magnetic domains, or to move a domain wall?
- How does the excitation and charge transfer initiated by photon absorption ultimately lead to a desired photochemical reaction?
- Which molecular-scale events and configurations enable or limit jamming and glass transitions?

- Which atomic-scale properties and correlations of dopants - among each other and with the host matrix - define the electronic behavior of a new material?

To address these challenges, major advances on two fronts are required: a) Maintaining single event sensitivity and high spatiotemporal resolution when studying mesoscale systems containing macroscopic numbers of atoms, and b) developing the tools and means to detect correlations of fundamental events across macroscopic length- and time-scales, to reveal the nature of transformation mechanisms. The research enabled by these major advances in characterization of multi-scale kinetics and dynamics will provide the basis for developing novel materials and processes with desired functionality.

The advent of DLSRs will provide new capabilities that bridge local dynamics to global kinetics, connecting fundamental electronic, structural, and chemical processes with the collective phenomena of extended systems. The characteristics of DLSRs, in particular, high coherent photon flux delivered at a high repetition rate, are ideally suited to facilitate such advances. Emerging, exceptionally powerful X-ray spectroscopy methods such as X-ray photon correlation spectroscopy (XPCS), resonant inelastic X-ray scattering (RIXS) with sub-natural line width, and pump-probe spectroscopy will be exploited to their full capacity through the unparalleled combination of high brightness and nanoscale focusing. Because of the near GHz repetition rate of storage ring facilities, a typical hour-long DLSR experiment will provide up to $\sim 10^{13}$ trials (pulses) with a total of $\sim 10^{21}$ SXR transversely coherent photons to probe a sample under extremely reproducible, tunable conditions, and with spatiotemporal, elemental, and chemical sensitivity unmatched by any other technique. These characteristics are uniquely suited to identify the rare events that govern the success of a superior catalyst, that trigger phase transitions, that nucleate a desired phase during the growth of novel materials, and that initiate cascades that drive material fracture, magnetization reversal, and beyond.

Two complementary classes of dynamical and kinetic measurements were actively discussed at the workshop: field driven and thermally driven processes. Field driven “pump-probe” techniques used to study dynamical events are well established in many branches of science, and high source brightness will significantly enhance photon pump – SXR probe experiments. Spontaneous, thermally driven processes occur over multiple time and length scales. Coherent, high-brightness X-ray beams with moderate pulse energies will provide revolutionary capabilities to monitor these important spontaneous processes. We discuss both classes of measurement briefly here, and many examples are provided in the remainder of this document.

In simple systems, driven and spontaneous dynamics are connected by the fluctuation-dissipation theorem. That connection, however, fails in complex media relevant to many systems discussed here. Additionally, driven dynamics are often measured far from equilibrium where the theorem is also not valid. Many of the systems discussed in this report have manifolds that are at least partly near equilibrium, e.g., reaction-diffusion systems, yet are hard to trigger efficiently and so are difficult to measure with pump-probe techniques. Coherent SXR beams will provide valuable new ways to examine the relationship between field driven and thermally driven dynamics.

Finally, we note that there was broad consensus at the workshop that, as in the optical regime, ultrafast pulsed and more nearly continuous X-ray sources support complementary classes of science and both are needed to understand the connection between atomic-scale excitations and macroscopic phenomena discussed above. X-ray FELs provide ultrahigh peak brightness in very short pulses. FEL science focuses on single-shot molecular imaging, corresponding pump-probe dynamics at the atomic and molecular length scale and ultrafast time scale, and temporal dynamics of elementary excitations in atoms, molecules and materials. By contrast, the stability and high repetition rate of a DLSR is uniquely suited for studying processes across their full time ranges from 10s of picoseconds to hours, while minimizing system perturbations due to the X-ray probe. DLSR science focuses on nanoscale multidimensional chemical imaging, spontaneous kinetic motion on mesoscale landscapes over broad time scales, and high resolution and high sensitivity spectroscopy.

Field Driven Processes

Perturbing a system and measuring its return to equilibrium has been used to probe many kinds of kinetic and dynamical phenomena. Classical reaction kinetics can be measured with temperature- or pressure-jump experiments, the motion of magnetic vortices can be initiated by applying a fast magnetic field pulse, and charge transfer dynamics in molecules can be driven with a fast optical pulse. The stable time structure of storage rings, as well as the chemical and magnetic contrast and nanoscale sensitivity of SXR techniques facilitates pump-probe measurements, which have become very popular in recent decades. High brightness sources will expand the power of these pump-probe measurements in the SXR regime.

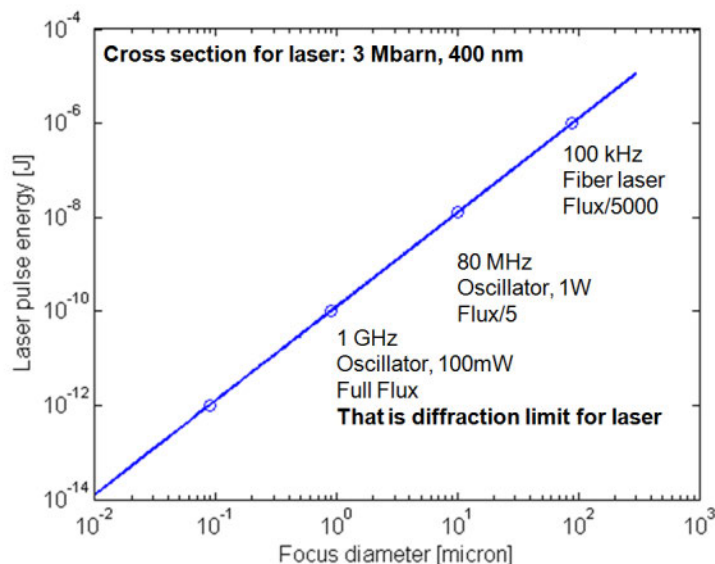


Figure I.2.6: Excitation laser requirements for optical laser pump – X-ray probe experiments. The pulse energy (y-axis) to excite 10% of the molecular population (3 Mbarn molecular absorption at a wavelength of 400 nm) decreases with decreasing spot size. For 100 μm spot sizes, a pulse needs to deliver 100 μJ, which is restricted to laser sources with 100 kHz repetition rate. Thus only 1/5000 of the synchrotron pulses are usable. With a one-micron spot size however, current GHz oscillator technology can be used, which allows for experiments at the full synchrotron repetition rate.

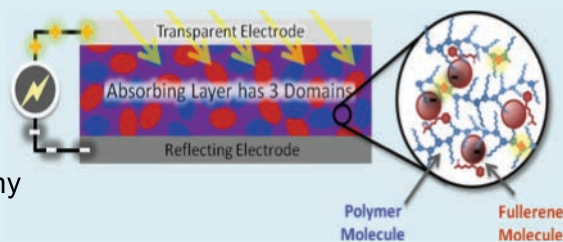
The development of laser-based high harmonic generation (HHG) sources and FELs has led to a burst of new research activities in the fast growing field of ultrafast X-ray science. In particular, chemical dynamics studies benefit from new opportunities to probe transient electronic and structural configurations, which may define the outcome of a chemical process but are often inaccessible in time-averaged measurements. DLSRs will open up a new class of storage-ring based multicolor experiments to understand processes at the electronic level and to follow chemical reactions with atomic resolution and, ultimately, control chemical processes.

Currently, the usable SXR flux in laser pump – X-ray probe experiments is usually limited by an insufficient average optical pump power. The optical laser needs to have a spot size larger than the X-ray spot. For large X-ray spots this requires high pulse energy lasers in order to excite a sufficient fraction of molecules to be probed by X-ray transitions. The same excitation fraction can, however, be accomplished with much smaller laser pulse energies provided a smaller

Killer Applications using Diffraction-limited Soft X-ray Beams:

#6 Nanoscale carrier motion in heterogeneous landscapes

Carrier transport on complex heterogeneous landscapes adversely impacts the performance of many materials proposed for emerging energy conversion, electronic, and spintronic technologies. For example, the external quantum efficiency of many second and third generation photovoltaics is much lower than the internal quantum efficiency because many photoexcited carriers decay before they can be collected (right). As discussed in chapters II.1 and II.4, soft x-ray beams from DLSR sources enable tools that address such multiscale problems by leveraging high coherent flux to measure transport, scattering, and recombination with nanoscale sensitivity and temporal resolution down to ps.



An bulk heterojunction organic photovoltaic (OPV) device integrates donor and acceptor materials into a complex mixture through which carriers need to drift and diffuse before they can be collected. Soft x-ray tools at a DLSR source will enable probing carrier motion with few nm sensitivity, and thereby help optimize devices like OPVs.

optical spot size can be used, which in turn permits the use of higher repetition rate laser sources. DLSRs will make common much smaller SXR focal spots, enabling the use of high repetition rate laser sources ideally matched to the bunch structure of synchrotron radiation facilities. Figure I.2.6 shows the scaling of the excitation laser energy with spot size. At spot sizes around one micron, current technology femtosecond oscillators operating at 1 GHz can deliver the required optical excitation density. Thus, one will be able to use the full repetition rate of the storage ring for time resolved experiments with low peak and high average flux.

Dynamics experiments performed at DLSRs will be complementary to those possible with HHG sources and FELs. However, DLSRs are unique because they offer a much higher average flux in the (soft) X-ray range as compared to HHG sources and a significantly higher repetition rate

(>100 MHz) than FELs, even those based on superconducting technology. This reduces the probability for unwanted multi-photon ionization events as well as challenges arising from sample perturbation from intense pulses and space charge in photoelectron spectroscopy experiments. It also significantly increases the achievable count rates in coincidence experiments, which are an important tool of chemical dynamics research.

Smaller focus sizes will also enable the X-ray based study of processes induced by multiple optical photons or higher laser harmonics at MHz repetition rates. This will enable, e.g., element-specific X-ray probing of laser plasmas and strong-field processes as well as pump-probe experiments with picosecond time resolution. X-rays focused to a few microns or even a few hundred nanometers allow selective probing of regions with different field strengths within the focus of a strong laser, thus reducing the effect of focal averaging.

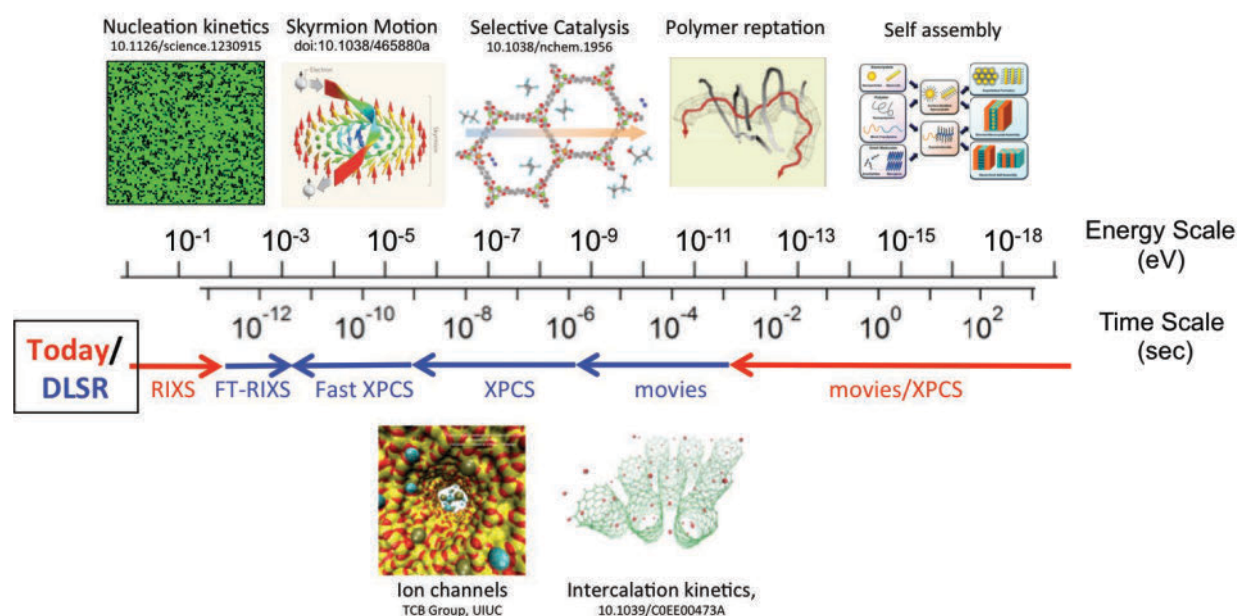


Figure I.2.7: Time/energy scales of some important spontaneous processes and temporal sensitivities for existing and proposed 4th Generation DLSR SXR sources using inelastic (e.g., RIXS) and quasielastic (e.g., XPCS) scattering in the energy and time domains, respectively. High brightness can be used to dramatically expand the temporal dynamic range over which such spontaneous processes can be measured. An aspirational goal is to connect the time/energy scales measured by RIXS and XPCS and most importantly to access energy scales well under $k_B T$ or time scales up to $h/k_B T$.

Spontaneous Processes

Many complex systems and phenomena are difficult to stimulate coherently and cannot be easily studied with pump-probe techniques. These include phase nucleation, chemical reaction-diffusion, polymer motion, drift and diffusion of electronic textures and domains, and many others that are crucial to functional materials and mesoscale structures. Just as high X-ray coherent flux can be leveraged with existing imaging techniques to probe heterogeneous (i.e., spatially incoherent) structures, it can also be leveraged to revolutionize our ability to measure spontaneous (i.e., temporally incoherent) processes (Figure I.2.7). Probing spontaneous

processes provided an important focus of the workshop and forms an important complement to the imaging and pump-probe tools discussed above.

Beyond serial imaging mentioned briefly above, statistical approaches to measure spontaneous processes can be borrowed from quasi-elastic and inelastic neutron and light scattering, which measure the dynamical structure factor $S(q,t)$ or its time Fourier transform $S(q,\omega)$. These functions can also be measured with X-ray scattering, in the time domain using XPCS (Figure I.2.8, right),¹⁸⁻²⁰ and in the energy domain using RIXS (Figure I.2.8, left).^{21,22} Though applied and analyzed differently, the two methods are fundamentally linked to the same process. For example, both are understood in terms of second order time dependent perturbation theory. As in quasi-elastic light or neutron scattering, XPCS is usually applied to low energy scale/long time scale processes and often probes over-damped modes, e.g., diffusion and polymer reptation. By contrast, as in inelastic neutron or Raman scattering, RIXS normally measures under-damped oscillatory modes, e.g. phonons and spin waves. In this way, RIXS and XPCS can in principle probe spontaneous kinetic and dynamic phenomena over a very broad time/energy range with nanoscale sensitivity (Figure I.2.7). Both also utilize SXR chemical, structural, and magnetic contrast discussed in previous sections. Neutron scattering relies primarily on isotopic contrast and rarely can be performed with a small beam to probe inside mesoscale structures.

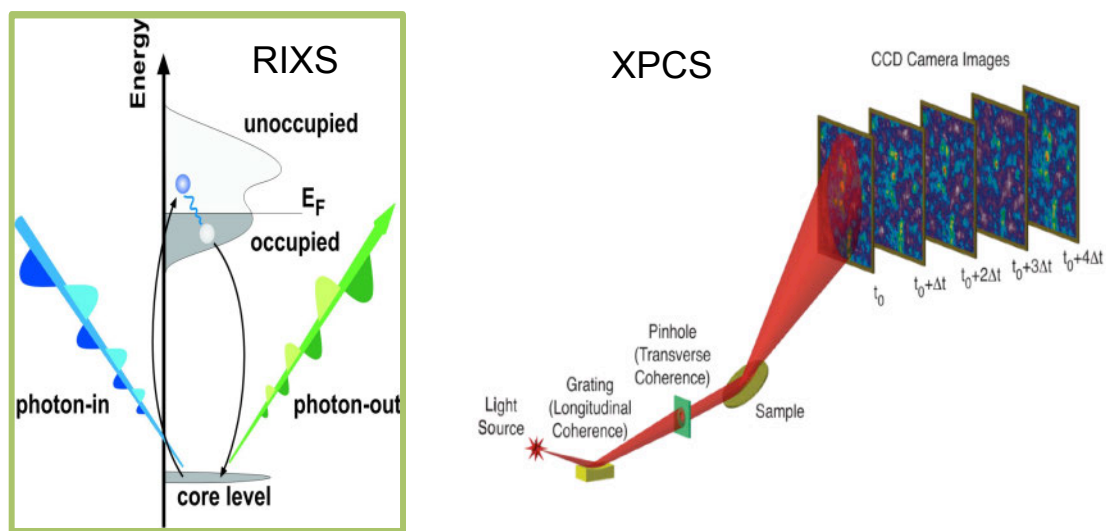


Figure I.2.8: Left: Schematic of a resonant inelastic scattering (RIXS) process, which is the X-ray analog of resonant Raman scattering. Core electrons absorb an incident SXR photon to make a virtual transition into unoccupied states involved in chemical bonding, magnetism, superconductivity, etc. In a coherent fashion, a valence electron decays into the core hole by emitting a second photon. The difference in photon energies (ω) and photon wave vectors (q) corresponds to the energy and momentum of an excitation in the material, which is measured through the dynamical structure factor $S(q,\omega)$. Right: Schematic of an X-ray photon correlation spectroscopy (XPCS) experiment, which is the X-ray analog of dynamic laser light scattering. A fluctuating sample is illuminated with a transversely coherent X-ray beam to produce a speckle pattern. Sample fluctuations at wave vector q are mapped into fluctuations in speckle pattern at a scattering wave vector also given by q . In the simplest implementation, the fluctuations in the scattered light are analyzed to determine the intermediate scattering function, $S(q,t)$, which is the Fourier transform of $S(q,\omega)$. $S(q,t)$ measures how quickly the structure of the system decorrelates at a length scale corresponding to $2\pi/q$.

To illustrate the unique power of the SXR RIXS/XPCS combination, note that $S(q, t)$ measures how quickly the structure of a system decorrelates at a length scale $2\pi/q$ (Figure I.2.8). This decorrelation might involve material diffusion, a chemical kinetic process, or motion of a magnetic texture. Any of these dynamic channels could be isolated in a mesoscale structure using a few-micron-sized SXR beam and by achieving the required contrast through an appropriately chosen photon energy. A similar statement applies to RIXS, though $S(q, \omega)$ is measured. Using the broad dynamic range offered by the combination of XPCS and RIXS, coupled reaction-diffusion systems could be studied with nanoscale sensitivity.

At present RIXS and XPCS are both challenging experiments, due primarily to low cross section and the desire to achieve high energy/time resolution. This leads to limited dynamic range for both methods roughly delineated by the red arrows in Figure I.2.7. Of particular interest, however, is to probe the $k_B T$ energy regime or the $\hbar/k_B T$ time regime (blue arrows in Fig. I.2.7) since these modes of the system are thermally activated and therefore are directly related to how a material functions. Probing spontaneous processes in this regime with SXR contrast would provide a truly revolutionary probe of material function.

What are the prospects for very high resolution SXR RIXS? Several RIXS beamlines and spectrographs under development around the world are designed to achieve an energy resolution ~ 15 meV at a photon energy of 1 keV, just barely below $k_B T$. To achieve even 1 meV resolution is impractical, both because the apparatus would be unmanageably large, but also simply because the signal would be so low that experiments would take an unmanageably long time. Workshop participants explored new concepts to improve the achievable energy resolution in RIXS. One possibility based on “double dispersion” in the sample and detector planes is shown in Figure I.2.9.²³ This promises a few-hundred-fold increase in data rate, which will address one limitation discussed above.

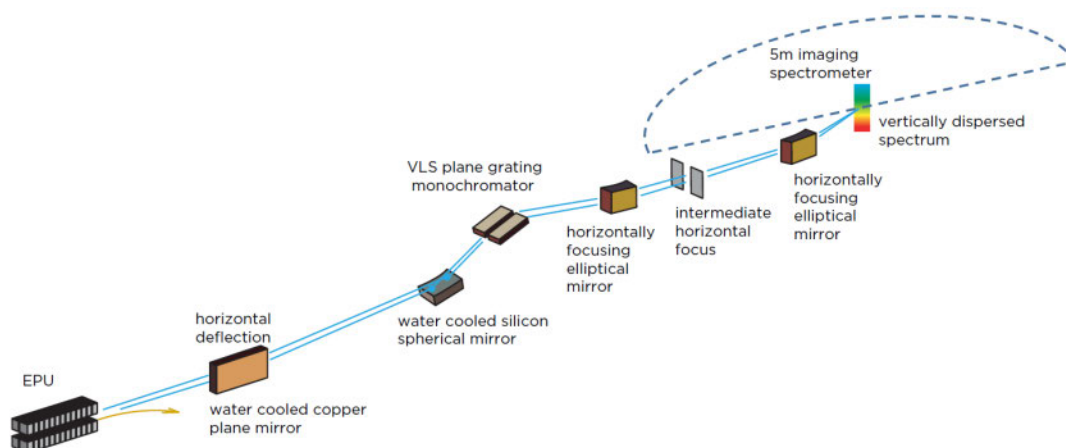


Figure I.2.9: Schematic of a double-dispersion RIXS beamline and apparatus. A broadband source is imaged and dispersed vertically on a sample, and a spectrograph is used to image and disperse the scattered light in the horizontal direction. The resulting RIXS map on the detector plots scattered intensity as a function of energy in and energy out and can be analyzed in various ways to achieve much higher throughput.²³

To achieve dramatic improvements in RIXS resolution beyond the above practical limits will require new thinking about revolutionary experimental approaches. There was much discussion of interferometric detection at the workshop, in many different contexts, but notably in Fourier Transform RIXS (called FT-RIXS in Figure I.2.7). This is very much an aspirational goal, but would provide resolving power in principle not limited by spectrograph size while potentially also providing large angular acceptance and so very good signal. One promising outcome of the workshop is that a few participants are already actively considering this idea. The most efficient approach to FT-RIXS will require coherent wave fronts and will therefore benefit directly from a DLSR source.

Achieving ps-scale time resolution XPCS presents at least equally daunting challenges as sub-meV resolution SXR RIXS. XPCS essentially measures the distribution of delayed coincidences in a single speckle at wave vector q . This distribution is related to the temporal autocorrelation function of the coherently scattered intensity, which in turn is related to $S(q,t)$. Measuring coincidences means that the XPCS temporal resolution scales as the square of the coherent flux, and a 100-1000x increase in source brightness will allow much faster processes to be measured than is presently possible and thereby revolutionize XPCS.

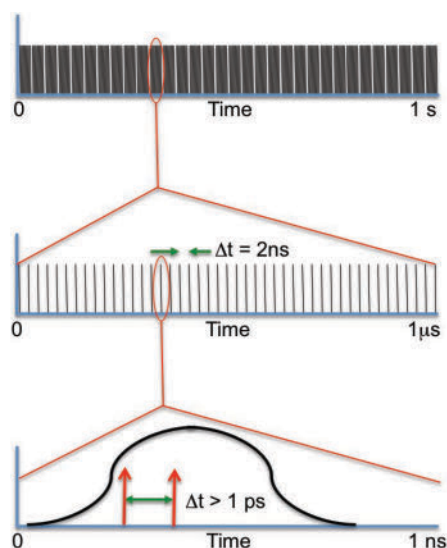


Figure I.2.10: Schematic of a typical storage ring pulse time structure and how this will impact faster XPCS measurements. Top: At scales longer than $\sim 1 \mu\text{s}$, a storage ring can be considered to be essentially CW. The time structure can be ignored or normalized in XPCS. Middle: Between the pulse period of $\sim 1 \text{ ns}$ and the ring cycle frequency of $\sim 1 \mu\text{s}$, the pulsed nature of the source needs to be explicitly utilized in XPCS by measuring the number of photons arriving in each pulse. Bottom: Between $\sim 1 \text{ ps}$ and the pulse width of $\sim 100 \text{ ps}$, an XPCS experiment will need to find and measure rare events where two photons are scattered into a single speckle from a single storage ring pulse. Note that there is a region of time delay that cannot be measured with XPCS between the pulse width and pulse period.

Figure I.2.10 shows schematically the time structure of a storage ring, which consists typically of 50-100 ps pulses at a few 100 MHz repetition rate. There are three conceptually different approaches to use this time structure to accomplish an XPCS experiment. In almost all experiments done to date, at both SXR and HXR energy, the source is treated essentially as continuous (Figure I.2.10, top panel). In this case all time scales down to a fraction of the pulse period, say $1 \mu\text{s}$, can in principle be measured if a detector with adequate bandwidth is available and if there is enough signal in a single speckle to allow measurement within a reasonable amount of time. To date such measurements are generally limited to $\sim 1 \text{ msec}$ time scales, but the quadratic dependence on source brightness mentioned above suggests that SXR DLSR sources will easily extend this to the sub- μs regime. As discussed in several sections of this

report, this will be a very important achievement in measuring chemical and material kinetics with nanoscale sensitivity, but still lies very far from the $h/k_B T$ times scale discussed above.

Measuring much faster than microsecond time scales will require that the pulsed nature of the source be taken into account (Figure I.2.10, middle panel). Conceptually the simplest detection scheme will simply stamp each pulse from the storage ring with 1 or 0, depending on whether a photon was detected in a given speckle. A fast 2D detector with the highest possible quantum efficiency would be needed to cover this range of q -space. Such detectors very nearly exist for the SXR regime, where microchannel plate electron multipliers can have high efficiency and are well suited for individual photon detection. Binning and normalizing delayed coincidences would produce the desired correlation to measure $S(q,t)$ with nanosecond resolution, thereby extending kinetic studies by nearly three orders of magnitude over the CW approach discussed above – but still not approaching the $h/k_B T$ time scale.

As with FT-RIXS, accessing the $h/k_B T$ time scale with XPCS is another aspirational goal that will require a revolutionary approach in which delayed coincidences inside a single storage ring pulse and a single speckle will need to be measured (Figure I.2.10, bottom panel). At the workshop there was discussion of accomplishing this with high time-resolution, high quantum efficiency, SXR streak camera framed at the storage ring radio frequency. A nice benefit of seeking delayed coincidences inside storage ring pulses is that the signal-to-noise increases by the inverse of the ring duty cycle, or by an additional order of magnitude beyond the quadratic dependence on brightness. This comes from the higher peak current in a pulse relative to the average ring current, coupled to the quadratic scaling mentioned above.

References: Section I

1. M. Eriksson and J. F. van der Veen, *Journal of Synchrotron Radiation* **21**, 1 (2014).
2. M. Gabay and J.-M. Triscone, *Nat Phys* **9** (10), 610-611 (2013).
3. A. Ohtomo and H. Y. Hwang, *Nature* **427** (6973), 423-426 (2004).
4. J. A. Bert, B. Kalisky, C. Bell, M. Kim, Y. Hikita, H. Y. Hwang and K. A. Moler, *Nat Phys* **7** (10), 767-771 (2011).
5. S. Gariglio, N. Reyren, A. D. Caviglia and J.-M. Triscone, *J. Phys.: Cond. Mat.* **21**, 164213 (2009).
6. D. Einfeld, M. Plesko and J. Schaper, *J. Synchrotron Rad.* (2014). **21**, 856-861 **14**, 856 (2015).
7. M. R. Howells, T. Beetz, H. N. Chapman, C. Cui, J. M. Holton, C. J. Jacobsen, J. Kirz, E. Lima, S. Marchesini, H. Miao, D. Sayre, D. A. Shapiro, J. C. H. Spence and D. Starodub, *Journal of Electron Spectroscopy and Related Phenomena* **170** (1-3), 4-12 (2009).
8. E. de Smit, I. Swart, J. F. Creemer, G. H. Hovelings, M. K. Gilles, T. Tylliszczak, P. J. Kooyman, H. W. Zandbergen, C. Morin, B. M. Weckhuysen and F. M. F. de Groot, *Nature* **456**, 222 (2008).
9. E. Rotenberg and A. Bostwick, *J. Synchrotron Rad.* **21**, 1048 (2014).
10. S. Eisebitt, J. Luning, W. F. Schlotter, M. Lorgen, O. Hellwig, W. Eberhardt and J. Stohr, *Nature* **432** (7019), 885-888 (2004).
11. B. Pfau and S. Eisebitt, in *Synchrotron Light Sources and Free-Electron Lasers*, edited by E. Jaeschke, S. Khan, R. Schneider and J. B. Hastings (Springer, Berlin, 2015).
12. K. A. Nugent, *Advances in Physics* **59**, 1 (2010).
13. H. M. Quinney, *Journal of Modern Optics* **56**, 1109 (2010).
14. R. Falcone, C. Jacobsen, J. Kirz, S. Marchesini, D. Shapiro and J. C. H. Spence, *Contemporary Physics* **52**, 293 (2011).
15. J. M. Rodenburg, A. C. Hurst, A. Cullis, G., B. R. Dobson, F. Pfeiffer, O. Bunk, C. David, K. Jefimovs and I. Johnson, *Phys. Rev. Lett.* **98**, 034801 (2007).
16. D. A. Shapiro, Y.-S. Yu, T. Tylliszczak, J. Cabana, R. Celestre, W. Chao, K. Kaznatcheev, A. L. D. Kilcoyne, F. Maia, S. Marchesini, Y. S. Meng, T. Warwick, L. L. Yang and H. A. Padmore, *Nat Photon* **8** (10), 765-769 (2014).
17. E. Malmerberg, C. A. Kerfeld and P. H. Zwart, *IUCrJ* **2**, 309 (2015).
18. M. Sutton, *Comptes Rendus Physics* **9**, 657 (2008).
19. M. Sutton, in *Third Generation Hard X-ray Sources*, edited by D. M. Mills (John Wiley, New York, 2002), pp. 101-124.
20. G. Grübel, A. Madsen and A. Robert, in *Soft-Matter Characterization* edited by B. Borsali and R. Pecora (Springer, Berlin, 2008), Vol. 1.
21. T. Schmitt, F. M. F. de Groot and J.-E. Rubensson, *J. Synchrotron Rad.* **21**, 1065 (2014).
22. L. J. P. Ament, M. van Veenendaal, T. P. Devereaux, J. P. Hill and J. van den Brink, *Reviews of Modern Physics* **83** (2), 705-767 (2011).
23. T. Warwick, Y.-D. Chuang, D. L. Voronov and H. A. Padmore, *J. Synch. Rad* **21**, 736 (2014).

II. Enabling Directed Chemistry at the Nanoscale

Thermally driven chemical processes tend to achieve low overall efficiency. Heterogeneous catalysts, for example, are normally optimized by trial and error, deploying multiple catalytic centers and additives into diverse nanostructured support materials. Often, however, only modest selectivity is achieved, which requires energy intensive purification. Even for many small molecule catalytic transformations, our abilities fall far short of biological systems: consider for example the difficulty of developing artificial photosynthesis technologies to produce solar fuels. An added complication is that ‘efficiency’ needs to be broadly interpreted. Energy efficiency is an obvious goal in any energy conversion or storage device. Similarly, an increasingly important goal in industrial catalysis is to achieve highly selective chemical synthesis using earth-abundant materials under mild conditions with high overall energy efficiency. We cannot at present design such catalytic systems from first principles.

Diverse chemical processes, e.g., electro- and photocatalysis, batteries and fuel cells, material self-assembly, and reactions in environmental systems and aerosol particles, occur on complex multidimensional free energy landscapes that govern correlated atomic and molecular motion over multiple length and time scales. Controlling incoherently-driven thermal processes on such a landscape presents a difficult inverse problem: how do we tailor a nanoscale structure to produce a desired energy landscape that supports a targeted chemical behavior? The combined spatial and temporal sensitivities of emerging SXR tools that will be able to answer this question were a major focus of the workshop.

At the heart of this challenge is the notion of “connecting scales”, which was a crosscutting theme of the workshop and is the focus of the next chapter. For example, chemical dynamics often focuses on ultrafast molecular-scale motion near saddle points of the above energy landscapes that are associated with breaking and making chemical bonds. Achieving efficient catalysis requires that these dynamical events be efficiently connected to kinetic events operating on more extended length and time scales. Leaving aside the issue of handling vastly different time scales, we might aim to make a ‘movie’ that stitches together thermally driven kinetic and dynamical events. But chemical kinetics are intrinsically statistical with many nearly degenerate paths contributing to a given chemical process, so a few such movies will provide a rather incomplete description. We need tools that provide statistical kinetic information on the nanometer length scale, and to work closely with theory and modeling efforts to connect kinetic information to ultrafast molecular dynamics - a challenging multiscale experimental and modeling effort.

Before examining a few classes of systems where directed chemistry is an important goal, we summarize a few crosscutting themes and associated experimental needs:

- Many such systems involve complicated reaction-diffusion processes, often in nanoscale confined spaces. Good examples are selective ion transport in nanoporous membranes used in most electrochemical systems, adsorption/absorption/reaction processes in colloids and aerosols, precipitation/dissolution in geochemical systems, and 3D self assembly of functional mesoscale structures. An important experimental need is chemically sensitive probing of nanoscale reaction diffusion processes. Ultrahigh

brightness SXR sources enable XPCS and RIXS techniques that will have major impact in this area in the time and energy domain, respectively.

- Many such chemical systems derive their functionality from ill-defined interphase regions. Good examples include the solid-electrolyte interphase, the chemically active interphase between an aerosol and its environment, and the selvage region between reacting nanomaterials. A prime goal of ultrabright SXR sources is to enable 3D chemical maps with few-nanometer resolution – in radiation hard materials. In some cases it will be possible to make a 2D image at 10 nm resolution with a single pulse of SXRs from the storage ring, thereby providing fast movies and tomographic reconstructions to examine these interphase regions in unprecedented detail.
- These systems often involve complicated correlations that operate over broad spatial and temporal scales. Multiple catalytic centers in a metal-organic framework compound might be located with the right spatial relationship to accomplish a concerted reaction. A nanoporous material can be functionalized in a particular way to achieve selective transport rivaling that of biological systems. Spatial correlations might be designed into a solid electrolyte interphase region to reduce dendrite formation or to facilitate ion charging/discharging. Scattering measurement directly probe spatial correlations, and high coherence enables XPCS and RIXS experiments that will probe how these spatial correlations evolve in time/energy with high chemical sensitivity.

The following chapters examine five areas where high brightness SXR beams will transform our ability to observe and ultimately control chemistry at the nanoscale. These examples are not intended to be exhaustive, but they do illustrate the impact of the crosscutting issues and capabilities discussed above.

II.1: Bridging Scales in Chemical and Material Dynamics

Contributions from Brian Stephenson, Oleg Shpyrko, Nora Berah, Daniel Rolles, Alexander Föhlisch, Fulvio Parmigiani, Markus Guehr, Oliver Gessner, Harald Ade, Sujoy Roy, Alex Hexemer

Many molecules have the ability to selectively and efficiently convert sunlight into other forms of energy like heat and electric current, or to store it in chemical bonds. Reactions triggered by optical photons from the sun power nearly all biological functions, either directly or indirectly. Similarly, as discussed in chapter II.3, artificial photosynthesis is a key technology on the path to clean and renewable energy. Since light is not selective concerning the energy conversion, the absorbing molecules or materials must provide this property. X-ray studies will continue to have a major impact on our understanding of these processes and to develop predictive power so that new and improved functionality can be achieved.

These energy conversion processes generally involve broad spatial and temporal scales. Molecular scale photoabsorption results in excited valence electrons, and the changed forces between the nuclei result in highly coupled ultrafast dynamics of nuclei and valence electrons in which the initial photon energy becomes transferred into other degrees of freedom just femtoseconds to picoseconds after photoexcitation. However intermediate states are stabilized by reaction barriers and exhibit lifetimes on the picosecond and longer time scales. Photogenerated charge drifts and diffuses through a complex energy landscape for which the key processes occur from nanoseconds to microseconds or even longer.

Understanding heterogeneous dynamical processes like these will be revolutionary since function is related to non-adiabatic coupling between different scales, whether at a conical intersection in a unimolecular reaction, electron-phonon and electron-spin interactions relevant to conventional and unconventional superconductivity, or interfacial electron transport and exciton dissociation in organic semiconductors. A primary goal of chemical and material dynamics and kinetics is to understand this flow of energy, charge, and mass on the most fundamental level while addressing systems ranging in complexity from the single-atom or molecule limit of gas phase targets to clusters and ensembles of solvated and surface-bound molecules to candidate photovoltaic/photocatalytic materials. This breadth of challenges requires a multifaceted approach in which both time- and energy-domain techniques are deployed to explore ground and excited state potential energy surfaces, molecular transformations and relaxation dynamics, as well as charge- and energy-transfer across molecular and interfacial boundaries.

Probing these optically excited states with X-rays opens new routes to understand chemical processes on the level of single atoms and electrons. Using x-ray absorption, emission or photoelectron spectroscopy provides element selectivity and site sensitivity, site specificity, and chemical sensitivity. DLSRs will offer currently unavailable access to complex electronic structures and coupled electronic/nuclear dynamics by combining high repetition rate, high average power x-ray flux, high spatial coherence, and small source size. Photon-hungry techniques such as RIXS, COLTRIMS, and time-resolved XPS can be exploited to their full potential. These types of measurement schemes are particularly well suited for photoelectron spectroscopy, where low single pulse photoelectron yields allows high resolution with a high average photoelectron yields. The small source/focus sizes will enable optical/x-ray multi-color

pump-probe experiments at storage-ring pulse repetition rates using readily available laser systems (see chapter I.2). The high spatial coherence will give rise to entirely new experimental techniques based on the translation of interferometric spectroscopy techniques from the visible and UV into the x-ray regime.

These ideas about bridging scales in chemical dynamics and kinetics apply to many classes of materials and candidate technologies:

- ***Dye-sensitized solar cells:*** an ultrafast photoabsorption event occurs in a surface-bound molecule or cluster is followed by interfacial charge transfer to and transport through a mesostructured host
- ***Organic photovoltaics:*** ultrafast exciton generation in a chromophore is followed by exciton hopping and interfacial dissociation in a material with designed heterogeneity
- ***Organometal perovskite photovoltaics:*** in this rapidly developing class of materials, local photoexcitation is (apparently) followed by transfer to electron and hole bands and surprisingly efficient transport.
- ***Transport and phase behaviors in transition metal oxides:*** many transition metal oxides also exhibit unusual transport and phase behaviors which may be related to intrinsic heterogeneity often observed in these systems.

In this chapter we describe these challenges across several classes of materials. These formed a major focus of discussion during several different breakout sessions in the workshop. The material in this chapter pertains directly to the complementarity between DLSR and FEL capabilities and science, and correspondingly there is a strong overlap between these two communities in this area. We return to this issue at the end of this chapter.

A. RIXS Maps of Ultrafast Dynamics on Molecular Potential Energy Surfaces

DLSRs will facilitate widespread implementation of highly differential, photon-hungry techniques such as RIXS for chemical dynamics studies. RIXS with vibrational resolution allows mapping of the potential energy surfaces of both the ground and excited states of gas and condensed phase systems from an element specific perspective.¹⁻⁵ The vibrational progression of the ground state monitors the development of the vibrational wave packet in the intermediate state and allows for an accurate determination of its potential energy surface and lifetime (Figure II.1.1). Since the bandwidth of the scattered radiation is conserved, sub-natural linewidth detection is feasible.

The presently developing complete description of RIXS processes in simple molecules will significantly enhance the applicability of RIXS to probe molecular materials and liquids. High-quality gas-phase results will give important contributions to the long-lasting debate about the interpretation of liquid water spectra. As has been demonstrated for liquid acetone.³ RIXS spectra associated with vibrational excitations in the electronic ground state do not suffer from broadening due to the environment that may affect experiments employing ionization or electronic excitations. In combination with the characteristic element specificity of x-ray

transitions, this facilitates a detailed mapping of the local electronic ground state potential energy surface from the perspective of well-defined reporter atoms. The sensitivity to symmetry furthermore makes RIXS sensitive to dynamic “symmetry breaking”. When vibronic coupling during the scattering process lowers the symmetry of the electronic wave function, lines appear that are forbidden in the symmetric case. Minute geometrical changes proceeding on (sub-) femtosecond timescales can thus be observed in the spectra.

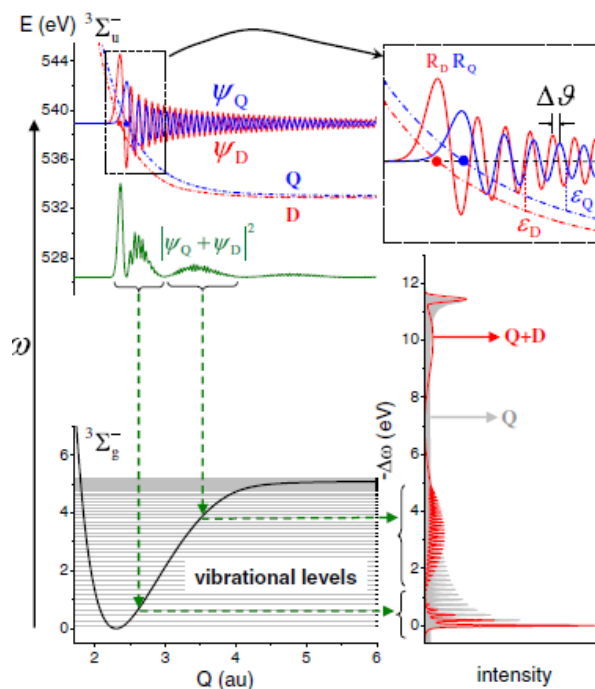


Figure II.1.1: Spatial quantum beats in vibrational resonant inelastic SXR scattering at dissociating states of Oxygen. Mapping of extended potential energy surfaces around selected atomic centers.³

The application of RIXS to liquids, wet systems and systems with high vapor pressure opens a wealth of opportunities for chemical and material dynamics studies. Prospects include *in situ* studies of catalytic and electrochemical processes pertinent e.g., to the development of solar photovoltaics and fuel cells, novel battery technologies, and a deeper understanding of corrosion. Moreover, application of RIXS to solutions promises access to processes of importance in pharmaceuticals and biochemistry.

B. Local Landscapes in Photochemistry: Intramolecular and Interfacial Charge Transfer

Charge transfer mechanisms are key in many areas of science and technology and occur across various length scales in molecules, solids and biological systems. A powerful methodology to measure and understand these processes is through optical pump/x-ray probe experiments in which the charge creation and migration is initiated by an optical pump pulse and the evolving electronic and chemical landscape is probed by a time-delayed x-ray pulse. These

techniques will be significantly enhanced by the routine availability of micron-sized and smaller focal spots at DLSR sources (see chapter I.2).

For gas phase targets, powerful ion-ion and electron-ion coincidence techniques (e.g. COLTRIMS) have been developed, which are capable of differentiating between reaction *pathways* even if their average final product *distributions* may be indistinguishable. The complete kinematic mapping of unimolecular reactions can give access to femtosecond temporal information even when using picosecond X-ray pulses. DLSRs will facilitate the efficient combination of these powerful techniques with multi-color schemes in order to initiate and probe unimolecular transformations and intramolecular charge transfer dynamics at unprecedented levels of detail.

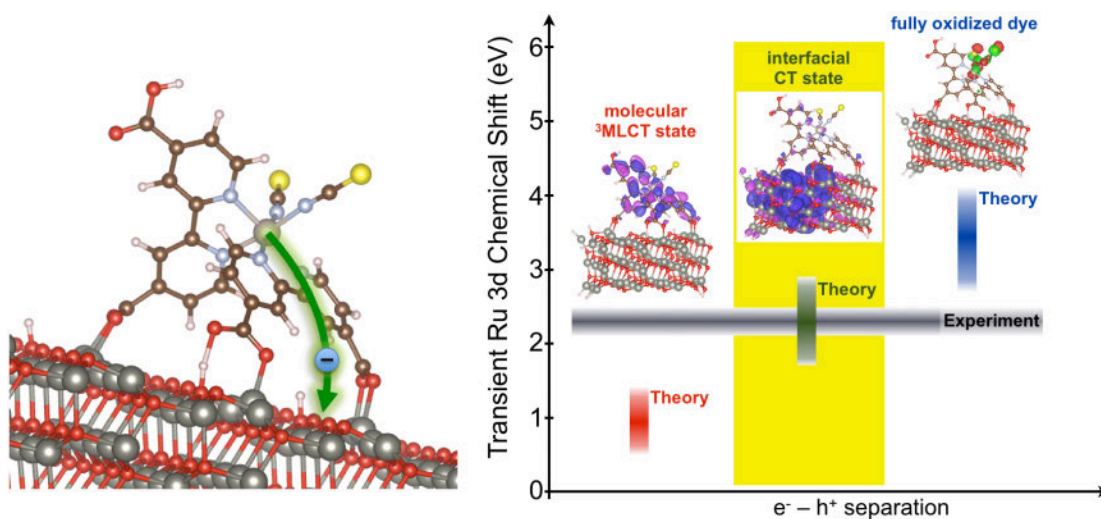


Figure. II.1.2: Interfacial charge transfer between ruthenium-based N3 dye molecules and a film of ZnO nanoparticles probed by time-resolved XPS.⁶ Left: schematic of the calculated adsorption geometry and the charge transfer process upon photoexcitation. Right: Calculated electronic configurations for three limiting cases of transient electron–hole states and associated ranges of expected Ru 3d core level binding energy shifts. The gray band represents the experimentally determined shift of $\Delta E_b = (2.3 \pm 0.2)$ eV at a delay of 500 fs after photoexcitation of the dye. While femtosecond studies are performed at the LCLS, the lower pulse energy and higher repetition rate of a DLSR offers important advantages to study systems like this in the picosecond domain with high sensitivity to local chemical and band structural dynamics.

Many emerging energy conversion technologies and atmospheric processes relevant to climate change are based on charge transfer processes in heterogeneous systems such as surface-bound or solvated molecules. Time-domain x-ray probing of optically induced processes has been demonstrated to provide new insight into interfacial charge transfer and chemical dynamics in these systems beyond the scope of traditional laser based techniques (Figure II.1.2). The high repetition rate, moderate peak power conditions at DLSRs in combination with small focus sizes are ideally suited to exploit the full potential of these novel experimental concepts. In particular, the quasi-CW characteristics of DLSRs facilitate the *simultaneous* x-ray probing of charge-transfer and chemical processes across time scales ranging from picoseconds to seconds. By combining these unique time-domain capabilities with *in operando*

x-ray spectroscopy techniques, real-time access to chemical reaction dynamics in operating electrochemical devices will be achieved.

C. Charge Generation and Transport in Complex Soft and Hard Matter

There are significant challenges to understand the limits of transport of charge in complex soft and hard matter systems. For example, electronic and structural disorder in blends of organic semiconductors on the ~10-100 nm length scale are critical to the efficient operation in energy conversion devices, such as photovoltaics and thermoelectrics, and for energy efficient light emitting diodes (Figure II.1.3). In addition to disorder, excitonic and biexciton carriers may form, thereby preventing facile measurement of the charge carrier concentration in many cases. However, because charge carriers in organic materials are usually polaronic, the electronic structure of the material is perturbed by the presence of the carrier leading to observable features in x-ray absorption spectra at the C, N, O or S edges, which present an opportunity to use SXR methods to uncover critical features in soft materials related to their electrical properties.

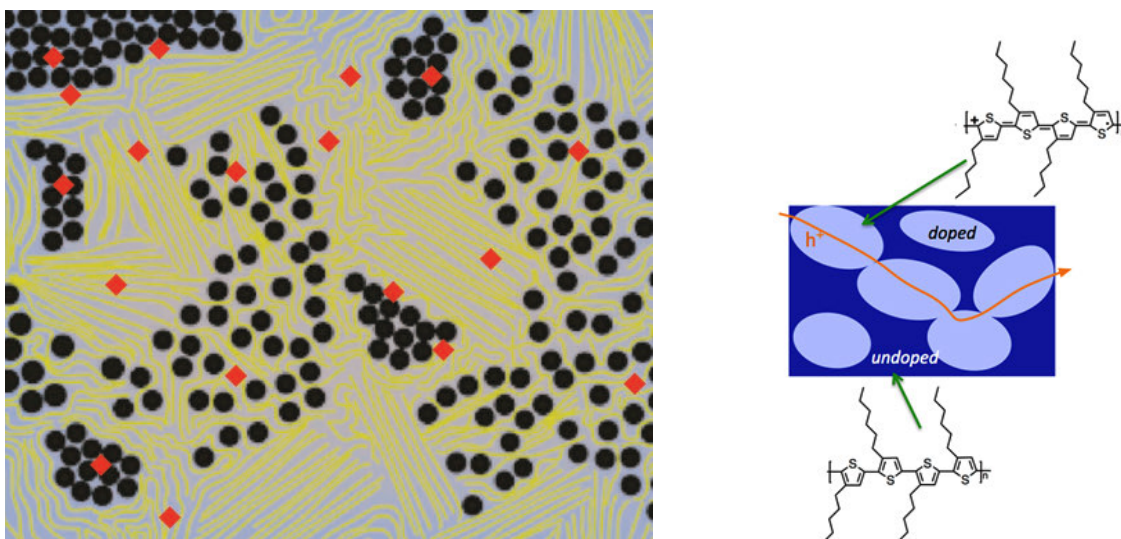


Figure II.1.3: Left: Schematic of electron donor (yellow) and acceptor (black) materials in an organic photovoltaic device with a complex structural and electronic landscape. Right: An OPV may comprise a percolation network of heavily doped and less doped regions. Resonant soft x-ray scattering and spectroscopy methods provide the necessary spectral contrast to reveal the spatial distribution of carriers in these domains. The high coherent flux available with a DLSR will push these measurements into the time domain with advanced pump-probe and XPCS techniques, which will be able to probe the nanoscale diffusive motion of charges, excitons, and bi-excitons between on this complex landscape.

The issue of complex electrical transport extends to many other classes of materials: dye-sensitized solar cells, emerging hybrid systems such as organometal halides, and many transition metal oxides where polaronic transport and heterogeneous phase behaviors are common. Organometal halide perovskites comprise inorganic layers separated by organic cations and exhibit significant molecular mobility due to vacancies in the lattice. These materials exhibit exceptional optoelectronic and photovoltaic performance. Using DLSR

sources, it will be possible to examine the motion of molecular species, e.g., methyl ammonium, using SXR energies specific to low Z species.

In many correlated electronic and magnetic materials, electronic, spin, orbital or chemical orders are intrinsically coupled, resulting in a variety of emergent phenomena, such as superconductivity, magnetism, metal-insulator transition, ferroelectricity, orbital ordering etc. These orders are often accompanied by nano- and meso-scale phase heterogeneity, for example in $(V_{1-x}Cr_x)_2O_3$ near its metal insulator transition (Figure II.1.4).⁷ Such heterogeneity is observed in many oxide materials and complicates of emergent electronic transport phenomena, magnetic and orbital phase properties, etc.

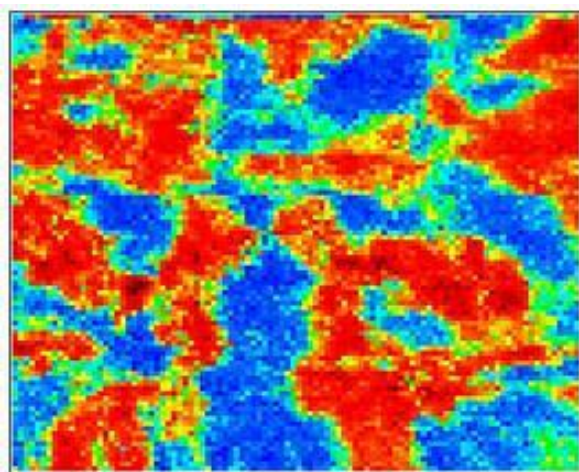


Figure II.1.4: Chromium doped vanadium sesquioxide, $(V_{1-x}Cr_x)_2O_3$, is the prototype system to study electronic correlation and associated Mott transitions. Temperature, doping or pressure are used to induce a metal-to-insulator transition (MIT) between a paramagnetic metal (PM) and a paramagnetic insulator (PI). In the phase diagram of $(V_{1-x}Cr_x)_2O_3$, a Cr concentration of $x=0.011$ makes it possible to cross the transition between the PI (red) and PM (blue) phases only by changing the temperature between 320 and 200 K explored using photoelectron microscopy (PEEM).⁷ Advanced imaging techniques on a SXR DLSRs will allow much higher spatial resolution and diverse spectral contrast mechanisms to probe complex electronic textures like this. Moreover, advanced XPCS and RIXS techniques described in Chapter I.2 will probe charge and spin transport in complex landscapes that are commonly observed in transition metal oxides.

The high coherence of DLSR sources will be used to address chemical, electronic, and spin transport, in systems ranging from organic photovoltaics to batteries to complex oxides, with simultaneous spatial and temporal sensitivity. This is particularly important in studying the heterogeneous systems discussed in this chapter since we need tools to track fsec-psec dynamics that occur on the scale of atoms and molecules to slower dynamic and kinetic processes like charge transport and trapping, exciton dissociation, and polaronic hopping that occur on a landscape that is structured on a scale from a few to a few hundred nanometers.

SXR sources offer resonant spectroscopies to probe a variety of atomic-scale degrees of freedom, but which can also provide contrast for scattering and/or microscopy techniques to probe nanoscale phase behaviors. The nature of the nanoscale domains, their fluctuations in

soft and hard systems, and transport of charge and spin can be probed by a combination of SXR nanoimaging techniques, XPCS in the time domain, and RIXS in the frequency domain.

For example, the characteristic excitation energy scale associated with stripe fluctuations cuprate superconductors is expected to be at the sub-10 meV level. Extending resonant XPCS temporal resolution to nanosecond, and perhaps even picosecond timescales and the RIXS energy resolution to well under 1 meV (see Chapter I.2) offer promising pathways for understanding the structure and dynamics of charged stripes in cuprates as well as their role in superconducting phase stability and their collective excitations. This process can obviously be extended to Goldstone modes in charge- or spin-density wave systems, Dirac excitations, dynamics of superconducting vortices, Kondo resonances, orbitons, and beyond.

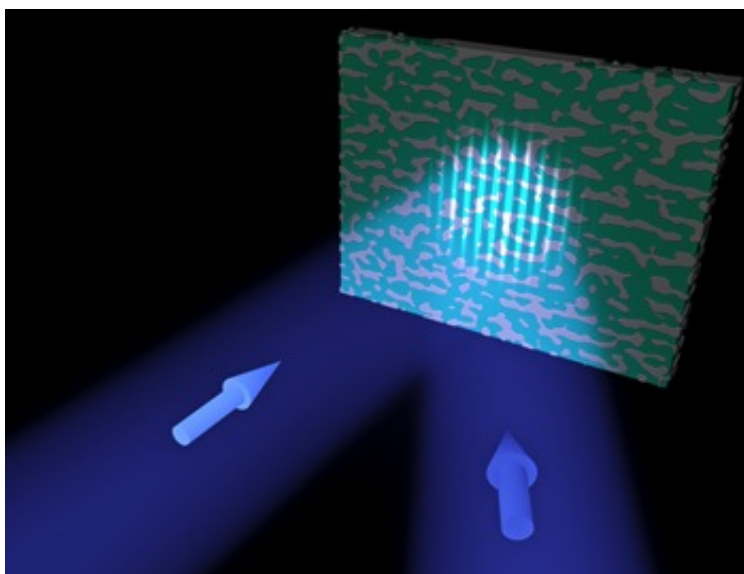


Figure II.1.5: Interference of two coherence X-ray beams to create a charge carrier grating inside a thin organic photovoltaic material.

An additional important goal is to connect the structural heterogeneity with the diffusive motion of charge carriers and spins, since this pertains directly to function. An aspirational way to accomplish this would be to perform a SXR transient grating experiment. Using a transversely coherent SXR source from a DLSR, the beam can be split and interfered at a specific angle to create an interference pattern at the sample, as shown in Fig. II.1.5. In areas of constructive interference charge carriers will be excited and form a 1D lattice. Due to the wavelength of the X-rays the periodicity of the interference pattern will be on the nanometer scale. Hence, the charge carriers are created in a regular lattice with nm pitch. By simply removing the first X-ray beam, the second beam can be used to perform transient grating experiment with resonant SXR scattering. By scanning the energy of the X-rays precisely and observing the decay of Bragg peak intensity, a detailed NEXAFS spectrum of the excited charge carriers can be obtained. Furthermore, the decay in the resulting Bragg peaks will be a direct measure of the diffusion and decay of the charges. The technique should be universal to a large variety of soft and hard materials.

A different approach using XPCS would allow studying diffusive motion of charged carriers and their statistical spatial distribution *at steady state*. In this case, the sample would be illuminated with continuous visible/UV light above the band gap energy to produce a steady state population of carriers. The motion of these excited carriers could then be probed with SXR XPCS or with high resolution RIXS. Crucially, as with the transient grating experiment discussed above, this experiment would provide nanoscale resolution and thereby would transform our ability to probe transport in heterogeneous landscapes.

D. Complementarity of FEL and DLSR Science Opportunities

The discussion in the previous sections provides a good way to think about the complementarity between DLSR and FEL science. Understanding and controlling the dynamics of photoexcitation, for example, will benefit from FELs in the ultrafast time domain, where a popular goal is to map charge and nuclear motion through a conical intersection. This is intrinsically dynamical: one can write down a time-dependent Hamiltonian and have some hope of solving it to deduce a real space trajectory. By contrast, kinetic motion on a complex energy landscape, e.g. in an OPV or a complex oxide, will ultimately need to be coarse-grained, parameterized, and treated statistically to model macroscopic function on longer time scales. Measuring statistical quantities like spectral functions with ARPES, dynamical structure factors with RIXS and XPCS, and space-time correlation functions with transient grating experiments and time-resolved microscopy provide robust, statistical approaches to connect experiment to theory on the relevant spatial and temporal scales. Just as experiments using FELs are very good at measuring dynamical events, experiments using DLSRs will be very good at measuring these statistical behaviors. The spectroscopic and spatiotemporal sensitivity of SXRs will benefit both kinds of study, and indeed will be crucial in drawing connections between them. Connecting the regimes of molecular- and unit cell-scale dynamics to few-nanometer-scale statistical kinetics is a tremendously important goal in diverse contexts that will require both kinds of facilities, and also provides an important focus in many of the following chapters.

II.2: Enabling Designed Catalysts

Contributions from Lou Terminello, Wolfgang Eberhardt, Jose Rodriguez, Maya Kiskinova, Jesper Andersen, Miquel Salmeron, Jinghua Guo, Selim Alaygolu, Hendrik Bluhm

Heterogeneous chemical reactions drive the majority of interfacial processes in industrial catalysis, alternative energy production, environmental and atmospheric science and geochemistry. It has been a long-standing goal - in particular in technical applications - to arrive at rational designs of more efficient catalysts instead of the currently used trial and error approach to optimization. At the industrial scale, a small increase in synthetic efficiency and selectivity translates into a large financial benefit. Moreover, the chemical industry relies heavily for starting products on non-renewal resources, and an additional goal is to develop approaches based on lower-value starting materials.

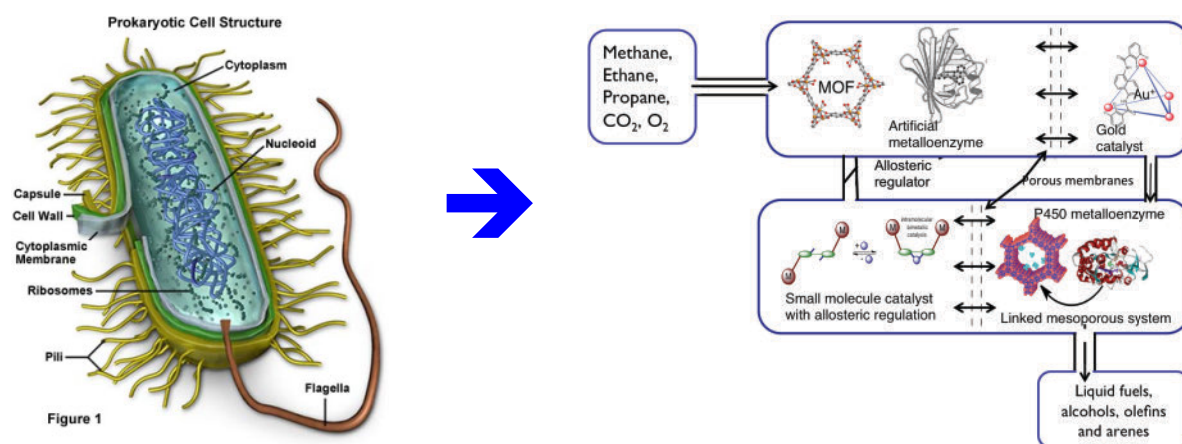


Figure II.2.1: An aspirational goal in catalysis is to mimic cellular biosynthesis in designed mesoscale reactors. These would convert low value starting materials, including biomass and biogas, to high value products with the high efficiency and selectivity and under moderate conditions. The synthesis would be energy efficient and high selectivity would eliminate much of the complication of separating chemically similar products. The notional catalytic network on the right deploys concepts familiar in cellular biosynthesis – compartmentalization, regulation, feedback, etc. [figure courtesy of John Hartwig, UC Berkeley]

Figure II.2.1 offers a conceptual target catalytic device, a “catalytic network”, which is motivated by this kind of thinking. This is inspired by cellular biosynthesis and will function under similarly moderate and tightly controlled conditions. It deploys a mesoscale, compartmentalized reactor and integrates feedback and regulation of the various steps in a synthetic reaction. As discussed in chapter I.1, such a device assembles a free energy landscape to control chemical kinetics to channel reactants to desired products under thermal stimulation. Accomplishing this level of control in a catalytic synthesis will entail a multi-decade effort and will require a basic understanding of the fundamental chemical reactions at interfaces under operating conditions, on the molecular level and at relevant time and length scales, to ultimately reveal which factors increase the selectivity and yield in a catalytic reaction. Higher selectivity means less waste products and thus more energy efficient and environmentally compatible processes in the production of fine chemicals, fuels, and other high value products. Such a catalytic reactor will

challenge our ability to distinguish reductionism from emergence (see Fig. I.1.1), since the goal is to rationally assemble subunits to achieve an emergent functionality.

The characteristics of SXR DLSRs enable new classes of experiments that are hitherto not feasible and which will provide the combined spatial temporal, and spectral sensitivities needed to study the properties of functioning catalysts and of ensembles of catalytic centers, an example of which is provided by the catalytic networks discussed above.

A. Imaging Functioning Catalysts

Figure I.2.2 from the introductory section of the report illustrates the power of a STXM to make chemical maps of a functioning nanoparticle catalyst. DLSR sources will enormously enhance spatial, spectral, and temporal sensitivities of SXR spectromicroscopies and will be a key feature in emerging efforts to design catalytic structures with optimum activity and selectivity. Figure II.2.2 shows two recent examples of synthetic structures that exhibit much enhanced activity for electrocatalytic reduction of oxygen and the catalytic reduction of CO to ethanol. The images were produced using electron microscopes, and so offer excellent spatial resolution but lack chemical contrast. SXR ptychography will change that, by offering nearly the same spatial resolution with full chemical contrast – and enough signal to make movies as the catalyst functions. An important limit in these imaging experiments will be sample damage, which can be a serious issue especially in aqueous environments.

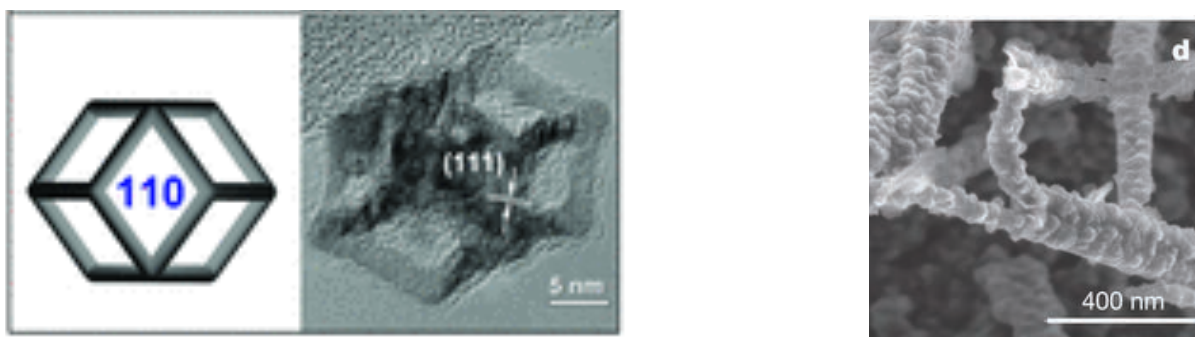


Figure II.2.2: Left: Crystalline Pt₃Ni nanoframes achieved a factor of 36 enhancement in mass activity and a factor of 22 enhancement in specific activity, respectively, for the were provided for oxygen reduction reaction relative to state-of-the-art platinum-carbon catalysts.⁸ Right: Nanocrystalline Cu prepared from Cu₂O produces multi-carbon oxygenates (ethanol, acetate and n-propanol) with up to 57% Faraday efficiency.⁹

B. Catalytic Correlations in Nanoporous Materials

A major initiative in areas of catalysis, energy, and environmental sciences is to understand chemical kinetics when molecules interact in confined geometries, for example, in nanoporous materials, in nanoscale cracks in minerals, and in complex interphase regions. In particular, recent developments in the synthesis of hybrid materials have resulted in new classes of nanoporous materials whose properties can be tailored for high and highly selective catalytic activity. Fig. II.2.3 shows two exemplary nanoporous structures: a zeolyte and a metal-organic framework (MOF). An important promise of these structures is that the inner surfaces can in

principle be physically and chemically tailored, e.g., the pore shape and size to control diffusion and the spatial distribution of accessible catalytic centers to optimize absorption isotherms and to direct catalytic selectivity. The goal is to enable design of highly selective, highly efficient “flow-through nanoreactors” operating at modest temperature. This is a second bio-inspired approach that would truly revolutionize the heterogeneous catalysis industry.

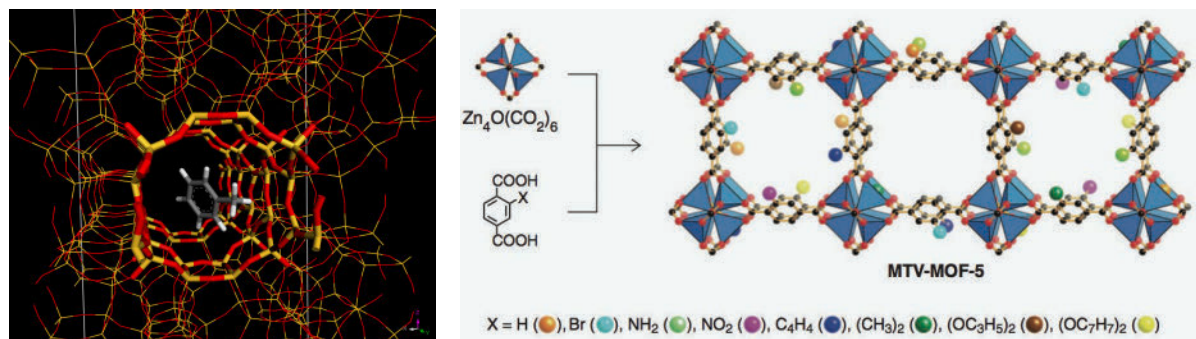


Figure II.2.3: examples of functionalized nanoporous materials for selective catalysis. Left - The most stable configuration of toluene adsorbed in a BEA-zeolite pore (<http://accelrys.com/products/materials-studio/quantum-and-catalysis-software.html>). Right: Multivariate metal-organic framework compound with designed distribution of metal centers.¹⁰

The static structure of these designed nanoporous systems is routinely measured in diverse environments with small angle x-ray scattering and x-ray diffraction, and macroscale kinetic measurements can be accomplished, for example, with infrared spectroscopy, mass spectroscopy, and other techniques. The crucial missing capability would combine these structural and kinetic sensitivities to probe the nanoscale spatial correlations between the atoms/ions/catalytic centers on the inner surfaces of the pores and the resulting catalytic activity. Again, this is a clear example of how DLSRs will allow us to measure a chemical (free energy) landscape and measure a thermally-driven chemical process on that landscape.

There are many ways to measure catalytic kinetics, but few of them provide the nanometer spatial sensitivity needed to probe kinetic correlations in space and time. X-ray scattering measures nanoscale spatial correlations directly, the high coherent flux from a diffraction limited storage ring enables XPCS to probe how those correlations evolve in time, and finally SXR provide the requisite chemical contrast to probe with high selectivity the different catalytic sites and species. Modern sample environments allow such SXR measurements to be performed at elevated temperature, at pressures well above atmosphere, and in solution. Emerging designs will enable studies of catalytic systems in even more robust environments.

A schematic of the experiment is shown in Fig. II.2.4. A beam of coherent x-rays tuned to an energy that provides contrast to a particular chemical species or functionality scatters off the functioning nanoporous sample and produces a speckle pattern in the far field.^{11, 12} For a static sample the speckle pattern remains constant and hence any two speckle patterns collected at two different times are fully correlated with each other. Any changes in the spatial configuration of the selected chemical species – through diffusion or chemical reaction - will result in a

different speckle pattern, and the patterns decorrelate. By measuring the decorrelation time at different wave vectors we obtain the intermediate scattering function $S((q, t))$. The use of X-rays provides tremendous advantage over dynamic laser light scattering because it allows probing kinetic events on a much smaller length scales and additionally, by using resonant edges, one can observe element-specific speckles and hence perform element specific dynamics studies. It will be an important challenge to model these structure factors to extract more traditional chemical kinetic mechanisms, rate constants, etc.

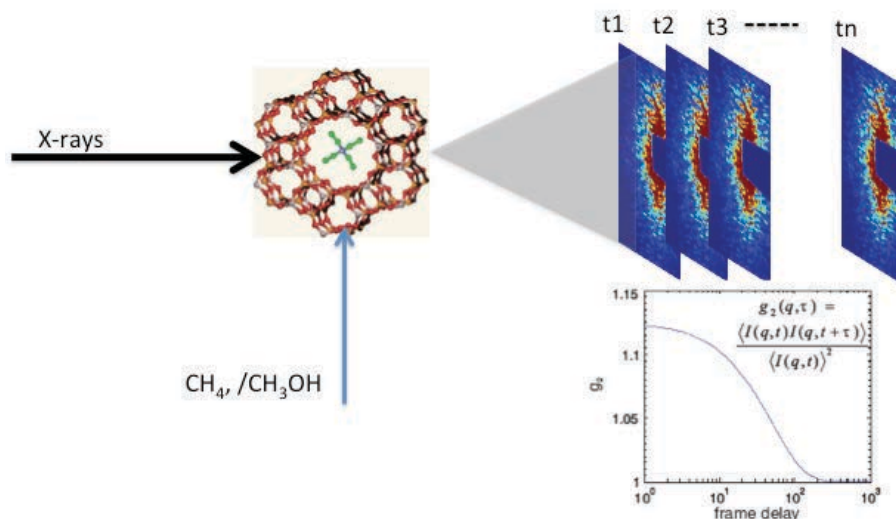


Figure II.2.4: Experimental set up for performing XPCS experiment on zeolite. Methane or methanol will be introduced onto a zeolite sample. Speckle pattern due to scattering of x-rays will be captured onto a CCD detector. Analysis of speckle pattern yield autocorrelation curves, shown on the right hand side corner.

C. Spatiotemporal Pattern Formation in Catalytic Systems

Imaging surfaces and interfaces with structural and chemical specificity is essential for understanding a variety of dynamic phenomena. Spontaneous formation of periodic and quasiperiodic patterns reflects nature's tendency towards order, controlled by cooperation or in some cases competition between both energetic and kinetic factors. In a wide range of magnetic and electrostatic systems, for example, the formation of quasi-equilibrium striped or labyrinthine patterns is driven by a balance or competition between short-range forces like the exchange interaction and long-range dipolar or strain fields. Heterogeneous catalytic systems have been found to exhibit a rich variety of nonlinear activities including reaction rate oscillations and spatiotemporal pattern formation. This was first observed in the oxidation of CO on Pt(110) using photoelectron microscopy (PEEM) or low energy electron microscopy (LEEM) over 20 years ago (Figure II.2.5).¹³ This and related systems have been heavily studied and modelled, both with reaction-diffusion kinetic models and with Monte Carlo simulations. These studies provide useful models for how to control a catalytic reaction, e.g., the circular reaction fronts in Figure II.2.5 can be transformed to spirals and other more turbulent structures by varying reaction conditions.

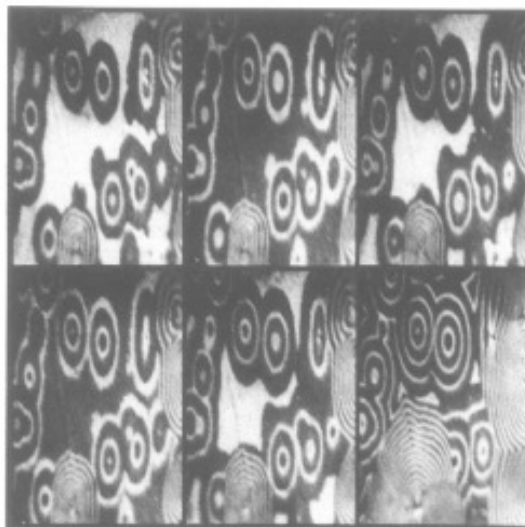


Figure II.2.5: A series of PEEM images revealing spatio-temporal pattern formation during CO oxidation on Pt(110), reflecting highly nonlinear reaction-diffusion kinetics in this fairly simple catalytic system.¹³

Surprisingly, similar nonlinear behaviors are often observed in catalytic reactors as well, even with nanostructured catalysts for which different parts are not in close physical contact, indicating important roles of thermal diffusion or fluid flow and diffusion.¹⁴ Even individual nanoparticles exhibit oscillations in catalytic activity; these are often not well understood but presumably involve structural or compositional rearrangements.

Much of the work discussed above was accomplished with PEEM and LEEM, tools that offer limited chemical contrast and moreover are most applicable to flat, nominally homogeneous surfaces. The mechanisms of these spatio-temporal self-organization phenomena, driven by the interplay between energetics and kinetics, opens a conceptually novel route to creating and/or utilizing a wide range of surface-supported functional structures at the micro- and nanometer length scales, provided we can overcome the micro-spectroscopy limits to understand how the local chemistry within the structures changes dynamically. Since fluctuations play an important role in the formation and dynamical evolution of these patterns, detailed characterization probes must be capable of accessing, in-situ, a wide range of length scales and time scales.

Nanoscale imaging with SXR spectroscopic contrast will provide these capabilities, and high source brightness of DLSR sources will enable simultaneous study of kinetic processes. A particularly interesting possibility will be to measure pattern formation in 3D, for example, in patterned mesoscale structure or in a hybrid catalytic system like one of the functionalized nanoporous materials discussed above. This might be possible in real space using tomographic microscopy, but a better way to measure kinetics would be the chemical XPCS experiment described in the previous section.

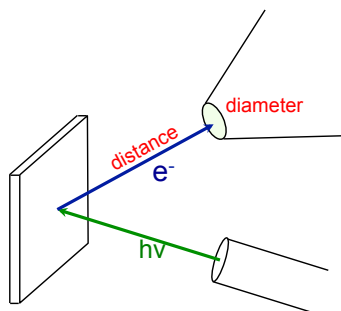


Figure II.2.6: Sample environment in an APXPS experiment.

Photoelectron spectroscopy at atmospheric pressures

Ambient pressure photoelectron spectroscopy has made enormous strides over the last 15 years, after the introduction of synchrotron-based APXPS at the ALS.^{15, 16} The number of instruments installed at synchrotrons around the world has sharply increased and so have the publications and the reach of APXPS experiments to research areas beyond classical surface science. One outstanding goal of the technical development of this spectroscopy is to finally be able to perform experiments at truly ambient conditions, i.e. 1 atmosphere. The pressure limit depends on the chemical composition of the gas or gas mixture and the partial pressures, the photon flux, kinetic energy as well as the distance that the electrons have to travel until entering the low-pressure region behind a differentially-pumped aperture (Figure II.2.6) In many cases the kinetic energy is chosen close to the minimum of the mean free path curve for maximum surface sensitivity, though this is often not ideal in APXPS since gas phase scattering is generally large there. The absolute pressure limit is thus determined by the distance that the electrons travel on their way to the differentially pumped aperture. This distance cannot be reduced beyond a certain limit; due to the pressure drop the sample has to be kept at a distance of about two aperture diameters to maintain equilibrium pressure conditions at the sample surface (Fig II.2.6). For optimum measurement conditions the incident X-ray spot should match the sample aperture size, and it is thus the focusing properties of the beamline that limit the maximum pressure in the experiment: Small beam spots allow the use of small apertures, facilitating small sample-to-aperture distances, this concurrently reduces the electron scattering and thus ultimately allows for an increase in the pressure limit. The high brightness of DLSR sources will make focal spot sizes under 10 μm diameter routine.

II.3 Optimizing Functional Energy Materials

Contributions from Wolfgang Eberhardt, Lou Terminello, Harald Ade, Gary Rumbles, Maya Kiskinova, Andrea Goldoni, Nenad Markovic, George Crabtree, Tony van Buuren, Miquel Salmeron, William Chueh, Jinghua Guo, Wanli Yang, David Shapiro

Worldwide the demands for energy are increasing, driven by the growth of the world population and the increase in the standard of living, mostly in non-OECD countries. The world population has doubled in the last 40 years and will continue to grow by another 50% by the year 2050. Over the same past 40 years the energy demand has increased by a factor of 2.5 and this has largely been met by an increase in the use of fossil energy resources. This has already caused significant increases in pollution and is leading us on a path toward world-wide climate change caused by the increase in the amount of greenhouse gases in the atmosphere. Moreover, there is a serious concern about being dependent of foreign sources for energy and - associated with this - a large cash flow into countries, which at least in some cases support terrorism.

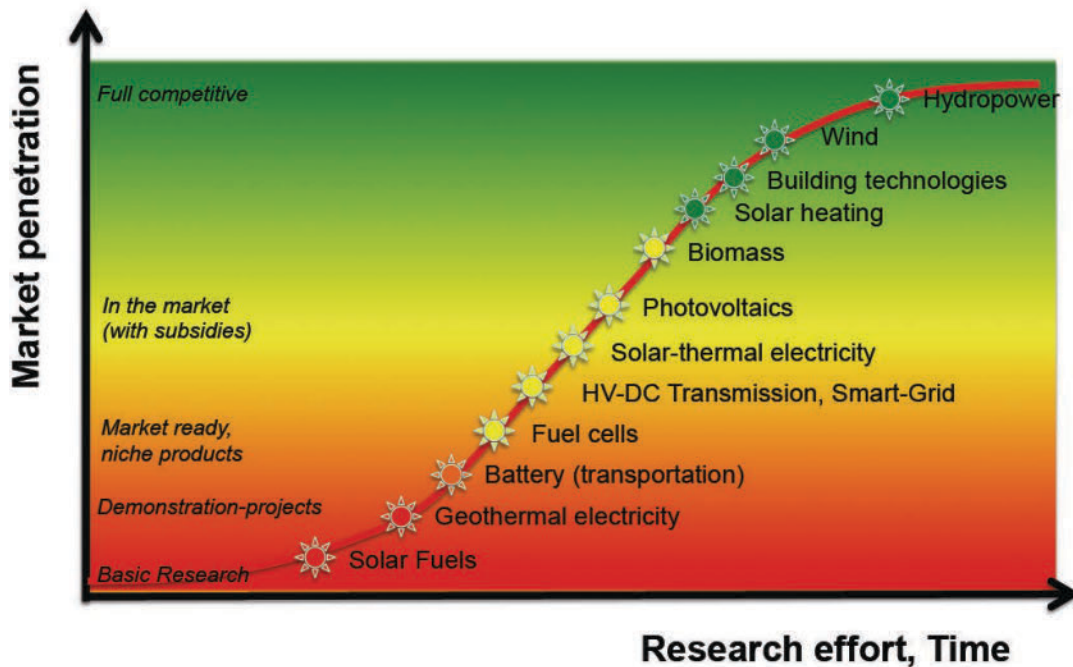


Figure II.3.1. Market penetration and estimated state of research and development for several essential energy technologies required for building an energy system based upon renewable energy.¹⁷

Worldwide the recognition has matured that we cannot continue along the established path forever and that we will need to rebuild our energy supply system. Additionally, several accidents in nuclear power plants and concerns about handling and long-term storage of nuclear waste, have increased the acceptance threshold for nuclear power as an alternate energy technology significantly over the last decades. On the positive side, all estimates¹⁸ point to the fact, that in the long term it will be possible to support the world's entire energy demand by using renewable sources, not only for the electric power supply, but also for transportation and heating/cooling of buildings as well as industrial demands. Rebuilding our energy system is a large challenge and requires a large effort for any country and society. The reward for the

countries that engage in or even lead that transition however will not only be realized at home, but also create a global economic opportunity.

As spelled out already several years ago by a BESAC report¹⁹ the energy system of the future will be based on three essential components. First, we will generate electricity without generating CO₂, and second, we will change the transportation and where not possible (aircraft, ships) provide fuels for transportation generated without increasing the overall CO₂ balance. In addition, increasing the energy efficiency at all levels will be an essential component that facilitates the transition.

Materials research is at the heart of research and development for energy technologies of the future. This includes both the development of novel materials and also the control and improvement of processes in materials production. Being able to characterize the electronic properties, structure and composition of any material even under in-situ/operational conditions will create many opportunities for advances in existing and new technologies. The energy system of the future will encompass many different components and technologies. In order to give an impression of the breadth of the field, the present state of development of several, but by no means all, essential technologies is roughly estimated by the graphical representation shown in Figure II.3.1.

In all these areas advances, enabled by materials research, are always welcome and possible. However, technologies near the bottom of this graph are closer to basic research and new materials discoveries are certainly very likely in this area. This includes for example thermoelectric materials and devices, which are not even shown in this graph. These convert heat directly into electricity. Here new quantum materials might lead to a significant improvement. Thin film solar cells, which are available in the market, present a large potential for innovation by improving the production technology and processes. A large solar panel manufacturing plant produces more than a square mile of panel area every year. The mass production methods do not reach the same performance levels as demonstrated in the laboratory prototypes and any improvement here will result in an enormous economic benefit.

Other technologies, such as fuel cells, are available for smaller market segments (submarines, buses). Full scale implementation to impact the main stream of individual passenger transportation or to balance loads on the electrical grid, requires that the noble metal based catalysts in the PEM fuels cells have to be replaced by more common materials, or at least the amount of catalyst required has to be drastically reduced.

Already at present synchrotron radiation is a highly valued tool for the study of materials and processes at the atomic scale. The significant increase in spectral and spatial resolution offered by a diffraction limited synchrotron light source in combination with the opportunity of studying heterogeneous materials under operational conditions or to follow individual production steps and processes in situ will be an invaluable asset for the technological advances required to meet the challenge of building the energy system of the future. In the following pages some examples are discussed in more depth.

A. Photocatalysis and Solar Fuel Production

The direct conversion of sunlight into energy stored in chemical bonds, termed artificial photosynthesis, mimics the natural photosynthesis process occurring in plants (Figure II.3.2). The overall process consists of two parts: light absorption and generation of excited charge carriers, and the utilization of photo-excited carriers to drive catalytic reactions. The former process typically uses semiconductors to absorb photons and generate carriers, which are subsequently separated at either a semiconductor/electrolyte interface or an embedded solid junction. The photo-generated carriers subsequently move to a catalytic center to drive oxidation/reduction reactions in the solution.^{20, 21} An integrated photocatalysis system spans from nanoscale building blocks to microscopic dimensions and always has inherent heterogeneity, whether it is the individual building block level or the individual interface level.

For the practical production of solar fuels, high solar-to-fuel conversion efficiency is necessary. The thermodynamic potential needed to drive the reaction is greater than 1.0 V, and an electrochemical overpotential must be overcome to achieve a high reaction rate. In analogy to natural photosynthesis, a dual light-absorber approach has been proposed in which separate semiconductor materials harness different portions of the solar spectrum. One semiconductor acts as a photocathode for reduction, while the other acts as a photoanode for oxidation. In these electrodes, photo-excited minority carriers move to the solution for a catalytic reaction, while majority carriers recombine at the interface connecting these light absorbers (Figure II.3.2(c)).

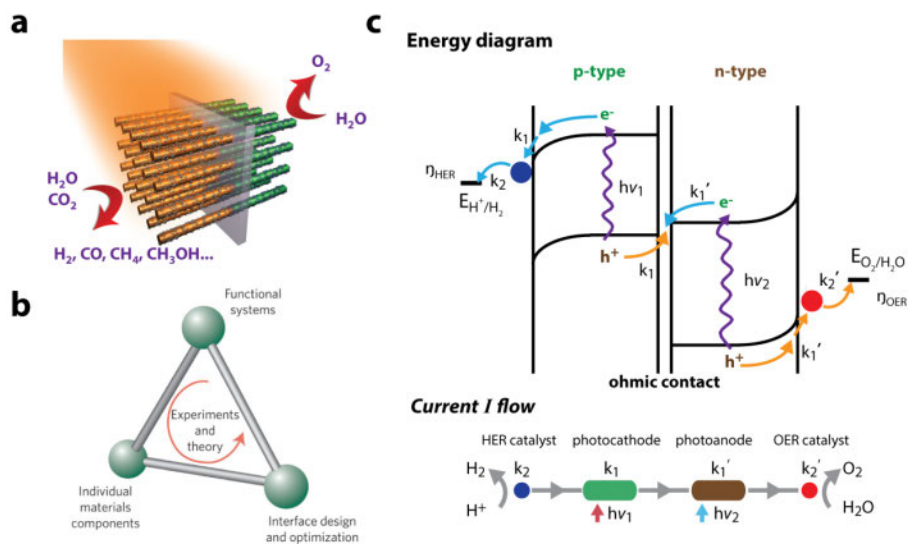


Figure II.3.2: Semiconductor nanowires for artificial photosynthesis. A schematic standalone device based on nanowires is shown in (a), which captures many of the features in natural photosynthesis. Its energy diagram under “Z-scheme” is depicted in (c), using water splitting as an example. In an ideal situation, the flux of charge carriers at different components, including the photocurrent from light absorbers (k_1 , k_1') and the TOF from electrocatalysts (k_2 , k_2'), should be comparable to ensure maximum efficiency. Because of the interrelated nature of the components in artificial photosynthesis, a system-level consideration is needed to consider the balances among the various components, and further device optimization should be based on such consideration (b).

In this approach, there are two major issues that need to be addressed that pertain to matching the flux through the different parts of a photocatalysis system:

- matching the flux between current-generating light-absorbers and the current-consuming electrocatalysts, *i.e.*, is the electrocatalyst capable of handling the chemical reactions efficiently and selectively under the flux of photo-excited carriers?
- matching the flux between different light absorbers, *i.e.*, could both the photoanode and photocathode provide the necessary photocurrent flux for practical applications, while maintaining a desirable voltage output?

These two questions are currently not fully answered, and the deployment of nanomaterials and nanostructures will contribute to tackling these issues in a variety of ways if the right experimental tools are available to help the optimization process.

Currently many studies on these active interfaces are based on ensemble measurement, but given the importance of nanoscale light harvesting and catalytic centers is crucial to study these systems microscopically at the single nanowire or nanoparticle level. For example, recent variants of SXR XAS, RIXS, and APXPS allows study of solid-liquid interfaces, and these techniques are providing important information to understand interfacial processes in catalysis in general and photocatalysis specifically. Of particular importance is developing advanced nanostructured electrocatalysts, especially for the oxygen evolution and CO₂ reduction reactions, and to study the interface between nanoscale electrocatalysts and light-absorbing semiconductors, which can present bottlenecks and increase overpotential. A DLSR opens the possibility of doing these experiments with sub 100-nm focused x-ray beam so that phenomena like these can be probed with valuable chemical contrast.

B. Interfaces and Microscopic Ion Diffusion of Energy Storage

Energy storage is a critical but weak link in the chain of renewable energy development to curb CO₂ emission. Developing high-efficiency, cost effective and sustainable energy storage devices has become one of the key challenges to allow broad deployment of technologies ranging from plug-in electric vehicles (EVs) to load balancing the electric grid, with projected market expansion of ten times in this decade. Today, lithium-ion battery technology remains a promising candidate for safe, low-cost, rechargeable, high-capacity and high-power energy storage solutions. However, the technology level is well below what is required to meet the need of this new phase of mid- to large-scale energy storage applications.²²

The formidable challenge of developing high performance battery system stems from the complication of battery operations, both mechanically and electronically (Figure II.3.5). Almost all Li-ion batteries operate beyond the thermodynamic stability of electrolyte.²³ Electronically, a stringent requirement of a stable, electron-insulating but ion-conductive solid-electrolyte-interphase (SEI) on the surface of battery electrodes is necessary to produce a functional battery cell. Inside the electrodes, Li-ion batteries operate with evolving electronic states. The dynamics are triggered by the transportation of the charges, including electrons and ions during the charging and discharging processes. This motion of charges, especially the diffusion of Li-ions, fundamentally regulates the functionality of batteries. At present, extensive efforts have

focused on discovering new electrode materials and enhancing mechanical properties. The effect of charge diffusion on the evolution of electronic states in battery compounds, including electrodes, electrolyte, and their interphases, remains elusive and largely unexplored. The high coherent SXR flux at DLSR sources will enable unprecedented spectroscopic probes with much-improved spatial, energy and temporal resolution. This is precisely what is needed to reveal the complex dynamics in batteries through both *ex-situ* and *in-situ* experiments. Below we focus on the benefits studying the aforementioned two critical elements in batteries, i.e., the SEI and the charge diffusion.

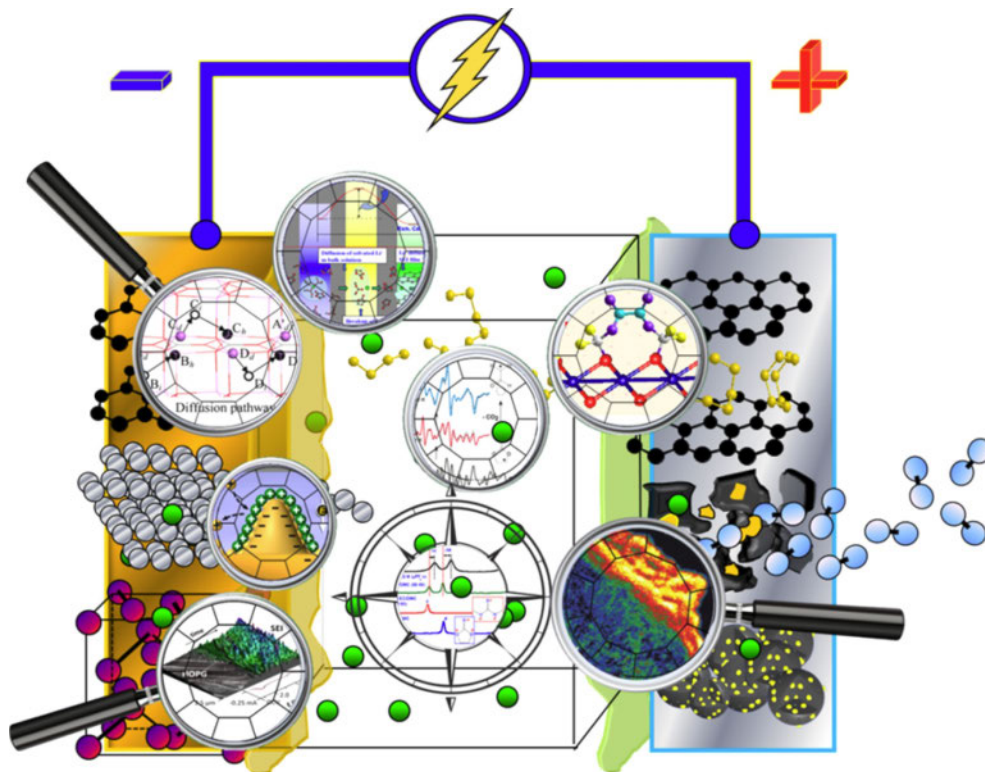


Figure II.3.5: Batteries are complex systems and their operations involve the formation of SEI and the multi-step charge transportation process, which are largely unexplored due to the spatial and temporal limitations of current experimental probes.²⁴

Solid-electrolyte-interphase (SEI)

Thermodynamically, the Li-ion battery operates far beyond the thermodynamic stability of the electrolyte. Fortunately, interphases known as SEIs form *in situ* on electrode surfaces from sacrificial decomposition (reduction) of electrolytes (Figure II.3.6). The SEI plays a double role in battery performance.²⁵ On one hand, the SEI blocks electron transport, thereby preventing parasitic reductions/oxidations on the reactive electrode surfaces, and transports Li^+ ions from the electrolyte into the electrode, thereby supporting the reversible (de)lithiation process.²⁶ On the other hand, because SEI formation is associated with the irreversible consumption of both the charge carrier and the electrolyte, this process is detrimental to the specific energy and cost

of the cell. Moreover, the SEI places restrictions on energy and power densities of the device by impeding Li⁺-transport and setting operating voltage limits.²⁷ Research activities aimed at controlling the chemistry of the SEI formation are arguably the most critical topic for maintaining the lifetime of commercial batteries.

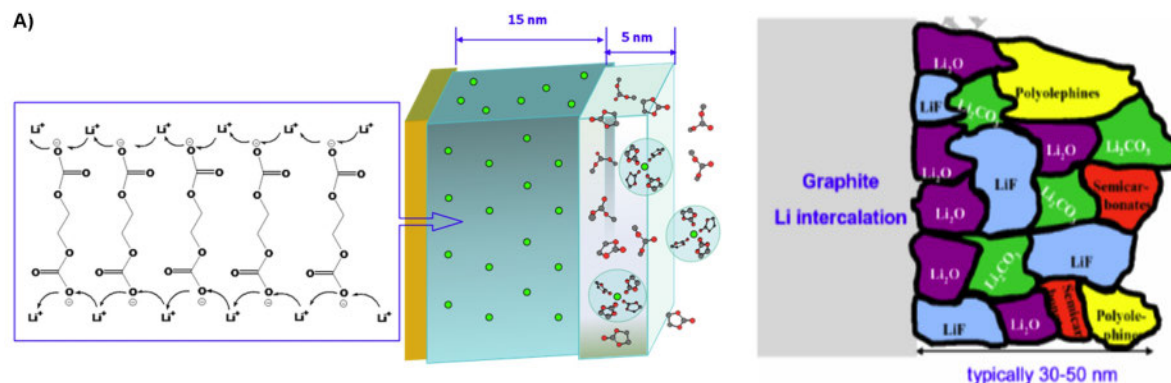


Figure II.3.6: (A) A proposed mechanism of ion transportation through SEIs on the battery anode surface.²⁸ (B) An “oversimplified” schematic of the chemical compositions of SEI on graphite anode.²⁵ Testing the SEI functionality requires chemical sensitivity, nanometer spatial resolution, as well as *in-situ* and *operando* sample environment.

Many crucial questions about how the SEI functions (and fails) remain unanswered. For example, what causes SEI failure, both chemically and mechanically, at the molecular level? What are the factors that control the charge diffusion through the SEI? How is the SEI formed? How does the SEI change during operation of the cell and with changes in temperature, voltage, and charge-discharge rates? How are the electrical properties related to SEI composition? How does Li⁺ diffuse through the SEI? And of course, lying at the center of all these questions is the key issue on how to tailor the SEI with desired properties so that it stabilizes the electrode surfaces but does not decrease the battery performance.²⁵ In general, the number of academic scientific studies/publications related to this topic is rather limited as compared with the actual scale of interest by the industry. With our current level of understanding, SEI films generally derive their stability from empirically discovered chemical additives, whose identities are commercial secrets.²⁹

The technical challenges to studying SEI stem from the stringent requirements on spatial, spectral, and temporal resolution, as well as the fact that SEI formation can be affected by a range of parameters: surface area, surface morphology, and surface chemical composition. The thickness of SEI formed on a graphite anode is believed to be around 20-50 nm.²⁵ Studying the mechanism and clarifying the mystery of SEI functionality require incisive tools that are capable to probe this dynamic process with nanometer spatial resolution under *in-situ/operando* conditions. In the past decade the value of SXR spectroscopy in detecting the chemical reaction products in the SEI has been demonstrated.³⁰ Several recent findings have revealed that the formation of SEI strongly depends on the surface properties of the electrodes³¹ and, *vice versa*, the formation of SEI strongly affects the electrode surface property.³² Recent instrumentation developments have enabled *in-situ* and *operando* SXR spectroscopic studies of various electrochemical devices. Figure II.3.7 shows one of the X-ray absorption spectroscopy (XAS) experiments of Mg batteries under *operando* conditions.

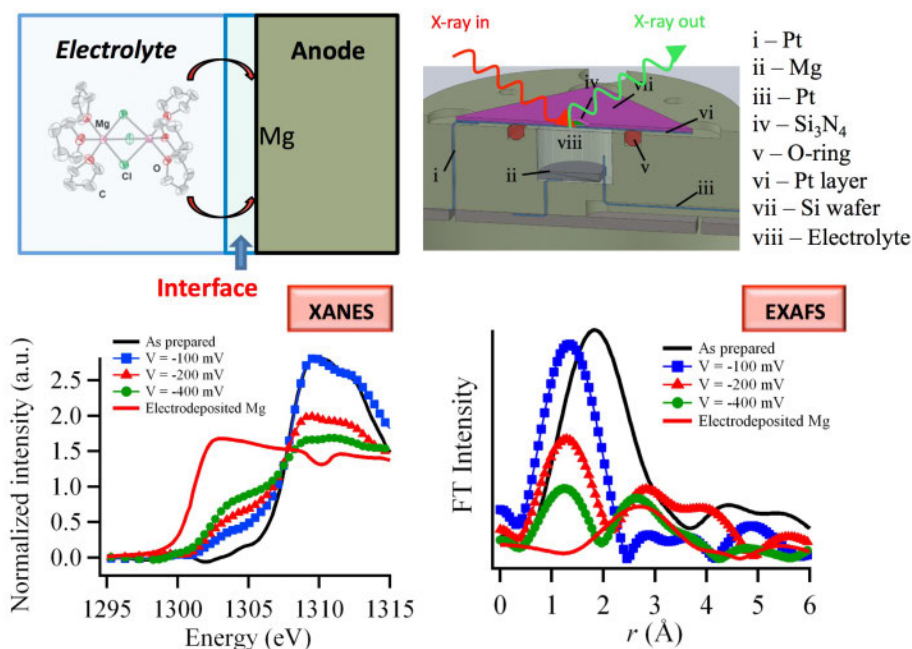


Figure II.3.7 (Upper) Mg electrolyte deposition and the in-situ electrochemical/XAS cell with annotations. (bottom) Near-edge and Fourier-transformed EXAFS spectra of the Mg K-edge at the Mg metal and electrolyte interface.³³

Although with good progress on both the fundamental understanding and instrumentation developments, revealing the mystery of the SEI remains a formidable challenge. Spectroscopic microscopy with nanometer spatial resolution could be achieved through STXM or with ptychography. However, the high SXR coherent flux available at a DLSR will be needed to make systematic measurements on a manageable time scale.

Charge diffusion in energy storage materials

Cathode materials lie at the heart of modern battery research, largely because there is still no perfect candidate that can maintain high-power and stable cycling comparable to that of anode materials.^{34, 35} The Li-ion diffusion and the resulting electrode phase transformation are often the key issues for designing high power Li-ion batteries. However, a clear picture of the phase transformation through ion diffusion in many electrode materials, e.g., LiFePO₄, is still under vigorous debate.³⁶⁻³⁸

Along the journey of inventing high-performance and safe cathode materials, the most striking discovery is probably LiFePO₄,³⁹ an insulator with unfavorable 1D Li diffusion channels (Figure II.3.8) and nominally two-phase transformation. In principle, mixed-valent TM cations are critical to maintain reasonable electric conductivity of the electrodes during charge and discharge. This is the reason that all other layered and spinel compounds feature continuous network of edge-shared TM octahedral array, where fluctuations of the mixed-valent TM cations essentially realize the electron motion. LiFePO₄, however, does not have such networking system. The FeO₆ octahedra are only corner-shared with PO₄ tetrahedra, further stabilizing the overall structure. In addition, it is believed that olivine LiFePO₄ structure only allows 1D diffusion

channels for Li-ions, which is not preferred and prone to impurity obstacles. Therefore, the fact that LiFePO_4 can provide impressively high performance⁴⁰ and could be successfully employed in commercial batteries challenges our conventional wisdom on understanding, choosing and developing cathode materials.^{38, 41}

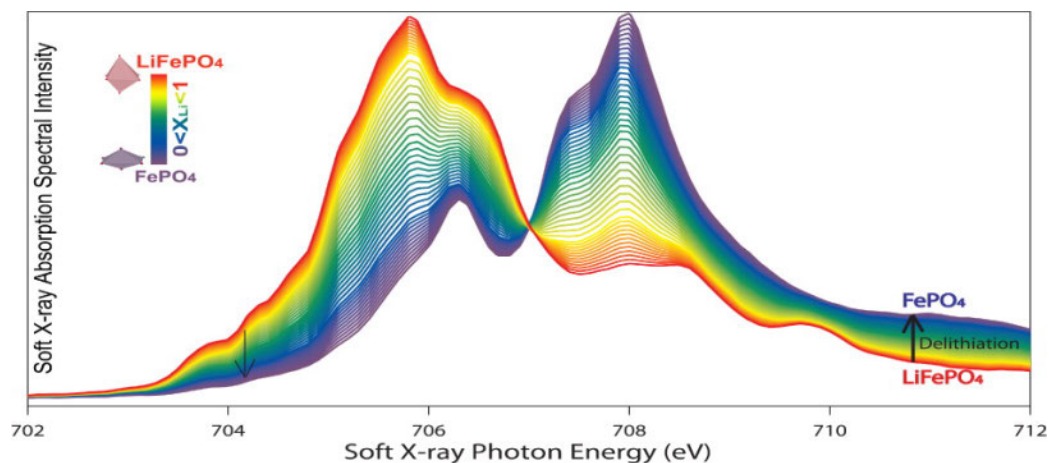


Figure II.3.8: SXR Fe-L edge XAS fingerprints the delithiation process from LiFePO_4 (red) to FePO_4 (purple). The isosbestic point provides spectroscopic insight into the ion diffusion mechanism in LiFePO_4 .³⁷

XAS at the transition metal L-edge measures the transition from $2p$ core level to $3d$ unoccupied states, thus revealing directly the valence states of transition metal $3d$ electrons. Due to this sensitivity, SXR XAS has been demonstrated to be a powerful tool to fingerprint the lithiation level of positive electrodes (cathodes), under both *in-situ*³⁷ and *ex-situ*⁴² conditions. Figure II.2.8 shows the Fe L-edge XAS spectra of a series of Li_xFePO_4 samples at different ion diffusion stages. The sensitivity and high-resolution of XAS spectra provide spectroscopic fingerprints of the ion diffusion process. Abundant information could be obtained based on the spectra and is relevant to battery performance, such as phase transformation, valence, spin states, and local structural distortions etc.³⁷

By virtue of the sensitivity of SXR to the transition-metal valence states in battery electrode materials, researchers are able to probe the phase transformation mechanism within the nanoparticles of LiFePO_4 through SXR STXM experiments.^{36, 43} Figure II.3.9 shows that the phase transformation in LiFePO_4 electrodes takes place through a particle by particle process.³⁶ Further studies reveal a strong asymmetry in the active particle population between charge and discharge. Contrary to intuition, the local current density of intercalating particles is nearly invariant with the global electrode cycling rate under typical cycling conditions. Rather, the electrode accommodates higher current by increasing the active particle population.⁴³ This active population behavior results from thermodynamic activation barriers in LiFePO_4 , and such a phenomenon likely extends to other phase-separating battery materials. Modifying the thermodynamic barrier and exchange current density can increase the active population and thus the current homogeneity. This could introduce new paradigms to enhance the cycle life of phase-separating battery electrodes.

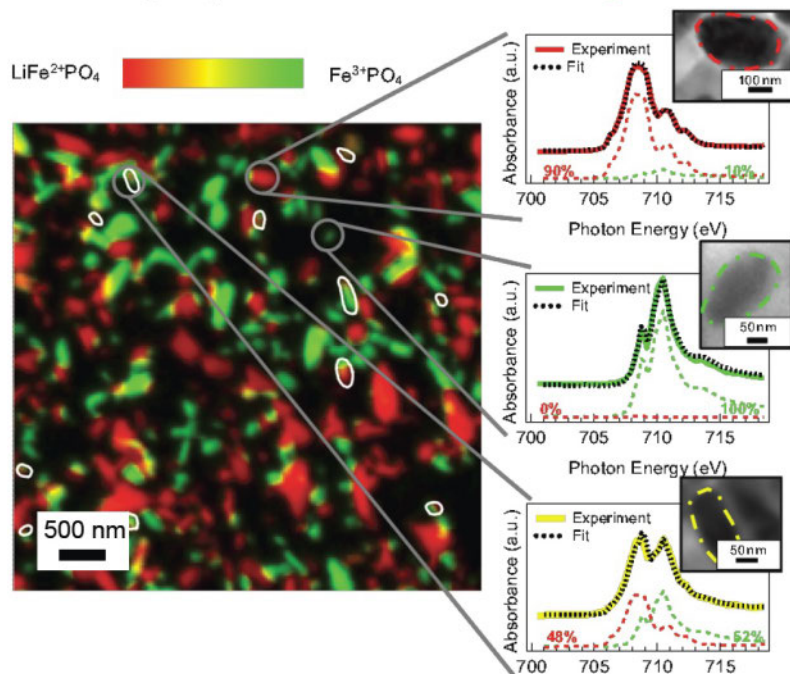


Figure II.3.9: STXM image of Fe states in a LiFePO₄ electrode. The color legend shows the phase distribution of individual particles at an averaged half delithiated electrode.

Recent development of SXR ptychography enhanced the spatial resolution of SXR spectroscopic microscope. Five nanometer spatial resolution is demonstrated using 25 nanometer focused beam size.⁴⁴ Such achievements will enable studying energy storage materials through SXR spectroscopy with nanometer spatial resolution.

Considering the dimensions of the ion diffusion, the intercalation-type cathode materials could be approximately categorized into groups with 1D, 2D and 3D ion diffusion channels.^{34,35} Clarifying the mystery of ion diffusion mechanism in battery electrodes relies on a systematic spectroscopy study with nanometer spatial resolution. The experimental feasibility relies on a great improvement of detector efficiency, especially for detecting the dynamics of the charge diffusion.

II.4: Measuring and Understanding Earth Processes at the Molecular Scale

Contributions from Gordon Brown, Ben Gilbert, Pupa Gilbert, Satish Myneni, Peter Nico and David Shuh

Fundamental research in the Earth Sciences attempts to understand the coupled evolution of life and minerals across geological time scales and to provide a framework within which some of the most pressing challenges for human societies and the planet can be addressed. This research is needed to inform our stewardship of water resources; to maintain the health and productivity of agricultural and marine systems; to improve upon ways of obtaining mineral and energy resources from the Earth while minimizing environmental impact; and to better establish the coupling between human and environmental processes and climate.

The study of Earth materials is typically very challenging because, as the products of more than 4 billion years of chemical and biological processes, Earth materials are distinguished by the heterogeneity and complexity they exhibit on a very wide range of length scales. Earth materials can contain any element from the Period Table, as well as a diverse assortment of complex organic molecules, and are typically hydrated. Key species for environmental reactions are frequently present in trace concentrations, are adsorbed to or substituted within another mineral phase, or are present as disordered or nanoscale minerals. A large number of fundamental reactions take place at the interfaces between minerals, fluids, and living organisms. Figure II.4.1 illustrates the use of soft-X-ray imaging and spectroscopy to identify the nature of amorphous calcium carbonate precipitates formed intracellularly by cyanobacteria.⁴⁵ That work exemplifies how X-ray imaging and chemical analysis performed at sub-20-nm resolution, enabled using a DLSR SXR source, can provide critical information about chemical speciation under ambient conditions that complements higher resolution imaging and elemental analysis offered by electron microscopy.

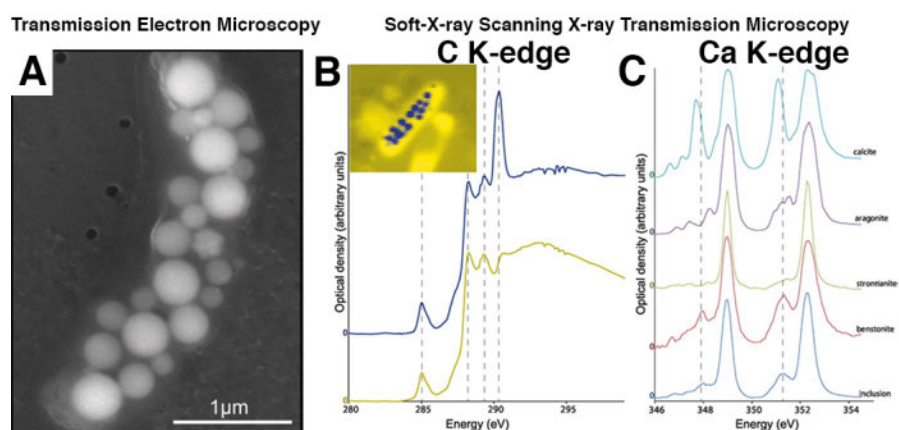


Figure II.4.1: The observation and identification of amorphous carbonate precipitates in a microbialite cyanobacterium by a combination of transmission electron microscopy (TEM) and scanning X-ray transmission microscopy (STXM). X-ray absorption spectroscopy of C and Ca with sub-20-nm spatial resolution provided intracellular characterization of the amorphous carbonate. Enhanced STXM using coherent soft-X-rays will provide X-ray absorption spectroscopy from sub-10-nm spots.⁴⁵

The diffraction-limited SXR methods described in this report represent a transformative advance in our ability to map and correlate essential chemical species and to understand processes in complex Earth materials under real-world conditions. The tunable soft-to-tender energy range will offer the ability to identify, image, and analyze all the relevant inorganic and organic species, including intracellular biological components in a minimally manipulated frozen hydrated form and three-dimensional fashion. For majority elements, (e.g., C, O, N, Si, Al, P and S) or critical but lower abundance elements, including transition metals and radionuclides, the SXR energy range is either essential for chemical analysis or offers chemical sensitivity superior to hard X-ray tools. The jump to true nanoscale imaging and spectroscopy will for the first time offer routine chemical analysis at the scale of single nanoparticles. The combination of fully coherent SXR imaging, scattering, and spectroscopy offers unprecedented ability to characterize light elements, and to distinguish disordered mineral phases or biopolymers by their complex optical properties.

Earth systems are dynamic and typically out of thermodynamic equilibrium. Basic molecular processes, such as the diffusion of ions or molecules remain poorly understood when they take place in the vicinity of mineral interfaces or within nanoscale pores (Figure II.4.2). Coherent scattering methods such as XPCS and RIXS will offer new approaches to understand molecular dynamics in confined fluids relevant to clay rich systems such as shales. Important outstanding questions concern the rates and pathways taken to move toward equilibrium. However, it is well established—mainly through simulation—that nanoscale chemical structure can emerge from the interplay of reaction (e.g., mineral dissolution) and transport (e.g., diffusion). Intense coherent SXR beams offer a valuable combination of atomic and molecular contrast and spatial and temporal resolution to make progress in understanding molecular-scale Earth processes that are presently most easily addressed through simulation.

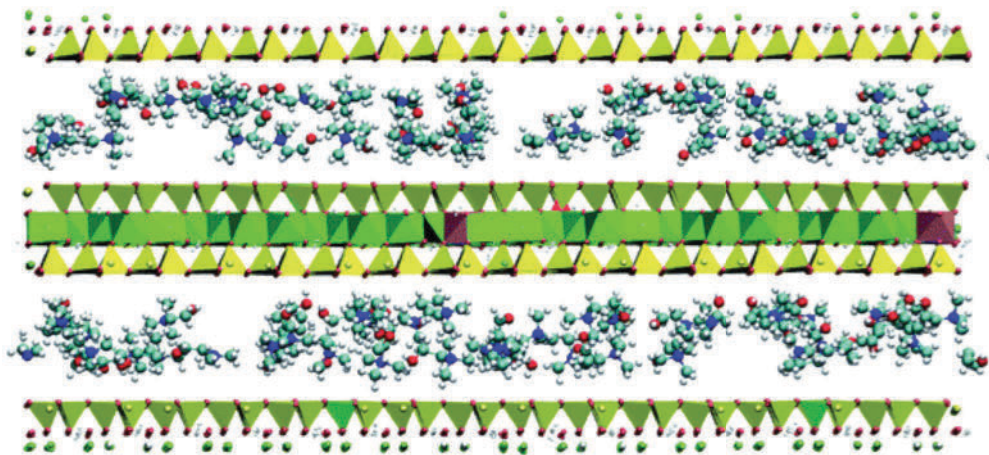


Figure II.4.2: Simulated adsorption-desorption-diffusion of sodium ions in water confined between smectite layers in a shale rock.⁴⁶ Understanding and correlating the nanoscale structure and multiscale chemical kinetic processes in these systems – adsorption/precipitation, desorption/dissolution, reaction, diffusion – is key for anticipating the effectiveness of barriers against radionuclide transport and for hydrocarbon extraction by hydraulic fracturing.

A further key benefit is that higher brightness, combined with optimal use of photons in diffraction imaging methods, will lead to a dramatic increase in data acquisition rate. Given the

heterogeneity of natural materials, statistically significant studies can require years of study, as exemplified by recent high-profile studies in astronomy and oceanography (Figure II.4.3).⁴⁷ A marked increase in throughput will enable dramatic increase in the quality and impact of the resulting science.

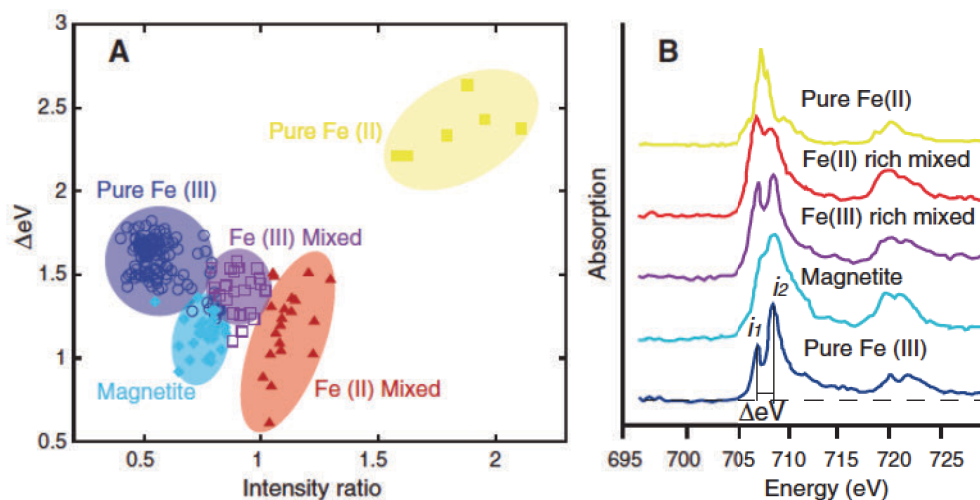


Figure II.4.3: STXM analysis of iron in over 60 colloidal samples from the Southern Ocean euphotic zone showed that the samples clustered into discrete mineral and chemical fractions. High-brightness STXM will dramatically decrease the throughput required for statistically significant analyses. Data from von der Hayden et al.⁴⁷

The use of coherent X-rays also marks an important switch from imaging materials via their X-ray attenuation contrast to providing a reconstruction of their full (complex) optical properties. As a consequence, we anticipate a significant improvement in our ability to image low X-ray absorbing materials, such as biomatter associated with more strongly absorbing inorganic components, and to distinguish between solid phases of similar elemental composition.

In this Chapter, we identify several emerging opportunities in which a diffraction-limited soft-X-ray source with world-leading brightness that will enable unprecedented new avenues for the analysis of complex Earth materials and new insight into environmentally important processes.

A. Pathways to Abiotic and Biological Mineral Nucleation and Growth

The nucleation and growth of crystalline and amorphous phases from fluids is a key process in all domains of the Earth sciences. For example, the precipitation of iron-bearing phases profoundly impacts ocean primary-productivity; salt crystal formation alters photochemical processes in atmospheric aerosols; and the nucleation of minerals of many kinds impacts soil and water quality through the incorporation or sorption of nutrients and contaminants. In subsurface aquifers proposed for geological sequestration of carbon dioxide, the precipitation of carbonate minerals offers the most stable trapping mechanism for CO_2 . Finally, many mineralizing life forms, including humans, have evolved with remarkable ability to produce crystalline or amorphous inorganic structures. The precipitation of diverse range of mineral nanoparticles by microorganisms can strongly alter the environment.

Although there is a long history of the study of crystal formation in both the Earth and materials sciences, it remains a grand challenge to understand how nucleation processes occur at the molecular scale. While the conditions under which mineral formation is favored can be predicted using thermodynamic calculations, knowledge of mineral saturation state is often not sufficient to predict with high certainty that nucleation will occur. Moreover, key attributes including mineral phase, morphology and particle size remain empirical aspects that cannot be anticipated because we lack knowledge of the pathway of the nucleation and growth process. These challenges are especially severe for all cases of biologically mediated nucleation.

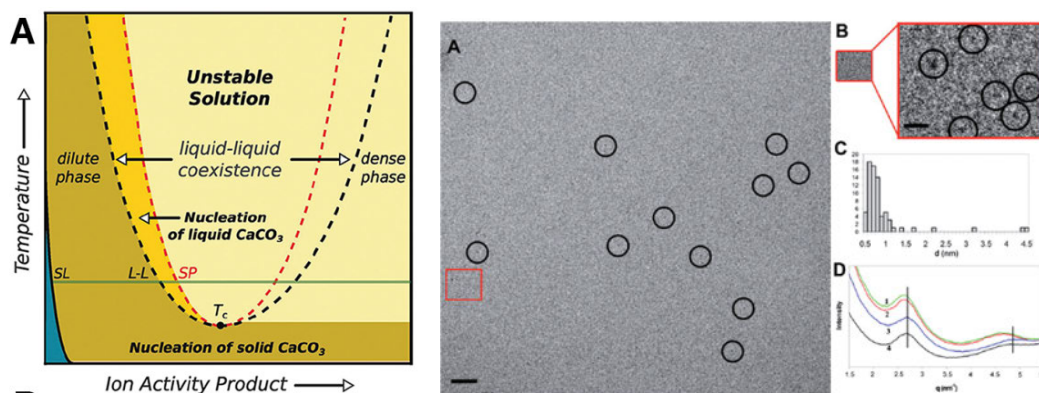


Figure II.4.4: Left: proposed phase stability relationships for systems exhibiting liquid-liquid phase separation.⁴⁸ Middle: Cryogenic TEM images of nanoparticles in a solution of calcium bicarbonate. Coherent soft-X-ray scattering will provide direct analysis of prenucleation clusters and reveal intrinsic timescales for cluster formation.⁴⁹

Understanding Abiotic Homogeneous Nucleation

In recent years, new and unexpected pathways for nucleation and growth in abiotic systems have been identified. For a growing number of systems, nucleation is now proposed to occur via the formation of thermodynamically stabilized pre-nucleation species such as hydrated molecular clusters,⁵⁰ contrary to the precepts of classical nucleation theory. In solutions that are supersaturated with respect to the solid phase, the solution is unstable to fluctuations, and the formation of dense liquid regions of hydrated CaCO_3 proceeds spontaneously (Figure II.4.4, left).⁴⁸ While there is some direct experimental evidence for this process (Figure II.4.4, right),⁴⁹ a confident description of the thermodynamic basis of the binodal for this system and the dynamics of solution fluctuations leading to liquid-liquid separation, coalescence, or dissolution are not known.

In addition, when nucleation produces low-solubility mineral nanoparticles, growth by oriented attachment of nanoparticles may outcompete growth by dissolution-reprecipitation. Figure II.4.5, right illustrates a nanoparticle-mediated growth pathway, and Figure II.4.5, left shows experimental evidence of this pathway observed recently by cryogenic transmission electron microscopy (cryo-TEM) for magnetite (Fe_3O_4).⁵¹ Chemically sensitive diffraction-limited imaging and dynamic scattering methods will offer highly complementary analyses of mineral formation processes.

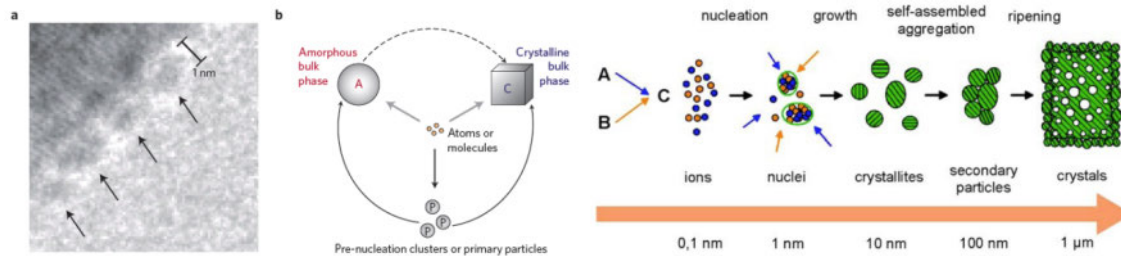


Figure II.4.5: Non-classical mineral nucleation and growth pathways. Left image: Cryo-TEM observation of magnetite growth surface with putative amorphous precursor nanoparticles attached. Right image: Proposed interrelationships relevant to mineral nucleation and growth pathways. Chemically sensitive diffraction-limited imaging and dynamic scattering methods will offer *in situ*, complementary analyses of mineral formation processes. Images from Baumgartner et al.⁵¹

The high SXR coherent flux provided by a DLSR will enable chemically-sensitive XPCS and RIXS measurements that will provide unique insight into the energy, spatial, and temporal scales of these nucleation and growth phenomena. XPCS and RIXS experiments performed as a function of solution saturation state and temperature will provide direct observation and analysis of the formation of dense liquid clusters, revealing intrinsic timescales for cluster formation, dissolution or coalescence.

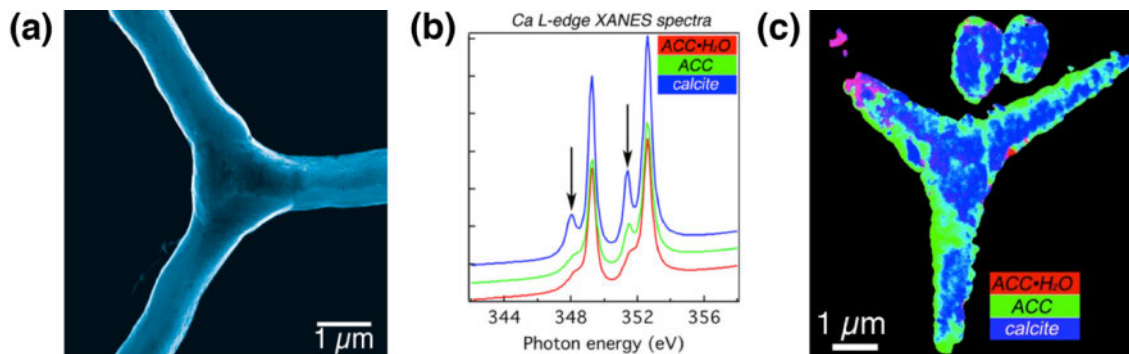


Figure II.4.6: (a) SEM micrograph of an embryonic sea urchin spicule showing the calcite rhombohedron at the center (c-axis normal to image plane) and rounded radii emanating from it. (Image courtesy of Pupa Gilbert. Unpublished.) (b) Ca L-edge spectroscopy of the 3 mineral phases detected in sea urchin spicules: hydrated amorphous calcium carbonate (ACC-H₂O), anhydrous amorphous calcium carbonate (ACC), and calcite. (c) Component map of the 3 mineral phases identified spectroscopically in (b) and displayed spatially here with the same colors. Data from Politi, et al.⁵²

Imaging the earliest stages of biomineralization

Biologically controlled mineralization processes can achieve remarkable control over material morphology and properties. Elucidating the pathways of biomineral formation will inspire new capabilities for directed synthesis of complex materials and is necessary in order to understand the current interactions between life, Earth chemistry and the climate, and to further interpret the fossil record.

A widespread strategy observed in biomineralization involves the initial formation of a transient amorphous phase that subsequently transforms to a more stable crystalline phase. This is exemplified by the growth of the sea urchin embryonic spicule which, when mature, is composed of two 1-micron sized rhombohedral crystals with spicule arms radiating from three termination surfaces (Figure II.4.6(a)). It was shown by soft-X-ray spectromicroscopy⁵² and by EXAFS methods⁵³ that crystal calcite formation is preceded by two distinct amorphous calcium carbonate phases. The organism appears to use and manipulate this intrinsic downhill thermodynamic landscape available to the carbonate system. This allows complex morphologies to be created through the addition of nanoparticles of the amorphous precursor, which creates a mechanically strong single crystal by an amorphous-to-crystalline transition that propagates through the resulting structure.

Although exceedingly challenging, coherent diffractive imaging methods with the resolution of the nanoscale precursor particles would permit unprecedented visualization of the mineralization pathway to directly test inferences obtained from current X-ray and electron microscopies and to answer new questions. For example, 3D images of the distribution of crystalline and amorphous phases within the central rhombohedral crystal and the spicule radii would provide new information as to the temporal correlations between simultaneously occurring growth and phase transformation. The small differences in electron density between ACC, calcite, and magnesium-rich calcite will be sufficient for delineating such nanostructure in complex biominerals. Due to radiation damage, *in vivo* analysis of biomineral growth will not be possible, but it is well established that spicule development can be followed at multiple time points following fertilization.⁵² Furthermore, polarization-dependent studies revealing relative orientation of crystallites would test the widely accepted concept of a single nucleation event. In addition, it has long been observed that while 6-7 calcite rhombohedral nuclei are formed, only two continue to grow to become spicules. Comparisons between candidate and final nucleation sites would establish whether there are mineralogical differences (e.g., crystal orientation) that are selected for spicule formation.

At around 50 μm diameter, the sea urchin embryo is rather large for transmission-geometry SXR analysis. However, the high spatial resolution, and exceptional sensitivity to biological structures and membranes justify the investment in the source characteristics and technique development that will be required. The analysis will require an intermediate energy (e.g., >5keV for >20% transmission), and will require the ability to perform an initial low-resolution analysis (e.g., stereographic or STXM-mode X-ray imaging or light microscopy) followed by region-of-interest high-resolution lensless imaging. The integration of optical microscopy into the on-line sample set-up would greatly facilitate the identification of ROIs. In the present case, the optically active calcite rhombohedra stand out in polarized light microscopy. Improved data analysis algorithms will be needed as the projection approximation fails for thick objects.

X-ray analysis provides crucial contrast for mixed inorganic/biological systems, and a majority of environmental samples belong to this category. X-ray absorption spectroscopy offers high energy resolution for finer distinction between chemical species, particularly between organic molecules and small changes in their chemical state, and metal complexes (Figure II.4.7).

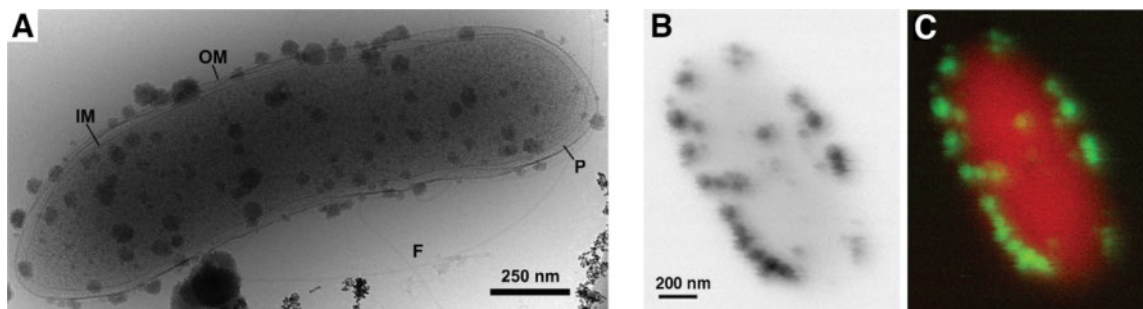


Figure II.4.7: Cryogenic TEM (A) and *in situ* STXM (B and C) observations of subsurface microorganisms decorated with iron-rich nanoparticle aggregates. The dense particles observed in cryo-TEM were identified using Fe L-edge spectroscopy in STXM (green regions in C). Ptychography using coherent X-rays will have the ability to image cell membranes as seen in cryo-TEM, and will retain the ability for detailed local chemical analysis through spatially resolved XAS. Data from Luef, et.al.⁵⁴.

Spectroscopy of fluids at high pressure

The implementation of highly focused X-ray beams will also enable SXR analysis of systems under regimes of high pressure and temperature that are completely inaccessible at present – where many subsurface nucleation processes occur. Currently, fluids held at pressures up to ~1 atm in windowed cells can be probed with SXR beams with focal spot dimensions in the 100- μm range. Reducing the window dimensions to the single micron scale dramatically increases resilience to pressure difference. For example a 1- μm thick, 2- μm square beryllium window can resist pressures exceeding 10 kbar, while retaining high transmission for X-rays at the O K-edge and all higher energies. With suitable fluid cell development, the small focus spot enabled by a diffraction-limited source will enable all soft-X-ray beamlines to interrogate materials under high pressure and high temperature.

This advance will enable SXR photon-in/photon-out spectroscopies to be performed on fluids under geologically relevant conditions, such as hydrothermal fluids, subsurface brines, deep-ocean waters, gas hydrates (clathrates), and supercritical CO_2 and CH_4 . Such methods can provide unique insights into the chemical bonding and structure of fluid molecules and solutes that are distinct from, and complement, information obtained from other complementary techniques such as vibrational spectroscopy, which are commonly used currently. For example, ALS studies have revealed the changes in aqueous hydrogen bonding networks that are caused by dissolution of an organic solute (methanol). There is currently very little knowledge as to the impact of solutes on water structure under conditions relevant to subsurface aquifers or deep ocean trenches.

B. Carbon Chemistry Affecting Energy and Climate

Organic carbon is the common and labile component in all Earth environments, and its chemistry plays a central role in many biogeochemical reactions occurring therein. The cycling of carbon between the atmosphere, living organisms, and their biomolecular products is crucial for the healthy functioning of the Earth systems that provide food, fibers and clean water to humankind. Carbon cycling is an important influence on the concentration of atmospheric CO_2

and hence on global climate. Carbonaceous materials also form the backbone of our global energy system, and the development of methods to improve our ability to extract, capture, transport or store key carbon materials will have major benefits. Thus, there is a strong ongoing need to better understand the roles of carbon in ecosystem health, climate reactions and energy resources and technologies.

Mineral controls on carbon cycling in soils

Soils are a major reservoir of organic carbon with estimates ranging from 2000 to 3000 petagrams — more than total terrestrial biomass or any of the atmosphere or ocean carbon pools. SXR imaging and spectroscopy have illuminated our understanding of soil carbon speciation and dynamics and helped establish the current paradigm that interactions between organic carbon and soil minerals are major controls on the rate of decomposition of organic

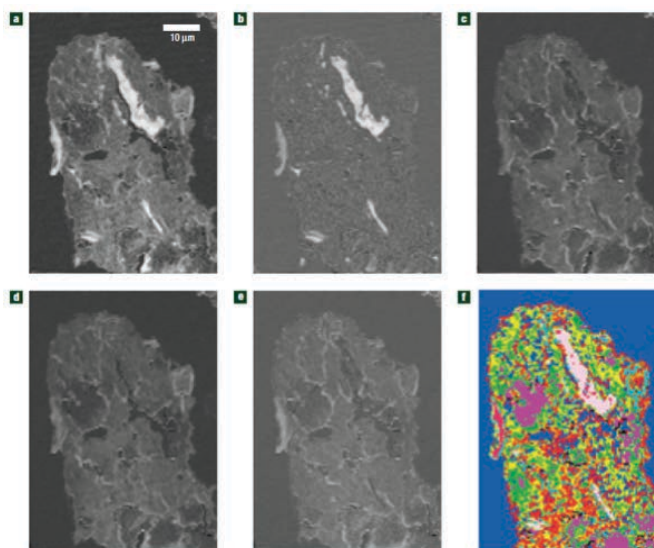


Figure II.4.8: STXM analysis of soil microaggregate showing the heterogeneity on all accessible length scales of carbon forms and associations that regulate larger scale carbon cycling: a) total carbon, b) aromatic, c) aliphatic carbon, d) carboxylic, e) and phenolic carbon, f) cluster map of carbon forms. From Lehmann, et. al.⁵⁵

matter by soil microbiota. As illustrated by Figure II.4.8, SXR methods provide unsurpassed descriptions of the spatial associations between carbon forms and mineral substrates,⁵⁵ information that is invaluable for understanding chemical and physical contributions to organic matter recalcitrance and bioavailability. Currently, however, the spatial resolution at STXM facilities does not yet quite approach the fundamental nanometer scales of macromolecules and mineral particles.

Figures II.4.9 C), D), and E) show STXM carbon maps of a soil aggregate compared with the SEM image of the same sample shown in panels A) and B). The SEM image clearly shows enormous amount of structural detail that is not captured in the STXM data. Figures II.4.9 F) show a SXR ptychographic image of a cement particle with the SEM image of the same particle. The ptychographic method reveals substantially greater detail of the nanoscale structure of the

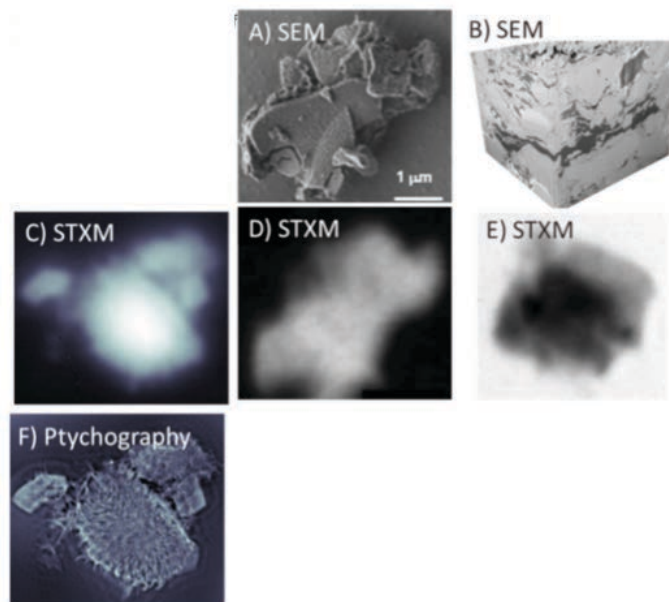


Figure II.4.9: Current limitations of STXM imaging and systems that will benefit from diffraction imaging. Unpublished data courtesy of P. Nico, D. Shapiro and T. Kneafsey (LBNL).

the particle, more closely attaining the resolution of SEM. Because ptychography additionally offers chemical spectroscopy with high spatial resolution, this method will for the first time allow clear correlations to be identified between the physical association of carbon and fine grained minerals, the chemical forms of such mineral associated carbon, and the mechanisms of carbon stabilization. Figure II.4.9 thus illustrates the high potential of SXR ptychography for attaining more accurate representations of soil particles and many other complex Earth materials, including shales. Shales are nanostructured, organic rich rocks that host enormous reserves of methane gas, and can provide a vital cap rock for subsurface sequestration of carbon dioxide. There are many unknowns about the coupling between shale rock mechanics, the mineral and geochemical evolution of shales subjected to stress, temperature variations or the introduction of high-pressure fluids, and the transport of methane and contaminant species. Ptychography will provide minimally destructive, 3D chemical information necessary to address these questions.

Links between global cycles of carbon, nitrogen, phosphorus and other key elements

Carbon availability and cycling is often limited or regulated by biogeochemical processes involving other key elements such as nitrogen, phosphorus, sulfur and metals. In particular, N and P cycles are intimately linked to the carbon cycle, frequently acting as limiting elements for ecosystem productivity. An outstanding challenge in Earth science is to understand the mechanisms of observed interdependencies among these global elemental cycles. Nitrogen availability in soils and sediments is frequently linked to the decomposition of organic matter and thus can be controlled by carbon association with minerals. For example, iron precipitates play a role in limiting the bioavailability of N in fungal mats in forest soils.⁵⁶ Phosphorus is an essential nutrient for all terrestrial ecosystems and a crucial input for modern agricultural practices. As a

non-renewable resource, obtained by mining from deposits that are more geographically concentrated than oil, phosphorus is a strategically vital element. Phosphorus is heterogeneously distributed in soils and sediments, with complex and varying distributions among mineral, sorbed and organic species.

There is abundant evidence from STXM studies, and other approaches for microchemical analysis, that determining the three-dimensional associations between carbon and other key elements, minerals, and soil flora and fauna is vital for understanding complex coupled natural cycles. However, all current and prior studies have been limited by low spatial resolution, the need to significantly manipulate samples prior to analysis, by the lack of 3D information, and by limited sample throughput. High-brightness, coherent SXR analysis methods offers exciting new solutions to each of these limitations.

Chemically sensitive imaging of natural organic matter

Assemblies of biologically derived macromolecules are common in the environment, in the form of biofilms and other extracellular polymers, as well as natural organic matter coatings and aggregates. The nano-to-microscale structure of such fragile molecule assemblies with low-Z atoms is exceedingly difficult to establish by electron or optical microscopy or high-energy X-ray scattering. Figure II.4.10 illustrates the use of soft-X-ray imaging for observing conformational changes in hydrated natural organic matter (NOM) when exposed to different environmental variables.⁵⁷

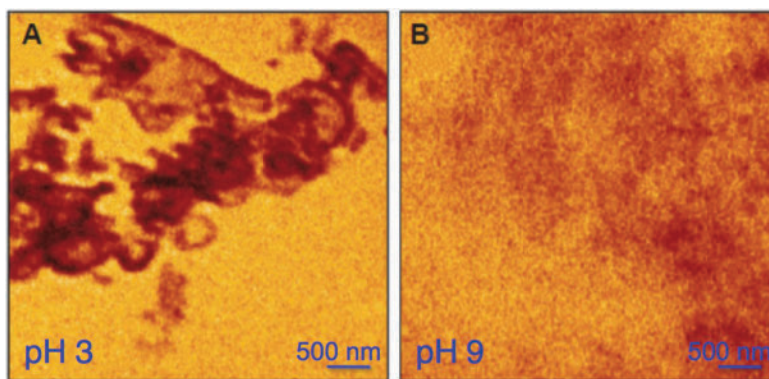


Figure II.4.10: Full-field soft-X-ray microscopy at 516.6 eV of fulvic acid in water at two pH values showing the high sensitivity of natural organic matter conformation to solution conditions. Chemically-sensitive soft-X-ray SAXS will be able to reveal structural correlations between low-Z elements and functional groups during dynamic flocculation processes. Images acquired at ALS and taken from Myneni et al.⁵⁷

High-brightness, chemically resolved SXR imaging will offer the ability to characterize the structure of the carbon backbone as well as to distinguish the distribution of chemically distinct species or functional groups within the network. These approaches will have application to membrane science more broadly, such as the long-standing challenge of correlating nanoscale structure, chemistry and the performance of ion-selective membranes such as Nafion. Because chemically-sensitive SAXS can be performed *in situ*, dynamic studies of NOM aggregation or

the disaggregation of biopolymers such as cellulose can be envisioned under conditions relevant to the natural environment or biofuel processing facilities.

C. The Behavior of Radionuclides in the Environment

A great challenge for the US Department of Energy (DOE) is the remediation and stabilization of both and high- and moderate-level radiologically contaminated materials and sites that are part of the US nuclear legacy. The costs related to these activities is one of the single largest fiscal burdens within the DOE complex and the commitments stretching well into the future represent a significant outlay of taxpayer resources. Improved fundamental scientific understanding of radionuclide biogeochemistry is vital to manage the environmental priorities of the DOE and to support the safe implementation of new advanced nuclear energy systems that could form one of the pillars for future carbon neutral energy sources.⁵⁸ Limits in our ability to anticipate and influence the environmental behavior of radiological waste has left contaminated sites, including Chernobyl and Fukushima, unremediated and relegated substantial land areas uninhabitable for some time. Thus, advances in this area will positively impact the U.S. public, DOE cleanup, DOE energy programs, and will provide leadership for similar efforts worldwide.

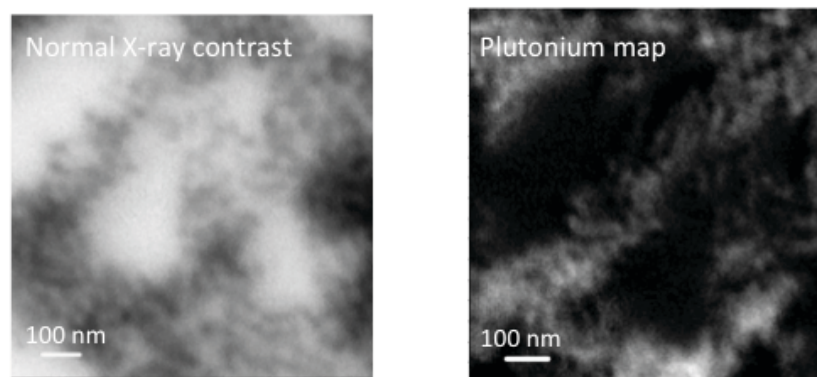


Figure II.4.11. Chemical imaging of synthetic plutonium dioxide (PuO_2) nanoparticles with ~ 20 -nm diameter. Left. Normal X-ray contrast image. Right. Elemental map of plutonium (light regions indicating Pu). Coherent soft-X-ray analysis will be able to image primary radionuclide particles in synthetic systems or complex environmental media. Data obtained at ALS Molecular Environmental Sciences Beamline. 11.0.2. Images courtesy of B. Dumas (CEA, Marcoule, France) and Minasian & D. Shuh (LBNL).

Radionuclide environmental science will benefit tremendously from the new capabilities provided by a DLSR source operating in the soft and intermediate energy ranges. Of particular concern, many environmentally mobile radionuclides form or associate with environmental nanoparticles. Current SXR spectromicroscopes that offer ~ 40 -nm spatial resolution can perform chemical analysis of nanoparticle aggregates and can identify spectral signatures of surface species, but cannot resolve individual particles. For example, Figure II.4.11, presents X-ray images of aggregates of ~ 20 -nm diameter PuO_2 nanoparticles. While individual nanoparticles could not be resolved, Pu $N_{V,IV}$ - and O K-edge X-ray absorption spectra could be interpreted as a combination of bulk and surface species. The use of ptychography for studies of radionuclide nanoparticles will enable primary particle imaging and the assessment of

chemical heterogeneities at the single-particle scale. True nanometer-scale analysis, coupled with the flexibility to translate the understandings from the nanoscale to the larger scale, will provide information from which more effective decisions can be made to mitigate the impacts of radionuclides in the environment.

Chapter II.5: Heterogeneous Aerosol Chemistry

Contributions from Kevin Wilson, Frances Houle, Mary Gilles, Hendrik Bluhm

The quantity and chemical composition of sub-micron particles (i.e. aerosols) play an important role in the Earth's climate system by directly scattering or absorbing incoming solar radiation or indirectly by modifying cloud properties.⁵⁹ Atmospheric aerosols are comprised of inorganic salts and complex mixtures of organic molecules (Fig. II.5.1).^{60, 61}

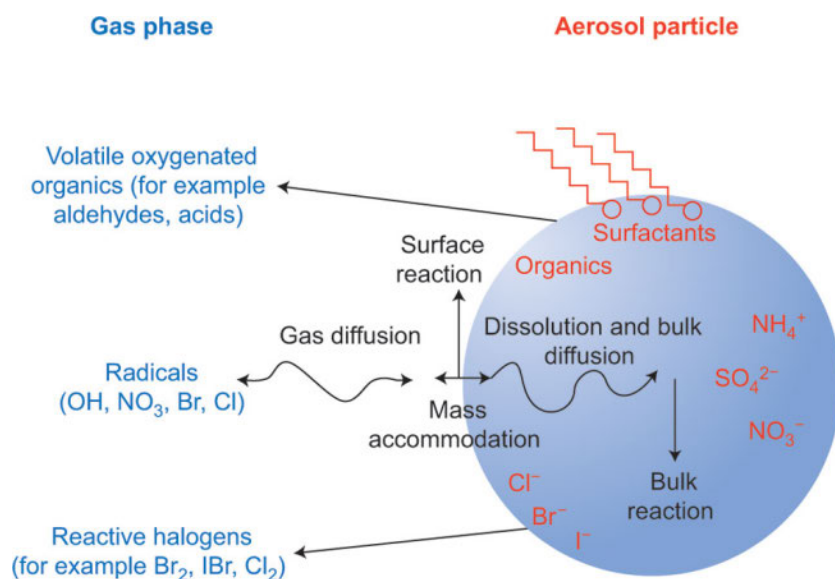


Figure II.5.1: Schematic of some of the complex chemical reaction-diffusion processes associated with an atmospheric aerosol particle.⁶¹

While much of the inorganic portion is well understood, the organic fraction is significantly more complex and is governed by complicated feedbacks that continuously transform both the chemical composition (via oxidation reactions) and the physical state of the aerosol (volatility, water content, size, etc.). Current atmospheric models parameterize organic aerosol formation and evolution using equilibrium partitioning theory,⁶² which assumes that molecules within the aerosol are well-mixed and respond instantaneously to atmospheric changes in chemical composition, temperature, aerosol concentration and relative humidity.

Recent studies report evidence that organic aerosols exist in the atmosphere not as well-mixed liquids – the traditional description – but rather as glassy or semisolid materials with extremely slow diffusion times.⁶³⁻⁶⁷ Moreover, an aerosol particle is not likely to have only one or two phase states during its lifetime in the atmosphere. In reality there are likely multiple transitions between liquid and glassy phases as well as transitions to phase-separated states, all of which can depend on the specific history of the particle. Drivers are changes in internal and external chemistry, temperature, and relative humidity, which all vary continuously during the particle's lifetime. This hypothesis is founded on well-known sorption behaviors in polymer

systems,⁶⁸ which resemble oligomeric material found in aerosols. Changes in temperature and small molecule content alter polymeric diffusion coefficients by 5 orders of magnitude, and we expect that similar processes are at play for aerosols. These observations suggest that the description of aerosols currently used in regional and global climate models is fundamentally incorrect. The lower evaporation rate of glasses may explain why models consistently under-predict the quantity of aerosol in the atmosphere by factors of 5 to 10. To accurately describe how chemical reactions couple with diffusive transport in aerosols, requires new and transformative ways to measure the formation and dissipation of compositional gradients induced by the uptake of atmospheric vapors and surface chemical reactions.

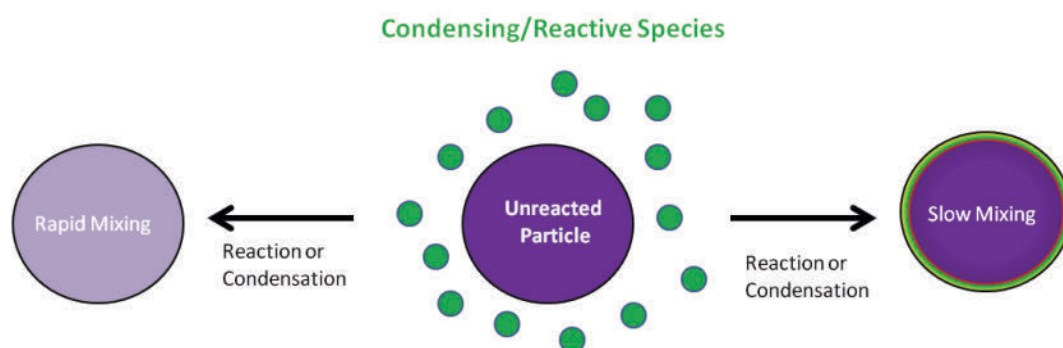


Figure II.5.2: Condensation and reaction mechanisms are highly dependent upon aerosol phase (i.e. Liquid vs. Glass)

When in a glassy state, the aerosol has slow internal mixing and low volatility, which greatly impacts the predicted quantity in the troposphere during aerosol transport from polluted urban regions to remote pristine environments. This is because the evaporative flux is not controlled simply by the specific molecular components of a particle, but also by transport of species to the aerosol surface. Similarly, there are many multiphase processes in the atmosphere from the uptake of water, condensation of gas phase species and oxidation chemistry, which would proceed at a much different rate and mechanism if organic aerosols are glasses rather than liquids (Fig. II.5.2).

When in a glassy state, the aerosol has slow internal mixing and low volatility, which greatly impacts the predicted quantity in the troposphere during aerosol transport from polluted urban regions to remote pristine environments. This is because the evaporative or condensational flux is not controlled simply by the specific molecular components of a particle, but also by transport of species to and from the aerosol interface. Similarly, there are many multiphase processes in the atmosphere from the uptake of water, condensation of gas phase species and oxidation chemistry, which would proceed at a much different rate and mechanism if organic aerosols are glasses rather than liquids (Fig. 2). Specifically, recent work has shown that heterogeneous uptake of a gas phase molecule onto an aerosol surface is an emergent property with complex relationships between gas phase concentration, particle size and viscosity.⁶⁹

These insights have significantly increased the difficulty of accurately describing, in computational efficient ways, aerosol microphysics and chemistry in regional and climate

models. Current experimental and modeling approaches by themselves simply cannot capture enough of these complex processes to develop an improved parameterization for use in atmospheric models. This is because there are currently no experimental approaches that can quantify the rate of formation and evolution of chemical gradients over 10's of nanometer length scales within a single glassy or semisolid particle. Furthermore these gradients are expected to have complex dynamics, which depend upon the coupling of chemistry with water uptake and diffusion. For example, in a glassy particle only the interfacial region is available for heterogeneous uptake (i.e reactive or non-reactive). As this thin shell becomes more oxidized by gas phase reactions with OH radicals or ozone water uptake and transport into the particle will be enhanced. As such we expect that these gradients will be transient and evolve during an aerosol lifetime in the atmosphere. Developing new experimental tools to observe these dynamics, which are governed by a broad range of timescales, will enable a more realistic parameterized descriptions to be developed for complex aerosol evolution histories found in nature. More generally, these are the first steps in developing an understanding of the dynamics in mesoscale ensembles with history-dependent properties.

Using single levitated droplets (micron size) or particles (~300 nanometer) provides an elegant way to study multiphase chemistry of organic aerosols. A single particle can be held in a laser trap for many days allowing the full range of atmospherically relevant conditions to be simulated and explored. Realistic atmospheric oxidation conditions (e.g. ozone or OH radical concentrations) can in principle be produced for single particles in the laboratory. Unfortunately, the suite of analytical tools currently available to probe single particles is limited to mainly Raman spectroscopy, which is not suitable for measuring the internal structure and dynamics of compositional gradients within a particle.

Fully coherent SXR beams from a diffraction-limited source will offer revolutionary opportunities to probe single trapped particles in the water window and above the carbon K-edge to achieve chemical contrast. As noted above a single snapshot with coherent diffractive imaging using a single pulse will provide an image with ~10 nm resolution and with little radiation damage. This will provide a measure of composition gradients at that scale, which are presently not known. Also efforts are underway to use single heavily over-sampled snapshots to produce 3D CDI reconstructions. If the droplet survives with little damage, a movie to probe reaction-diffusion kinetics or provide tomographic reconstructions.

Key experiments will focus on quantifying the atmospheric loss pathways of glassy and semisolid aerosols. In particular we will determine how particle phase viscosity impacts oxidative aging chemistry and how this chemistry either enhances water uptake and diffusion or decomposition through chemical erosion. The competition between these processes control atmospheric lifetime of aerosols either by wet deposition (cloud formation) or through the formation of gas phase reaction products. It is expected that the dynamics of internal gradients near the particle interface will be controlled by both interfacial oxidation chemistry and liquid water content. We expect that the chemical composition and dynamics of this interfacial region, which is transformed by heterogeneous oxidation or the condensation of gas phase reaction products will be key in controlling the competition between water uptake and decomposition.

Model particles that are representative of the chemical functionality and phase behavior of ambient aerosol, will be levitated in an optical trap. The phase state of the particle, governed by liquid water content, will be controlled experimentally by the relative humidity in the reaction cell. Oxidative aging of the particle will be simulated by introducing OH or ozone. As a glassy particle become more oxidized, interfacial gradients will form and be imaged with chemical contrast by monitoring changes in carbon oxidation state at the carbon K edge. Similarly the dynamics of water diffusion inside the particle will be observed at the O K edge. Decomposition chemistry will be observed via changes in particle size and by an overall decrease in carbon K edge intensity in the interfacial region as reaction product evaporate from the particle. The dynamics of chemistry and water diffusion will be explored over a range of oxidation rates and particle viscosity to explore the full complexity of aerosol aging during its lifetime in the atmosphere. Coherent SXRs will enable for the first time the direct observation a range of dynamic processes driven by chemistry that include dynamic phase transformations and reaction driven changes in viscosity, which are features of extreme importance for understanding atmospheric aerosol chemistry and more generally for elucidating and controlling chemical reactions at the mesoscale.

References: Section II

1. C. Århammar, A. Pietzsch, N. Bock, E. Holmström, C. M. Araujo, J. Gråsjö, S. Zhao, S. Green, T. Peery, F. Hennies, S. Amerioun, A. Föhlisch, J. Schlappa, T. Schmitt, V. N. Strocov, G. A. Niklasson, D. C. Wallace, J.-E. Rubensson, B. Johansson and R. Ahuja, *Proceedings of the National Academy of Sciences* **108** (16), 6355-6360 (2011).
2. F. Hennies, A. Pietzsch, M. Berglund, A. Föhlisch, T. Schmitt, V. Strocov, H. O. Karlsson, J. Andersson and J.-E. Rubensson, *Physical Review Letters* **104** (19), 193002 (2010).
3. A. Pietzsch, Y. P. Sun, F. Hennies, Z. Rinkevicius, H. O. Karlsson, T. Schmitt, V. N. Strocov, J. Andersson, B. Kennedy, J. Schlappa, A. Föhlisch, J. E. Rubensson and F. Gel'mukhanov, *Physical Review Letters* **106** (15), 153004 (2011).
4. Y.-P. Sun, A. Pietzsch, F. Hennies, F. Rinkevicius, H. O. Karlsson, T. Schmitt, V. N. Strocov, J. Andersson, B. S. Kennedy, J., A. Föhlisch, F. Gel'mukhanov and J.-E. Rubensson, *J. Phys. B* **44**, 161002 (2011).
5. Y.-P. Sun, F. Hennies, A. Pietzsch, B. Kennedy, T. Schmitt, V. N. Strocov, J. Andersson, M. Berglund, J. E. Rubensson, K. Aidas, F. Gel'mukhanov, M. Odelius and A. Föhlisch, *Physical Review B* **84** (13), 132202 (2011).
6. K. R. Siefertmann, C. D. Pemmaraju, S. Neppl, A. Shavorskiy, A. A. Cordones, J. Vura-Weis, D. S. Slaughter, F. P. Sturm, F. Weise, H. Bluhm, M. L. Strader, H. Cho, M.-F. Lin, C. Bacellar, C. Khurmi, J. Guo, G. Coslovich, J. S. Robinson, R. A. Kaindl, R. W. Schoenlein, A. Belkacem, D. M. Neumark, S. R. Leone, D. Nordlund, H. Ogasawara, O. Krupin, J. J. Turner, W. F. Schlotter, M. R. Holmes, M. Messerschmidt, M. P. Minitti, S. Gul, J. Z. Zhang, N. Huse, D. Prendergast and O. Gessner, *The Journal of Physical Chemistry Letters* **5** (15), 2753-2759 (2014).
7. S. Lupi, L. Baldassarre, B. Mansart, A. Perucchi, A. Barinov, P. Dudin, E. Papalazarou, F. Rodolakis, J. P. Rueff, J. P. Itié, S. Ravy, D. Nicoletti, P. Postorino, P. Hansmann, N. Parragh, A. Toschi, T. Saha-Dasgupta, O. K. Andersen, G. Sangiovanni, K. Held and M. Marsi, *Nat Commun* **1**, 105 (2010).
8. C. Chen, Y. Kang, Z. Huo, Z. Zhu, W. Huang, H. L. Xin, J. D. Snyder, D. Li, J. A. Herron, M. Mavrikakis, M. Chi, K. L. More, Y. Li, N. M. Markovic, G. A. Somorjai, P. Yang and V. R. Stamenkovic, *Science* **343** (6177), 1339-1343 (2014).
9. C. W. Li, J. Ciston and M. W. Kanan, *Nature* **508** (7497), 504-507 (2014).
10. H. Furukawa, K. E. Cordova, M. O'Keeffe and O. M. Yaghi, *Science* **341** (6149) (2013).
11. M. Sutton, *Comptes Rendus Physics* **9**, 657 (2008).
12. G. Grübel and F. Zontone, *J. Alloys and Compounds* **362**, 3 (2004).
13. S. Jakubith, H. H. Rotermund, W. Engel, A. von Oertzen and G. Ertl, *Physical Review Letters* **65** (24), 3013-3016 (1990).
14. M. Bär, E. Meron and C. Uetzny, *Chaos* **12**, 204 (2002).
15. H. Bluhm, K. Andersson, T. Araki, K. Benzerara, G. E. Brown, J. J. Dynes, S. Ghosal, M. K. Gilles, H. C. Hansen, J. C. Hemminger, A. P. Hitchcock, G. Ketteler, A. L. D. Kilcoyne, E. Kneidler, J. R. Lawrence, G. G. Leppard, J. Majzlan, B. S. Mun, S. C. B. Myneni, A. Nilsson, H. Ogasawara, D. F. Ogletree, K. Pecher, M. Salmeron, D. K. Shuh, B. Tonner, T. Tylliszczak, T. Warwick and T. H. Yoon, *Journal of Electron Spectroscopy and Related Phenomena* **150** (2-3), 86-104 (2006).
16. D. F. Ogletree, H. Bluhm, G. Lebedev, C. S. Fadley, Z. Hussain and M. Salmeron, *Rev. Sci. Inst.* **73**, 3872 (2002).

17. W. Eberhardt, in *Research for Sustainable Electricity-Heat System (translated from German)*, edited by F. Giovannetti, D. Krüger, M. Nast, W. Platzer, M. Krause and M. Reuß (FVEE, Berlin, 2010), pp. 18-25.
18. A. Cho, *Science* **329** (5993), 786-787 (2010).
19. BESAC, edited by U. D. o. Energy (2008).
20. J. Turner, *Nat Mater* **7** (10), 770-771 (2008).
21. O. Khaselev and J. A. Turner, *Science* **280** (000073159600044), 425-427 (1998).
22. R. van Noorden, *Nature* **507**, 26 (2014).
23. J. B. Goodenough and K.-S. Park, *Journal of the American Chemical Society* **135** (4), 1167-1176 (2013).
24. K. Xu, *Chemical Reviews* (2014).
25. J. B. Goodenough, H. D. Abruña and M. V. Buchanan, edited by D. o. Energy (Washington, DC, 2007).
26. J. B. Goodenough and Y. Kim, *Chemistry of Materials* **22** (3), 587-603 (2009).
27. P. B. Balbuena and Y. Wang, *Lithium-Ion Batteries Solid-Electrolyte Interphase*. (Imperial College Press, 2004).
28. K. Xu and A. von Wald Cresce, *Journal of Materials Research* **27** (18), 2327-2341 (2012).
29. K. Xu, *Chemical Reviews* **104** (10), 4303-4418 (2004).
30. A. Augustsson, M. Herstedt, J. H. Guo, K. Edstrom, G. V. Zhuang, J. P. N. Ross, J. E. Rubensson and J. Nordgren, *Physical Chemistry Chemical Physics* **6** (16), 4185-4189 (2004).
31. R. Qiao, I. T. Lucas, A. Karim, J. Syzdek, X. Liu, W. Chen, K. Persson, R. Kostecky and W. Yang, *Advanced Materials Interfaces* **1** (3), 1300115 (2014).
32. R. Qiao, Y. Wang, P. Olalde-Velasco, H. Li, Y.-S. Hu and W. Yang, *Journal of Power Sources* **273** (0), 1120-1126 (2015).
33. T. S. Arthur, P.-A. Glans, M. Matsui, R. Zhang, B. Ma and J. Guo, *Electrochemistry Communications* **24** (0), 43-46 (2012).
34. B. L. Ellis, K. T. Lee and L. F. Nazar, *Chemistry of Materials* **22** (3), 691-714 (2010).
35. M. S. Whittingham, *Chemical Reviews* **104** (10), 4271-4302 (2004).
36. W. C. Chueh, F. El Gabaly, J. D. Sugar, N. C. Bartelt, A. H. McDaniel, K. R. Fenton, K. R. Zavadil, T. Tyliszczak, W. Lai and K. F. McCarty, *Nano letters* **13** (3), 866-872 (2013).
37. X. Liu, J. Liu, R. Qiao, Y. Yu, H. Li, L. Suo, Y.-s. Hu, Y.-D. Chuang, G. Shu, F. Chou, T.-C. Weng, D. Nordlund, D. Sokaras, Y. J. Wang, H. Lin, B. Barbiellini, A. Bansil, X. Song, Z. Liu, S. Yan, G. Liu, S. Qiao, T. J. Richardson, D. Prendergast, Z. Hussain, F. M. F. de Groot and W. Yang, *Journal of the American Chemical Society* **134** (33), 13708-13715 (2012).
38. R. Malik, F. Zhou and G. Ceder, *Nat Mater* **10** (8), 587-590 (2011).
39. A. K. Padhi, K. S. Nanjundaswamy and J. B. Goodenough, *Journal of The Electrochemical Society* **144** (4), 1188-1194 (1997).
40. S. Y. Chung, J. T. Bloking and Y. M. Chiang, *Nature Materials* **1** (2), 123-128 (2002).
41. M. Thackeray, *Nat Mater* **1** (2), 81-82 (2002).
42. X. Liu, D. Wang, G. Liu, V. Srinivasan, Z. Liu, Z. Hussain and W. Yang, *Nat Commun* **4**, 2568 (2013).
43. Y. Li, F. El Gabaly, T. R. Ferguson, R. B. Smith, N. C. Bartelt, J. D. Sugar, K. R. Fenton, D. A. Cogswell, A. L. Kilcoyne, T. Tyliszczak, M. Z. Bazant and W. C. Chueh, *Nat Mater* **13** (12), 1149-1156 (2014).

44. D. A. Shapiro, Y.-S. Yu, T. Tyliczszak, J. Cabana, R. Celestre, W. Chao, K. Kaznatcheev, A. L. D. Kilcoyne, F. Maia, S. Marchesini, Y. S. Meng, T. Warwick, L. L. Yang and H. A. Padmore, *Nat Photon* **8** (10), 765-769 (2014).
45. E. Couradeau, K. Benzerara, E. Gérard, D. Moreira, S. Bernard, G. E. Brown and P. López-García, *Science* **336** (6080), 459-462 (2012).
46. J. L. Suter, P. V. Coveney, R. L. Anderson, H. C. Greenwell and S. Cliffe, *Energy & Environmental Science* **4** (11), 4572-4586 (2011).
47. B. P. von der Heyden, A. N. Roychoudhury, T. N. Mtshali, T. Tyliczszak and S. C. B. Myneni, *Science* **338** (6111), 1199-1201 (2012).
48. A. F. Wallace, L. O. Hedges, A. Fernandez-Martinez, P. Raiteri, J. D. Gale, G. A. Waychunas, S. Whitelam, J. F. Banfield and J. J. De Yoreo, *Science* **341** (6148), 885-889 (2013).
49. E. M. Pouget, P. H. H. Bomans, J. A. C. M. Goos, P. M. Frederik, G. de With and N. A. J. M. Sommerdijk, *Science* **323** (5920), 1455-1458 (2009).
50. D. Gebauer, M. Kellermeier, J. D. Gale, L. Bergstrom and H. Coelfen, *Chemical Society Reviews* **43** (7), 2348-2371 (2014).
51. J. Baumgartner, A. Dey, P. H. H. Bomans, C. Le Coadou, P. Fratzl, N. A. J. M. Sommerdijk and D. Faivre, *Nature Materials* **12** (4), 310-314 (2013).
52. Y. Politi, R. A. Metzler, M. Abrecht, B. Gilbert, F. H. Wilt, I. Sagi, L. Addadi, S. Weiner and P. U. P. A. Gilbert, *Proceedings of the National Academy of Sciences of the United States of America* **105** (45), 17362-17366 (2008).
53. Y. Politi, T. Arad, E. Klein, S. Weiner and L. Addadi, *Science* **306** (5699), 1161-1164 (2004).
54. B. Luef, S. C. Fakra, R. Csencsits, K. C. Wrighton, K. H. Williams, M. J. Wilkins, K. H. Downing, P. E. Long, L. R. Comolli and J. F. Banfield, *Isme Journal* **7** (2), 338-350 (2013).
55. J. Lehmann, D. Solomon, J. Kinyangi, L. Dathe, S. Wirick and C. Jacobsen, *Nature Geoscience* **1** (4), 238-242 (2008).
56. M. Keiluweit, J. J. Bougoure, L. H. Zeglin, D. D. Myrold, P. K. Weber, J. Pett-Ridge, M. Kleber and P. S. Nico, *Geochimica Et Cosmochimica Acta* **95**, 213-226 (2012).
57. S. C. B. Myneni, J. T. Brown, G. A. Martinez and W. Meyer-Illse, *Science* **286** (5443), 1335-1337 (1999).
58. J. Roberto and T. Diaz de la Rubia, 2006.
59. IPCC, *Climate Change: The Physical Science Basis - Contribution of Working Group I to the Fourth Assessment Report of the Intergovernmental Panel on Climate Change*. (Cambridge University Press, Cambridge, 2007).
60. Q. Zhang, J. L. Jimenez, M. R. Canagaratna, J. D. Allan, H. Coe, I. Ulbrich, M. R. Alfarra, A. Takami, A. M. Middlebrook, Y. L. Sun, K. Dzepina, E. Dunlea, K. Docherty, P. F. DeCarlo, D. Salcedo, T. Onasch, J. T. Jayne, T. Miyoshi, A. Shimono, S. Hatakeyama, N. Takegawa, Y. Kondo, J. Schneider, F. Drewnick, S. Borrmann, S. Weimer, K. Demerjian, P. Williams, K. Bower, R. Bahreini, L. Cottrell, R. J. Griffin, J. Rautiainen, J. Y. Sun, Y. M. Zhang and D. R. Worsnop, *Geophysical Research Letters* **34** (13), L13801 (2007).
61. I. J. George and J. P. D. Abbatt, *Nat Chem* **2** (9), 713-722 (2010).
62. J. F. Pankow, *Atmospheric Environment* **28** (2), 189-193 (1994).
63. B. J. Murray, *Atmos. Chem. Phys.* **8** (17), 5423-5433 (2008).
64. B. J. Murray, T. W. Wilson, S. Dobbie, Z. Cui, S. M. R. K. Al-Jumur, O. Mohler, M. Schnaiter, R. Wagner, S. Benz, M. Niemand, H. Saathoff, V. Ebert, S. Wagner and B. Karcher, *Nature Geosci* **3** (4), 233-237 (2010).

65. A. Virtanen, J. Joutsensaari, T. Koop, J. Kannosto, P. Yli-Pirila, J. Leskinen, J. M. Makela, J. K. Holopainen, U. Poschl, M. Kulmala, D. R. Worsnop and A. Laaksonen, *Nature* **467** (7317), 824-827 (2010).
66. B. Zobrist, C. Marcolli, D. A. Pedernera and T. Koop, *Atmos. Chem. Phys.* **8** (17), 5221-5244 (2008).
67. T. D. Vaden, C. Song, R. A. Zaveri, D. Imre and A. Zelenyuk, *Proceedings of the National Academy of Sciences* **107** (15), 6658-6663 (2010).
68. J. Crank and G. S. Park, *Diffusion in Polymers*. (London, 1968).
69. F. A. Houle, W. D. Hinsberg and K. R. Wilson, *Physical Chemistry Chemical Physics* **17**, 4412 (2015).

III. Controlling and Deploying Emergent Electronic and Magnetic Phases

Largely through astounding miniaturization over several decades, the power drawn by a single CMOS gate has decreased exponentially for many years. The number of gates on a chip has also increased exponentially, and the net result is that the power needed to run a single microprocessor chip has increased by 20-25% per year for a couple of decades. Devices connected to the Internet now consume 10% of the world's electrical energy, and consumption is projected to increase by over 50% by 2020. Switching a CMOS gate presently consumes about a million times more energy than the Landauer thermodynamic limit of $kT \ln(2)$. There are several emerging platforms that promise much lower power consumption (Figure III.0.1), and SXR science with ultrahigh brightness has played and will continue play an important role in helping to discover and perfect materials and material structures to enable further development of these platforms. Enabling materials for power efficient information processing formed another major focus of the workshop and is examined in this section of the report, which contains chapters on magnetism and spin structures, quantum materials, and emerging transformative technologies in this area.

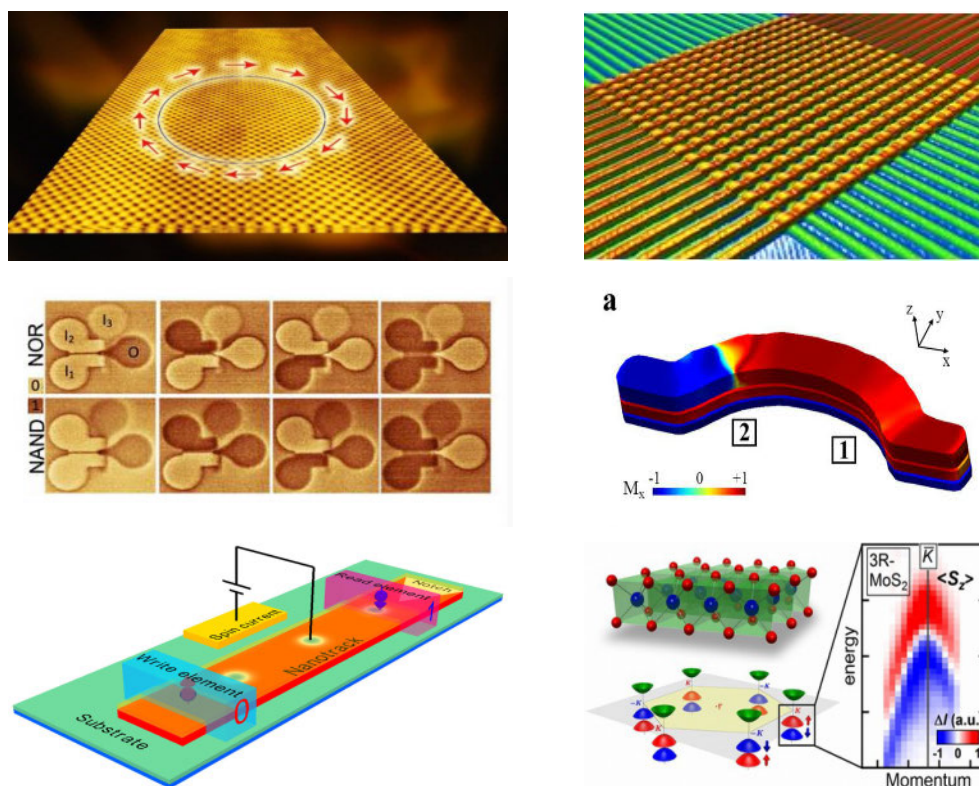


Figure III.0.1: A sampling of paradigms for low power information processing where SXR science has already had a significant impact that will be dramatically amplified by ultrahigh brightness. Clockwise from the upper left: spin currents and quantum computing with topological insulators; memristor crossbar array (courtesy of Stan Williams, HP Labs), spintronic memristor¹; quantum computing with with valleytronics²; skyrmion racetrack memory and processing³; magnetic logic gates⁴.

Creating and controlling currents of spins and spin textures (e.g. skyrmions) are common ingredients in these emerging technologies due to the potentially much lower resistive dissipation and the possibility of quantum computing. Topological insulators were first observed using angle-resolved photoemission with SXR and are now proposed as internal spin sources, spin FETs, and other classical and quantum spintronic logic devices. The advent nanoAPRPES with spin resolution, combined with ultrahigh brightness for efficient focusing, will play an important role in optimizing such devices. For example, the magnetic contrast of SXR imaging and scattering techniques has recently been applied to study skyrmions, and high brightness will revolutionize studies of skyrmion motion and interactions.

Bioinspiration provides another approach to low power processing in the form of neuromorphological devices. CMOS-based neural simulators have made great strides in scalability while vastly reducing power requirements, and are starting to demonstrate useful applications. There is much interest in nonlinear circuit elements like memristors and spin-memristors that promise even much lower power consumption and higher density in 3D architectures. Most memristors operate via electro-migration in a 10-20 nm thick insulating film, a complex process that needs to be optimized by mapping oxidation states with low-nm resolution, on a functioning device. The spatial and temporal resolution and spectral contrast offered by SXR beams from diffraction-limited storage rings will enable such studies.

Before examining a few classes of electronic and magnetic materials in greater detail, we summarize a few crosscutting themes and associated experimental needs:

- Virtually all systems discussed involve hierarchical systems, with magnetic and/or electronic textures extending from an atomic layer to a micron or more, either intentionally patterned or forming spontaneously. SXR probes offer the requisite spectral contrast and spatial sensitivity to probe and understand these structures in detail.
- To process information these structures must also be functional, that is, various degrees of freedom or material textures are in motion, either through an external drive or spontaneously. While many materials proposed for application in information processing have been studied using SXRs, only a few of these studies (e.g., magnetic vortex structures) have probed a nominally functioning structure. Leveraging high brightness to include temporal sensitivity into these studies is an important challenge.
- Finally, the goal is low power processing at or near room temperature, which means that to study a functioning system will require high energy resolution in many instances. The Landauer limit noted above suggests that probing an energy scale for switching of less than kT , or a time scale faster than h/kT , will be very beneficial.

III.1 Magnetism and Spin Structures

Contributions from Hermann Dürr, Y. Idzerda, Z.Q Qiu, John Freeland, Bastien Pfau, Peter Fischer, Hendrik Ohldag, Andreas Scholl, and Elke Arenholz

The magnetic sensitivity and ease of focusing SXR beams have resulted in their providing key information to understand diverse modern magnetic materials and structures. For example, 20 years ago it was just becoming possible using SXR spectroscopy to probe element-resolved magnetic moments in alloys – despite the enormous historical and practical importance of alloys in magnetic materials. Since that time, this sensitivity has been deployed in numerous microscopies offering 10s of nm resolution to routinely probe magnetic textures with enough signal to support a dazzling array of pump-probe studies of magnetization dynamics. Leveraging all this progress with the improved brightness and coherence provided by DLSR sources will further empower many of these now ‘traditional’ SXR techniques. Aside from improved focusing of the laser-like SXR beam, the new sources will enable new techniques that strongly rely on spatial coherence of the beam, such as coherent imaging, ptychography, and holography for imaging at the crucially important scale of magnetic domains, and interferometric detection for high sensitivity spectroscopic imaging of dilute spins and spin currents. These techniques are currently hampered by the low coherent fraction provided by 3rd generation sources, leading to low signal levels and exposure-time-limited resolution and sensitivity.

In the field of magnetism we envision the development of new techniques, which allow vectorial measurements of the spin and orbital moments by using polarization dependent spectroscopy at nanometer resolution. We envision tomographic measurements with nanometer depth resolution, either through 3-dimensional imaging or diffraction techniques, or by using standing wave methods combined with nanometer spatial resolution. We envision measuring ultra-small magnetic effects at interfaces or produced by spin currents and spin accumulation in nanostructures using fast differential and interferometric measurement techniques.

These advances will be realized by combining powerful spectroscopic techniques, such as XMCD and XMLD, vector magnetometry, and resonant x-ray scattering with ultrahigh resolution imaging techniques such as STXM, ptychography, CDI, and holography, ultimately limited by diffraction to about 1 nm in the SXR range. In the following sections we provide more details about a few examples of classes of materials that were discussed at the workshop where these sensitivities will be crucial to develop a firm understanding of emergent material properties and how these materials function in devices.

Nano-Engineered Transition Metal Oxides for Energy Applications

Semiconductor based electronics have revolutionized how we collect, process, use and store information. However, semiconductor devices rely on electrical currents and transient electric states, causing them to be inherently dissipative and therefore energy-inefficient. New materials and designs are needed for future information processing that combine and dramatically expand the characteristics of Si based devices with energy-efficiency rivaling that of information processing in the human brain. The function of a semiconductor material is governed by the

doping controlled electronic density of states and the shape of the electric potential at interfaces. The next materials breakthrough will come from atomic-scale integration, based on advances in materials engineering. Such nano-engineered materials offer new opportunities for the efficient control of information processing.

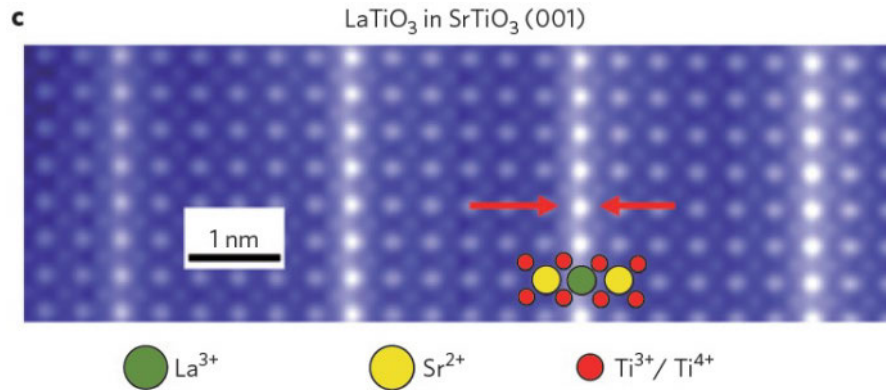


Figure III.1.1: Scanning transmission electron microscopy image of a LaTiO₃/SrTiO₃ superlattice, which supports metallic interfaces – which become superconducting at low temperature - even though both components are wide gap insulators. The red arrows show the lanthanum layer.⁵

An important highly flexible class of materials to explore are complex oxides, which possess emergent phenomena that arise from strongly competing interactions.^{6,7} In heterostructure form, they offer many opportunities to create new phases in a controlled manner.⁸⁻¹⁰ One compelling example is the recent observation of a 2-dimensional highly conductive interface layer formed in stacks of otherwise insulating materials LaAlO₃ and SrTiO₃ (Figure III.1.1).¹¹ Transition metal oxides exhibit a wealth of phenomena that can be exploited in devices, reaching from magnetism, superconductivity, multiferroicity to more exotic phenomena such as the fractional quantum hall effect, charge and orbital order, and the spin Hall effect.

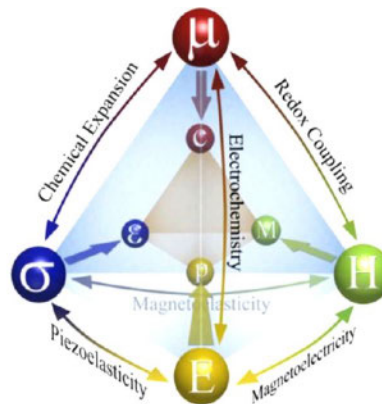


Figure III.1.2: Diagram illustrating the relationships between mechanical, chemical, electrical, and magnetic properties of a crystal. The corners of the outer tetrahedron may be thought of as 'forces' applied to the crystal, with the corners of the inner tetrahedron representing the direct response of the crystal to these forces. The bold arrows from the outer to inner tetrahedron represent principal effects.¹²

Beyond simply creating unique phases is the ability to rationally control the state in these emergent materials. From an energy perspective the control with optical¹³ or electric fields¹⁴ is potentially an efficient pathway if we can understand the fundamental science. While many people have focused on trying to use electric field for direct charge control in oxides, new

opportunities have arisen with respect to control of materials that can be programmed in new ways by their chemical and electrochemical environment (see Figure III.1.2).^{12,15} Recent work has highlighted the controlled stabilization of related oxygen deficient phases using oxide hetero-structures.^{16,17} This approach allows direct control of metal vs. insulating phase as well as possible elements of brain-like (neuromorphic) electronic circuits. In the context of magnetism, it also offers the potential of creating ferromagnets that could be dynamically converted to drastically different magnetic phases (antiferromagnetic) in a reversible manner, which would create wholly new avenues for the realm of spin based electronics or other applications since no such materials exist today.

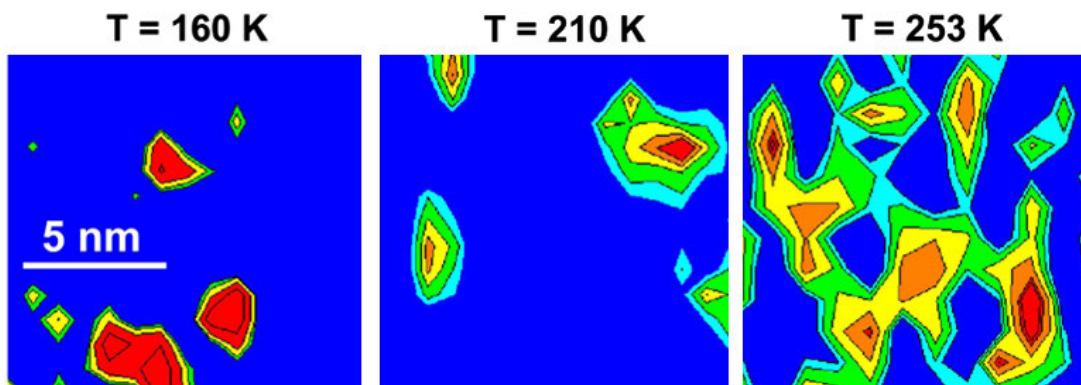


Figure III.1.3: Phase separation in $\text{La}_{0.55}\text{Ca}_{0.45}\text{MnO}_3$ visualized using scanning electron nanodiffraction as the temperature is raised through a metallic ferromagnetic – insulating paramagnetic transition.¹⁸ The color scale corresponds to the intensity of charge-ordered Bragg reflections, and reflect intrinsic heterogeneity on the scale of $\sim 3\text{-}4$ nm.

The functionality of transition metal oxides is governed by their response to changes in temperature and other thermodynamic variables. Often systems undergo hysteretic transitions, show nanoscale phase separation, phase coexistence, and complex phase diagrams. Some effects such as colossal magnetoresistance depend on the nanoscale structure near a phase transition and result from percolative transport. Phase separation in complex oxides can be the result of variances in chemical doping, strain, or an electronic phase separation. As an example, Figure III.1.3 shows nano-diffraction images of competing structural phases in LCMO at the phase transition between an insulating, paramagnetic high temperature state and a metallic, ferromagnetic low temperature state.¹⁸ The regions are 3-4 nanometers in scale. Nano-scale x-rays spectroscopy, diffraction and scattering are ideal for the study of such competing ordered phases and can go beyond structural measurements because of their selective sensitivity to charge order, chemistry, orbital, and spin magnetism. Nanoscale phase separation in manganites and fluctuating stripe patterns in cuprates¹⁹ are dynamic phenomena and current static imaging techniques rely on weak disorder pinning the pattern near a quantum critical point. Fast, coherent x-ray enabled imaging techniques, such as STXM and ptychography, will allow us to image fluctuating stripes and phase separated regions in real time without the need to rely on disorder stabilizing and freezing the fluctuating state.

Designing next-generation atomic-scale integrated materials will require tools sensitive to electronic and magnetic properties on a nanoscale, down to 1 nm in dimension, the ability to distinguish surface and interface properties and the extension to 3D imaging in layered structures. The ability to apply magnetic fields and supply voltages and currents during imaging will be essential for in-operando studies. Transition metal oxides are just one prototypical new class of materials that require atomic control and sensitivity. High brightness enabled x-ray spectroscopy and microscopy techniques will be similarly needed in next generation electronic materials such as topological insulators or graphene based systems and high-brightness techniques will find broad application in material design and optimization.

Topological Insulators

X-ray techniques have been instrumental in understanding the electronic properties of novel materials, in particular of a new class of matter: topological insulators (TI). TIs are characterized by a bulk band gap similar to that of a conventional insulator but have conducting surface states. The band structure of a TI resembles that of an integer quantum hall state system but the surface conductivity is created intrinsically through spin-orbit interaction without an external magnetic field (Figure III.1.4).^{20, 21} The conductive surface state is topologically protected and insensitive to impurity scattering, the electron transport occurs with little or no dissipation. The carriers resemble massless Dirac fermions and show very little interaction with lattice excitations or defects while the direction of the spin is locked to the electron momentum, causing spin-up and spin-down electrons to flow in opposite directions.

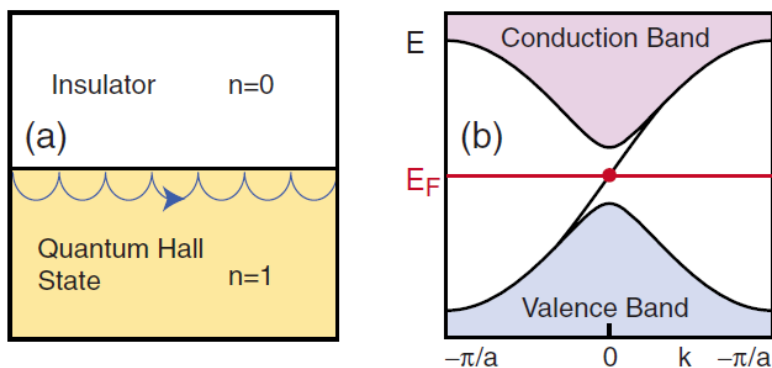


Fig. III.1.4, left: Chiral edge mode at the surface of a quantum hall state. In a topological insulator the extrinsic magnetic field is replaced by the intrinsic spin-orbit interaction, doubling the spin split surface states and locking momentum with spin direction. Right: The surface state has a Dirac-like dispersion inside the band gap of the bulk electronic structure.²²

The peculiar surface band structure and the transport properties of TIs have led to a wide array of proposed applications in the area of spintronics and low-power computing, utilizing the dissipationless charge transport and the unusual interaction of the surface of a TI with other materials. Interaction with an s-wave superconductor is predicted to create a Majorana fermion quasiparticle state, which is its own antiparticle and may find application in quantum computing. Interaction with ferromagnets has been shown to generate an extremely large spin-transfer

torque, greatly exceeding the torque produced by conventional high Z conductors based on the regular spin hall effect. Magnetization switching through this giant spin-orbit torque demonstrated recently²³ promises a much more efficient method of controlling and generating spin accumulations in spintronics devices (Figure III.1.5).

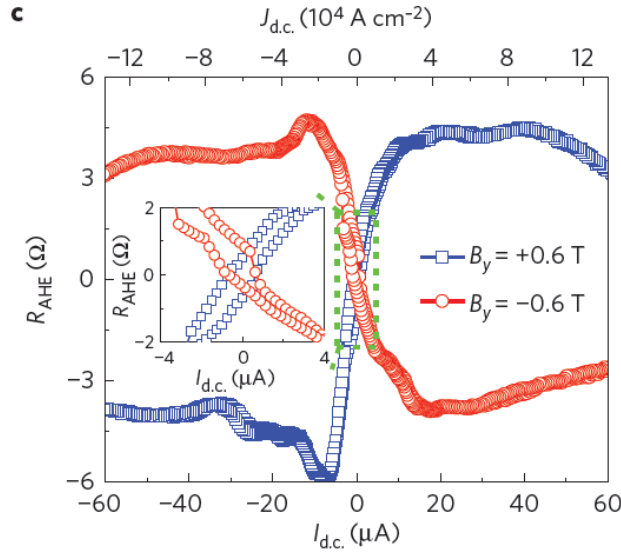


Fig. III.1.5: Switching of a ferromagnetic chrome telluride film by a current running through a TI for two directions of an external magnetic field, visible as hysteretic change of the Hall resistance as function of current.²³

X-rays techniques have proven the Dirac-like dispersion of electron bands near the Fermi level and the existence of conductive surface states. They can be used to study the intrinsic symmetry of the system and they are instrumental in understanding the interaction of quasiparticles with other degrees of freedom, for example magnons and phonons. Next generation light sources with unprecedented brightness and coherence will allow us to study the band structure and excitations with much higher energy resolution through interferometric techniques, combined with much higher spatial resolution using nanofocusing or holographic techniques. Combining spectroscopy with spatial resolution will be critical for studying the interaction of novel materials near defects, electrodes, and patterned overlayers. For actual device application, knowledge of the electronic structure on a length scale of nanometers will be needed to account for effects of domain boundaries and edges. For example, a magnetic material brought in contact with a TI should open the surface band gap while a domain wall with opposite direction of the magnetization to left and right of the wall should create a 1D chiral edge state across the wall (Figure III.1.6).²² Both effects can be characterized using x-ray techniques such as ARPES and RIXS and require next generation light source to reach the required energy and spatial resolution of nanometers, typical for the width of a magnetic domain wall.

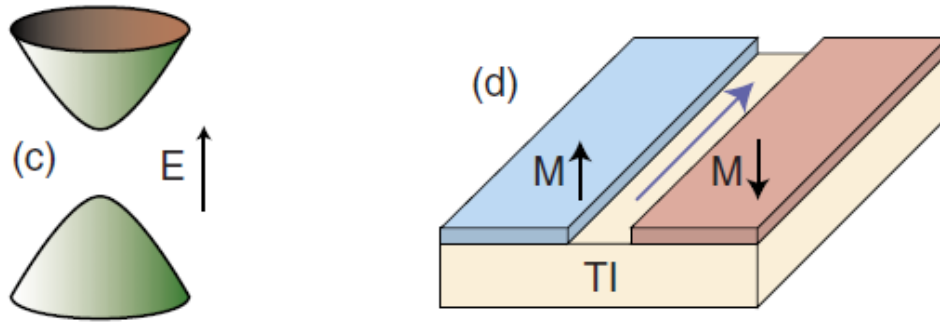


Fig. III.1.6: Predicted opening of the band gap in contact with a ferromagnet and chiral edge state near a domain wall or transition between opposite magnetic states.²²

Data Storage and Skyrmions

Magnetic storage approaches fundamental limits as the magnetic recording density reaches 1 Tbit/ inch². At this density the surface approaches the volume in the fraction of magnetic centers. The response to magnetic fields and the environment starts to be dominated by the non-collinear magnetization near the surface. The fundamental length scale governing non-collinear magnetic structures is the magnetic domain wall width, which is just a few nanometers for high anisotropy magnetic materials. Methods that can image the non-collinear magnetic state of a magnetic domain wall are of critical importance to emerging magnetic materials and technologies.

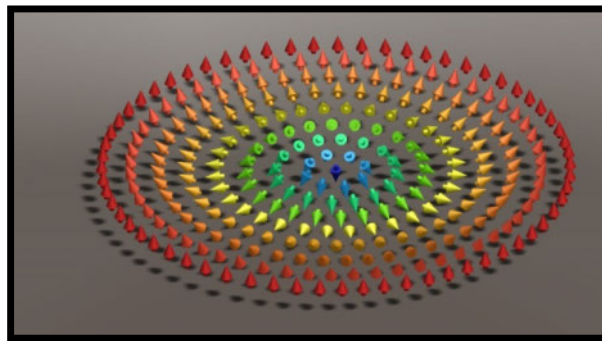


Figure III.1.7: Micromagnetic model of a ~10 nm-size skyrmion spin spiral. Skyrmions are ideal containers of magnetic information because of their topological stability and the low coupling to the lattice, which leads to low threshold for current-driven transport and low dissipation.

Skyrmions constitute particularly interesting nanoscale, chiral magnetic structures because of their stability and their intriguing transport properties (see Figure III.1.7).²⁴⁻²⁶ Skyrmions can be interpreted as 3-dimensional magnetic states of a sphere, projected onto a 2-dimensional surface. Skyrmion states are related to magnetic vortices and their structure is characterized by a single, integer number, the skyrmion number. Because of their particular topology, skyrmions cannot be continuously transformed into a collinear domain state without transitioning through a singularity. The skyrmion state is therefore topologically protected, it is stable against external

magnetic fields and Skyrmions repel each other, forming lattices reminiscent of vortex patterns in type II superconductors. Skyrmion ground states can be found in materials with non-centrosymmetric structure²⁵ but they can also be created in more generalized structures that lack inversion symmetry, e.g. thin films with a vacuum interface,²⁷ or in magnetic bilayers consisting of materials of different anisotropy.²⁸ The quest for systems with a skyrmion ground state at room temperature is open and high-resolution element-specific imaging techniques will be particularly useful for heterogeneous systems, for example magnetic multilayers.²⁹

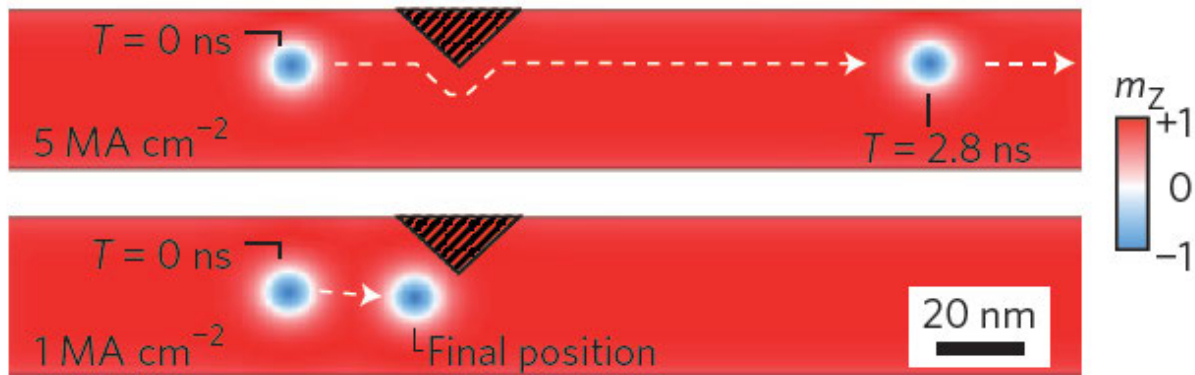


Figure III.1.8: Simulated motion of a skyrmion in the presence of a defect at high (top) and low current density (bottom).³⁰ Time-resolved x-ray imaging will be capable of resolving the micromagnetic structure of the skyrmion while interacting with the defect.

Skyrmions may find application in racetrack-like memory devices as topologically protected storage of information (see Figures III.0.1 and III.1.8).³⁰ Studies have shown an extremely low electrical current threshold driving skyrmion motion compared to traditional domain wall devices, promising much low power consumption and higher reliability for a non-volatile magnetic memory.³¹ The potentially small size of thin film skyrmions (nanometers) compared to regular domains (10s of nanometers) will greatly increase the achievable storage density and the reading and writing speed, which is limited by the speed of their motion divided by their size.

Imaging and controlling the creation, transport, detection, and annihilation of a skyrmion in a magnetic nanowire is a critical stretch goal for synchrotron radiation based imaging techniques. Because of the very small size of the of the skyrmion spin spiral a spatial resolution of nanometers is required. A high temporal resolution is also desirable in dynamics studies aimed at understanding the creation of skyrmions and the pinning and depinning process at defects. Coherent imaging techniques, such as holography or ptychography will have the resolution required to image the spiraling magnetization within a skyrmion, the deformation of the magnetic structure near defects and the interaction of skyrmions with each other. High brightness coherent x-ray sources are needed to reach the required spatial resolution and will allow imaging the dynamics of skyrmions.

Electrical Control of Magnetism

Magnetic memory technology is based on the long-time stability of stored magnetic information and the simple readout scheme provided by giant magnetoresistance or tunnel magnetoresistance. However, traditional writing methods based on macroscopic magnetic fields are cumbersome and require a high investment in energy per bit of information because magnetic fields have to overcome the high anisotropy of the storage material and are not well localized. Direct electrical control has been explored as an alternative and experiments have tested a variety of control schemes based on intrinsic magnetoelectric coupling in magnetic multiferroics, strain coupling, the converse piezoelectric effect, and electrically manipulated exchange coupling and bias.³² Recent experiments tested an electrical writing scheme using multiferroic BiFeO₃ and demonstrated reversible switching by 180° of magnetic islands through exchange coupling with the weak Dzyaloshinskii–Moriya interaction induced magnetic moment of bismuth ferrite (see Figure III.1.9).³³ The domain structure within the device is a result of the complex, nanoscale electric and magnetic domain structure of multiferroic BiFeO₃.

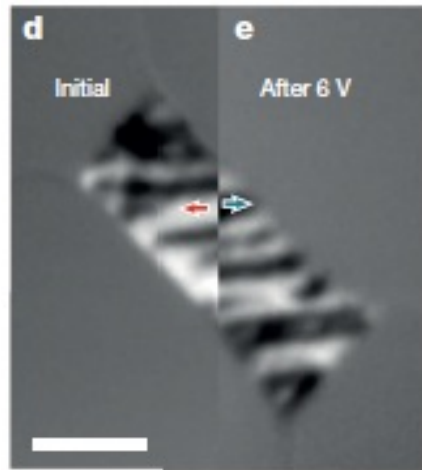


Figure III.1.9: Magnetic domain structure in a micron-scale CoFe/BiFeO₃ bilayer magnetoelectric device before and after applying a voltage to the multiferroic BiFeO₃.³³

A grand challenge in the field of electrical control is imaging the ferroelectric and magnetic microstructure and the kinetics of the switching process of devices that are scaled down in size by two or even three orders of magnitude. This will localize the device within a single ferroelectric domain and will lead to storage densities competitive with other technologies. Imaging of sub 10 nm size multiferroic structures and speed of sound limited switching kinetics will require significant advances in imaging techniques. X-ray imaging, in particular based on scanning probe techniques, will play a significant role because of the ability to detect ferromagnetism, antiferromagnetism, and ferroelectricity in parallel³⁴ and will be needed to disentangle the switching mechanism, determined by the complex magnetic and electric energy landscape of the material.

Current Induced Spin Dynamics

Classic magnetization dynamics are observed when a magnet is exposed to a fast rising magnetic field pulse. These phenomena are relevant for magnetic switching in today's magnetic devices, like e.g. hard drives or acceleration sensors. However, the challenge for field induced switching processes is that while they are well understood and can be easily engineered on a scale of a few hundred of nanometer, they are not easily applicable to the smallest nanostructures. Crosstalk between devices in close proximity is just one of several road blocks in this field. For this reason, the scientific as well as the technological community has pushed new disruptive ideas forward to manipulate magnetization on the nanoscale by engineering complex nanostructures. These new concepts allow for e.g. manipulation of magnetization assisted by heat application or magnetic switching by local currents. The latter one employs the fact that any electric current consists of spins with a distinct magnetic moment. The interplay of charge and spin current results into a plethora of new and exciting spin transfer and spin current induced effects that have been reported over the past decade.³⁵

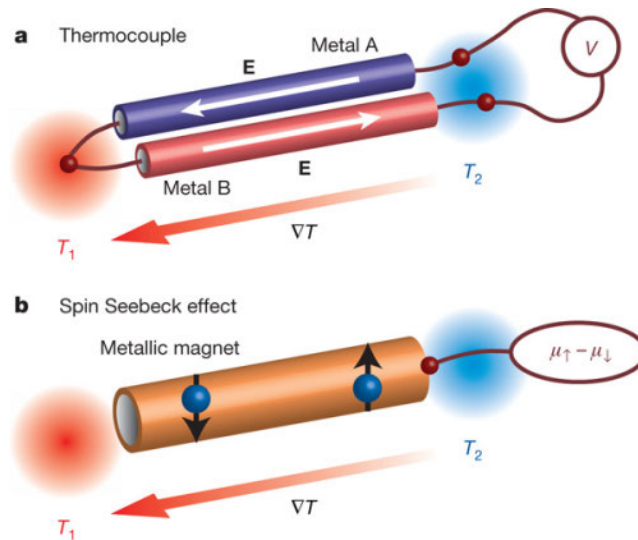


Figure III.1.10: **a)** Illustration of a thermocouple.³⁶ A thermocouple consists of two conductors (metals A and B) connected to each other. They have different Seebeck coefficients and, thus, the voltage V between the output terminals is proportional to the temperature difference $T_1 - T_2$ between the ends of the couple. **b)** Illustration of the spin Seebeck effect. In a metallic magnet, spin-up (\uparrow) and spin-down (\downarrow) conduction electrons have different Seebeck coefficients. When a temperature gradient is applied, a spin voltage $\mu_{\uparrow} - \mu_{\downarrow}$ proportional to the temperature difference appears.

For this reason the field of current induced spin dynamics has evolved into one of the most active fields in magnetism. Many experimental studies rely on evaluation of the macroscopic transport properties but do not provide any insight into heterogeneity of the spin dynamics or the role of different materials or elements in the nanostructures, which often exhibit a complex composition. Recent advances in instrumentation have opened the door to observe the small changes in magnetization that occur when a spin polarized current flows from a ferromagnet into a non magnet.³⁷ Combination of high spatial resolution in a STXM (25 nm), with a time

resolved (50 ps) bunch-by-bunch detection method enables us to detect changes of the magnetization of 10^{-5} in state of the art nanostructures. With these experimental tools now available and in mind it is possible to look forward and address new challenges in the area of current induced spin dynamics as well.

One possible example that we would like to mention in this context is the Spin-Seebeck effect, reported by Uchida et al.³⁶ Similar to the classic Seebeck effect that is used in a thermocouple and leads to a voltage across two terminals due to a temperature difference, the Spin-Seebeck effect leads to a spin voltage or magnetic moment across a conductor in response to a temperature gradient, see Figure III.1.10. The detection of the Spin-Seebeck effect in real space and the correlation between device structure, composition and lateral variation of the spin voltage requires a probe that provides ultra high sensitivity to magnetic moments. The ability to do so will provide critical information about the atomic processes that are relevant for the Spin-Seebeck effect. Such insight cannot be directly obtained using macroscopic probes. An ultimate storage ring with its creased coherent flux, intrinsic high stability and reproducibility between x-ray bunches provides exactly the probe which is needed for these experiments.

III.2 Quantum Materials

Contributions from Peter Johnson, Peter Abbamonte, Hong Ding, D. J. Huang, Alexei Preobrajenski, Zahid Hussain, Ernie Glover, Yi-De Chuang, Sujoy Roy, Allan MacDonald, T.-C. Chiang, Yves Petroff, Thorsten Schmitt, Tom Debereaux, Aaron Bostwick, Luca Moreschini, Karsten Horn, Sung-Kwan Mo, Aexei Fedorov, Jonathan Denlinger, Eli Rotenberg,

The most pressing issue our world faces is reducing the impact of energy generation, conversion, transport and consumption. Without doubt new materials will be the key to addressing these global problems. For example, if we increased the temperature at which superconductors operate, we could reshape how the world generates, distributes and consumes energy. But this is only the beginning of the vision that controlling the properties of new materials could realize.

Today, computer logic uses only the basic aspect of electrons- their charge - to manipulate information. By also using another basic property - their spin - we could transform computing, not only making it consume far less energy, but also go beyond today's limitations in computer speed and facilitating new paradigms of quantum computing and neuromorphological processing.

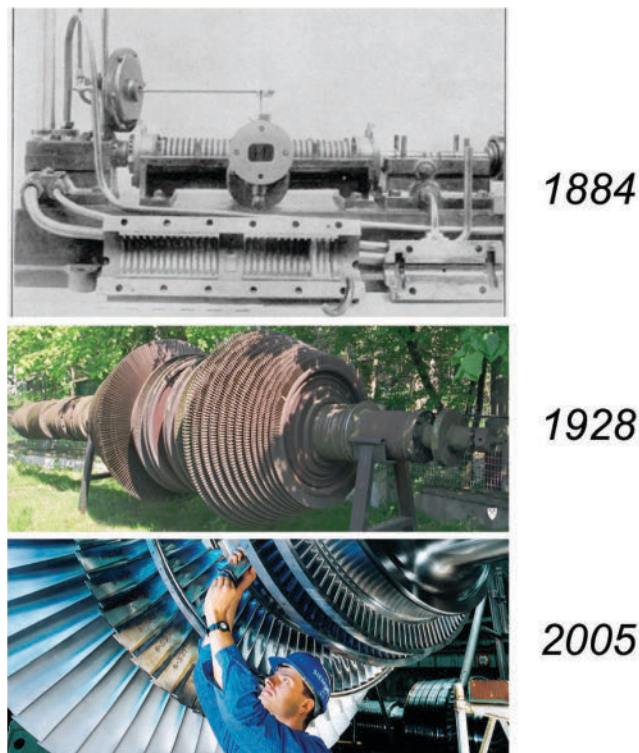


Figure III.2.1: Energy Conversion over the years hasn't changed much.

To convert power from the easiest form to generate (heat) into a useable form (electricity) we use a mechanical technology (steam turbines) that has hardly changed in form since its

invention in the 19th century (see Figure III.2.1). But if we can create solid-state materials to efficiently convert heat into electricity, we could transform the power generation from expensive, centralized, environmentally costly sources (fossil fuel and nuclear plants) to smaller, cheaper, decentralized renewable sources (solar, geothermal).

In order to achieve these goals, we need to answer the most important question we can ask about any material: “Where are the electrons, and how do they move and interact with each other and other excitations in the system?”

The answer to this question for simple materials developed in the modern era of cheap, accessible technology from transistors to smartphones – all powered by cheap accessible energy. But further progress is difficult unless a “quantum leap” forward in understanding how electrons move can be accomplished. The key problems that we have to deal with are:

- the complexity of materials is increasing, in terms of
 - number of elements of the periodic table combined in a material
 - the hierarchy of length scales that are needed to achieve functionality
 - the combination of multiple functionalities in a single material
- the multiple degrees of freedom that are important
 - electrons interact with atoms and each other, both through the charge and spins of the electrons and nuclei
- the rules of the game are changing
 - We know how one or two electrons interact with each other when we push them around, but when many electrons get together, how they behave can be very hard to predict.
 - We know how perfect materials behave, but new functionality can arise from intrinsic and extrinsic disorder in ways that are difficult to describe.

And yet, out of this complexity have emerged new materials with highly ordered, coherent ground states like high temperature superconductors that, while providing tantalizing new properties that are already changing our lives, point to the possible existence of even better materials. The problem is that we still don’t know, nearly 30 years after their discovery, how these materials work. The study of such materials, how such degrees of freedom as electron charge, orbit, and spin interact with material structure, requires an exquisite understanding of quantum mechanics, and such materials are called quantum materials (QMs).

As in the past, the development of new materials requires the new tools to learn how to measure and control their properties. These tools will have a two-fold purpose:

(1) Guiding our understanding. Developing the tools to study the most fundamental properties of the electrons, in order to enhance our ability to understand them and improve their properties.

- Where are the electrons?

- How do they move when we push them around?
- How does their behavior change when we play with the structure and composition of their host materials?
- How do these properties change as material performance improves?

(2) Discover new paradigms and platforms. Developing the tools to screen new materials for optimized properties, in order to perform systematic studies (combinatorial, or “shotgun” approach), or to accelerate serendipitous discovery.

Tool Box to Study Quantum Materials

We know a lot about the right kind of tools that we need to understand how things work. Can we guess how a piano works only by hearing its sound? A good start is to analyze the sound when different parts are hammered until a picture of the overall structure emerges. By analogy, we can learn how a material works by “hitting” the electrons, and “listening” to their frequencies. One of the best hammers for hitting the electrons is a high-energy beam of light that can excite the different degrees of freedom in the material. This means we need to generate suitable x-rays.

There are several good ways to listen to the electrons:

- (1) Knock the electrons out of the sample and interrogate their properties directly, using x-ray angle-resolved photoemission spectroscopy (ARPES). This tells us the energy and momentum of the charged excitations in materials.
- (2) Measure the light that the electrons give off in response using resonant/non-resonant inelastic x-ray scattering (RIXS/IXS). This tells us the energy and momentum of neutral excitations in materials, which is critical to understand the internal degrees of freedom. We can also convert this information to spatio-temporal images of electronic excitations.
- (3) Optical measurements such as near-edge x-ray absorption fine structure (NEXAFS).

So, we will need not only suitable x-rays to perturb our materials, but the means to detect x-rays and electrons. Why are substantial improvements needed in the generation of suitable x-rays? What detector improvements are needed? We will discuss this in the next sections.

Brighter X-ray Sources Open New Horizons in Space and Time

A very important theme arises when interactions between particles occur in nanoscale materials: non-locality. Particles interact with each other, but because of their confinement, the environment can mediate this interaction in complicated ways. In the nanoworld, there is a convergence of length and time scales: electron interactions occur on the 10-100 attosecond time scale, but in 100 asec, the speed of light carries the information about the interactions a distance of 30nm. So a full understanding of interactions in nanomaterials requires characterizing both the spatial and temporal landscape of the interactions.

In the previous century, we were interested in materials like semiconductors whose properties did not change much when they were reduced in size, except in easily predictable ways that could be modeled without considering multiple interacting degrees of freedom. So, the size of the sample studied was often not terribly important.

As the introduction emphasized, we are now interested in materials whose behavior is qualitatively different, and depends on the sample geometry in ways that are difficult to predict. For example, two well-known simple materials, SrTiO₃ and FeSe, become superconducting at very low temperatures (1K and 15K), but it was recently shown that a thin film of FeSe deposited onto SrTiO₃ is a superconductor at much higher temperature than the bulk material.³⁸

This example shows how very important the role of heterogeneity can be, in the form of new properties that develop at interfaces between materials. But substantially more heterogeneity is possible. In particular alloying Te with FeSe can further enhance superconductivity, but when alloys are created, a substantial variation *in composition can be observed, especially near the boundaries in phase diagrams*. We will need to characterize this innate inhomogeneity, and relate it to performance metrics (such as superconducting transition temperature). Can we control this inhomogeneity by engineering means, such as patterning through lithography or selective implantation? This will be essential in order to continue progress in superconductivity research, and indeed, in research on many classes of complex materials.

The ultimate goal for QM research is the enhancement of global properties of materials - things that can be measured with simple tools like a voltmeter - through the control of nano-, meso-, and microscopic degrees of freedom. But when such freedom exists, it is very difficult to work back from the global properties how these degrees of freedom are important. Our probes need to work on these same length and time scales as the inherent fluctuations in properties so that we can learn how the different pieces come together. We now list four examples of how energy research can be impacted.

Superconductivity

As a classic example, the superconducting gap of so-called Bi2212 high temperature superconductors was shown to vary dramatically with position (see Figure III.2.1).³⁹ It is highly desirable to know both the chemical distribution and electronic properties that are behind this inhomogeneity, which can be probed by the ARPES and resonant inelastic XSR scattering (RIXS) methods. Presently nanoelectronic probes (ARPES, RIXS) are envisioned with 50 nm (although not better than about 100 nm was achieved to date). This is useful for many materials, but as Figure B indicates, such resolution is useless for the probing of high T_c materials on the length scales relevant to this heterogeneity. By focusing the x-rays down to the 5 nm scale, we will gain a factor of about 20 spatial resolution beyond what is presently available. This will enable nanoscale dynamics of emergent properties like high temperature superconductivity for the first time.

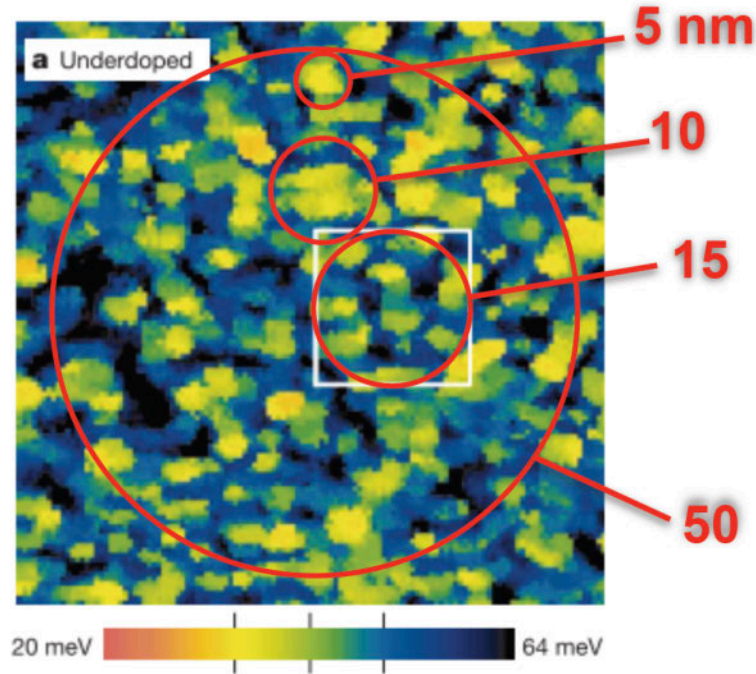


Figure III.2.2: Spatial inhomogeneity of electronic properties in Bi 2212 high T_c superconductors,³⁹ compared to length scales probed by possible DL light sources. 50 nm is the current target resolution enabled by the MAESTRO beamline at the ALS. 5 nm is the minimum resolution needed for isolating pure domains.

Single nano-object analysis

A second example concerns the flow of energy in nano-objects such as quantum wires (See figure II.2.3). What happens in a nanowire, in which the phonons and the electrons are both confined to one-dimension? The electrons and the phonons will interact not only with the wire, and any functionalization, but also with each other. This will affect both the entropy and charge transport in a way that can be potentially useful for advanced thermoelectrics or sensors.

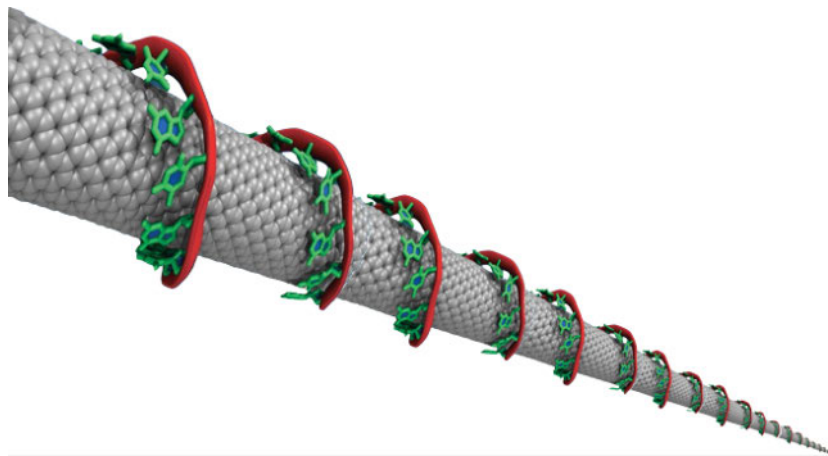


Figure II.2.3: A functionalized nanoobject, optimized for interacting with the environment, heat conduction and electronic transport. Illustration: adapted from Ref. 40.

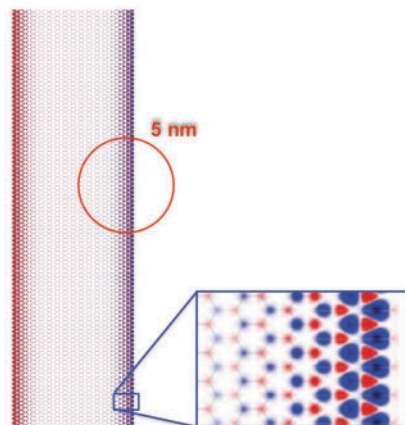


Figure III.2.4: Nanoribbons are expected to have spin-polarized edge states.⁴¹

Low energy electronics/spintronics:

Reducing the energy consumption of electronics is in principle possible when spin, not charge degree of freedom is used for logical manipulation in circuits. One of the most promising material systems are the edge states of graphene nanoribbons, which are predicted to be spin-polarized depending on their atomic arrangements (Figure III.2.4).⁴¹ Equally promising are the spin-polarized edge states of topological insulators, which are expected to be robust against disorder. Spin-polarized ARPES will be revolutionized by recent developments of extremely efficient spin polarized detection.^{42,43}

Brighter X-ray Sources Accelerate the Pace of Discovery

Although synchrotron radiation sources are traditionally thought of as characterization tools, qualitatively different kinds of experiments can be performed at DL light sources. In particular, far more efficient focusing of light is possible, not only at nanoscale resolution, but also at the microscale (1-5 μm). These complementary spatial resolutions enable not only nanoARPES and nanoRIXS/IXS, for the smallest sample volumes, but also microARPES and microRIXS/IXS, which will have more than 100 times the flux and 10 times better energy resolution than their nano- counterparts. These new tools will dramatically lower the required sample volumes, enabling studies of a far wider range of materials than have heretofore been possible to study. In particular, the factory production of samples for combinatorial analysis will be enabled. This can be expected to greatly enhance the pace of discovery, as well as the validation of new theories that are expected to be developed to explain emergent and complex phenomena.

Other Enabling Technologies

In order to fully exploit the brighter beams that will be offered by DL light sources, there are additional developments that shall be needed, in the areas of detector efficiency, photon delivery systems and ancillary facilities.

Detectors

One of the most important new developments are spin-polarized electron detectors. Notoriously inefficient, spin detectors have recently made huge strides by exploiting new scattering materials and parallel detection schemes. These schemes rely on short-lived materials and complex data analysis and need to be improved both to enable turn-key operation and longer detector lifetime.

High-resolution particle imaging detectors should also be improved, especially by enabling higher pixel densities. This can increase the energy resolution of RIXS detectors, or increase the spatial resolution of RIXS experiments, or conversely reduce the size of RIXS spectrometers to increase detected angular range, reduce cost and increase instrumental stability.

Photon Delivery Systems

A rule of thumb is that to study a phenomenon that occurs at a temperature T [°K], the energy resolution needed in meV is about $T/10$. Judging by this standard almost all light sources fail to achieve the desired resolution at $T=10\text{K}$, the temperature of typical normal superconductors. So all of the tools discussed require high energy resolution, and none more demanding than x-ray scattering requires high energy resolution at relatively high photon energies. New beamlines coming on line will achieve 15 meV at 1 kV photon energy, but the next generation needs to aim for even better resolving powers.

Sample Delivery Systems

DLSR sources will require sample pipelines with sufficiently high throughput to exploit their capability for systematic studies. Traditionally, photoelectron spectroscopy has required atomically precise surfaces, but as X-ray scattering detection efficiency improves, RIXS and IXS will be applied to ever smaller sample volumes in the future, making surface contamination an issue there as well. Control of surface quality will therefore depend on placing sophisticated sample preparation facilities in closer proximity to the beamlines, ideally so that sample surfaces that are prepared can be transferred to the analysis chambers without leaving the ultra-high vacuum envelope.

III.3 Enabling Transformative Information Processing Technologies

Contributions from John-Paul Strachan, Jeff Bokor, Mike Crommie, Peter Fischer, Z.-Q. Qiu, Hendrik Ohldag, Andreas Scholl, and Elke Arenholz

Understanding the materials physics of multiferroics, graphene, topological insulators and many other emerging electronic and magnetic materials is often related to an important practical goal: to enable transformative technologies for ultralow-power information processing. Smaller microelectronic devices operate with lower power, but this is more than offset by the ever-increasing density of transistors on a chip: the power dissipated by a microprocessor has increased by typically 20% per year even though the energy consumed by a single logic operation has fallen exponentially with Moore's law. For this reason there is a pressing need to develop materials that enable ultralow-power electronic devices and device architectures that reduce power consumption.

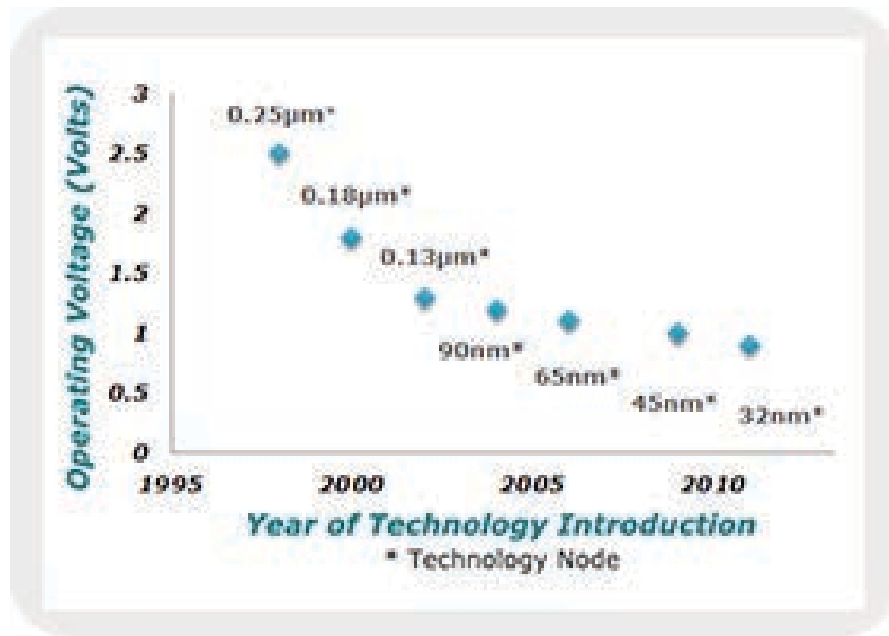


Figure III.3.1: As a transistor becomes extremely small, the operating voltage has not decreased substantially because of increasing leakage in the OFF state. The wires connecting the transistor, however, could function with only a few millivolts if there were a millivolt switch. Since energy consumption is proportional to the square of operating voltage, the energy used to manipulate a single bit of information today is 10^6 times greater than needed in an ideal system. Besides energy for switching, an IC chip also consumes energy for communications among the transistors, through the interconnects has continued to rise steadily to a larger portion of the total consumed power. Thus, the entire problem of energy consumption by ICs must include tackling the energy consumption by transistors and interconnects. [Ref. <http://www.e3s-center.org/research/index.htm>]

To engineer these functional systems and to control material function we need to be able to characterize and correlate composition, atomic, electronic, and magnetic structure on the nanometer scale and on time/energy scales relevant for fluctuations induced by thermal energy. SXR spectroscopy, scattering and imaging techniques are powerful characterization tools to address and fill this need and the capabilities of all of these will be dramatically expanded with

the commissioning of DLSR sources. Utilizing resonant excitations from tightly bound core states to empty low energy electronic states characterized by lattice symmetry, electron localization as well as spin order, x-ray absorption provides detailed element-specific information about atomic, electronic and magnetic structure with very high contrast. ARPES and RIXS measure minute details of the electronic structure and important low energy excitations, respectively. Scattering experiments probe local order on the nanometer scale of the x-ray wavelength. Scanning a tightly focused x-ray beam across the samples or inverting diffraction pattern to real space images allows nanometer spatial resolution for all techniques mentioned/listed above.

Unlike charge currents, spin currents travel in materials without dissipating energy, and furthermore spins may be used to store information. Spintronics, the manipulation of spin currents in devices, not only promises to consume less energy than today's electronics, but can also enable new technologies like quantum computers and cyber-secure encryption schemes. Magnetic and spintronic materials can be ideally studied with polarization-dependent SXR techniques, since these provide quantitative magnetic information with element specificity, sensitivity to the valence state of the absorber, and the symmetry of the absorber site. Moreover, photon-in/photon-out SXR microscopes provide nanometer spatial resolution with ~100nm probing depth that is ideal for probing individual components in multilayer stacks and nanoscale patterned devices in applied magnetic and electric fields. DLSRs will provide unique capabilities for imaging domains and domain walls in 3D with nanometer resolution as well as quantifying magnetization dynamics and fluctuations on the timescales relevant for domain wall motion.

Many structures using emergent electronic and magnetic materials discussed in the previous two chapters have been proposed for applications in information storage and processing, both classical and quantum. The spectral, spatial, and temporal dynamic range of SXR techniques using DLSR sources will be ideally suited to probe many of these candidate structures as they function. The following sections provide brief descriptions of a few of these, and indicate the relevant SXR capabilities.

Devices Based on Magnetic Domain Walls and Textures

Magnetic nanostructures are already at the heart of devices in information storage today; best known is the computer hard drive where information is stored in magnetic domains imprinted in media and read using giant magnetoresistance in magnetic thin film heterostructures as read heads. But hard drives based on mechanical motion pose power consumption challenges, a paradigm shift toward novel solid state magnetic storage devices is occurring. An example is the racetrack memory based on magnetic domain walls moved by spin currents in 3 dimensions (see Figure III.3.2).⁴⁴ The concept is evolving to include other magnetic textures like skyrmions (Figure III.0.1), which are both topologically stable and very weakly coupled to the lattice and therefore can be moved with little dissipation. Also, information processing relies on conventional logic devices based on semiconductor gates that are volatile and suffer from constant power consumption. Using magnetic logic (see below) with movable magnetic domain walls or skyrmions as information will provide an energy efficient and non-volatile alternative to

the leaky transistors of today. Skyrmions offer the intriguing possibility to use the information stored in internal degrees of freedom for classical or quantum computation.

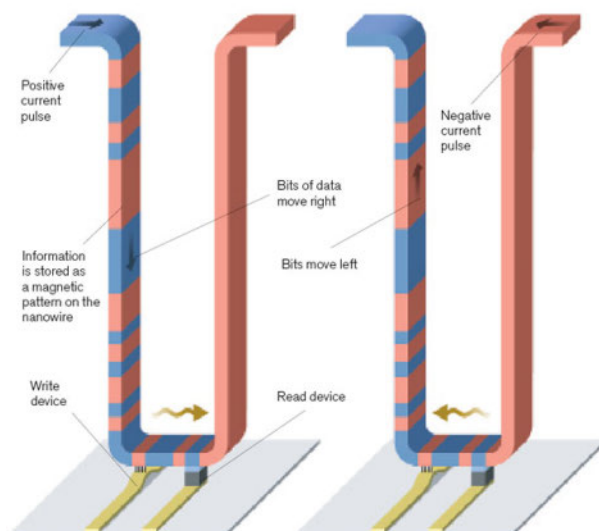


Figure III.3.2: In one implementation of racetrack memory,⁴⁴ information is stored on a U-shaped nanowire as a pattern of magnetic regions with different polarities. Applying a spin-polarized current causes the magnetic pattern to speed along the nanowire; the data can be moved in either direction, depending on the direction of the current. A separate nanowire perpendicular to the U-shaped "racetrack" writes data by changing the polarity of the magnetic regions. A second device at the base of the track reads the data. Racetrack memory using hundreds of millions of nanowires would have the potential to store vast amounts of data. [Figure from <http://www2.technologyreview.com/article/412189/tr10-racetrack-memory/>]

Figure (below) shows tomographic x-ray microscopy images of a cobalt-coated buckyball shaped polymer scaffolds and suggests a fascinating approach to combine concepts from self-assembly and nanomagnetic logic.⁴⁵ Each such structure will have several magnetic configurations at low energy, and these could be used for information storage and processing. This structure is probably too large for highly efficient processing, but it is a step toward ordered arrays of smaller structures having more diverse shapes that might well be useful in this context.

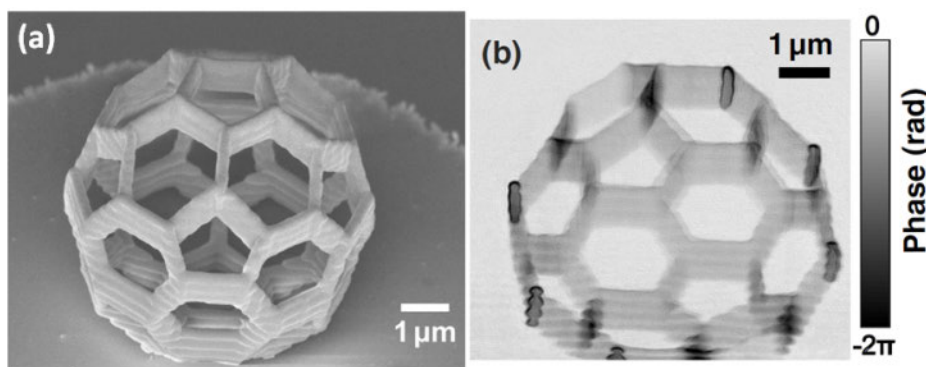


Figure III.3.3: (a) Scanning electron micrographs of a Co-coated buckyball-shaped polymer scaffold.⁴⁵ (b) Reconstructed phase of the 2D complex-valued transmission function at an x-ray photon energy of 6.20 keV.

The size of the domain walls governs the achievable miniaturization and thus device density and is determined by material parameters (saturation magnetization, exchange constant, and anisotropies) as well as the geometry that influences the stray field energy. The speed at which the domain wall can be manipulated by magnetic fields or spin polarized current governs the device performance. Both can be ideally quantified using x-ray nanospectroscopy and x-ray imaging enabled using coherent SXR beams. SXR magnetic linear and circular dichroism provide element-specific and quantitative information about magnetic moments, ordering temperatures and magnetic anisotropies on the nanoscale. Today the available signal-to-noise is limited to spectroscopy experiments sampling an area of hundreds of square microns. High coherent flux will allow focusing these photons into spot size of 10nm x 10nm and probing these characteristics on the length scale important for devices which will enable evaluating the impact of patterning and nanoscale confinement for the first time. New imaging techniques like magnetic tomography and ptychography will allow characterizing the vector character of these domain wall structures and their dynamics in 3D on the relevant time scales.

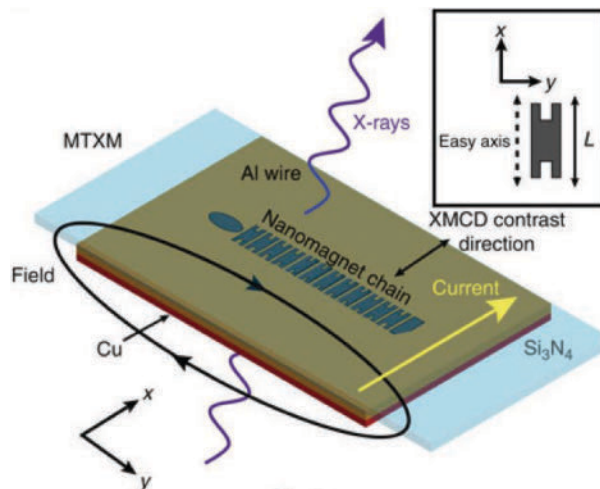


Figure III.3.4: Schematic of SXR transmission microscopy experiments on a nanomagnetic chain.⁴⁶ The magnetic contrast of SXR microscopy is already being applied to study the magnetic structure and field-driven switching in diverse nanomagnetic structures. DLSR sources will expand those applications with 3D vector imaging of magnetization higher resolution pump-probe microscopy, and correlation spectroscopy studies of thermal fluctuations as the switching energy approached $k_B T$.

Nanomagnetic Logic

Nanomagnetic logic (NML) is an emerging information processing technology where binary information is represented by the magnetization state of nanomagnets and that is processed via dipolar field-coupling (see Figures III.3.4 and III.0.1).⁴⁶ Nonvolatility, low-power computing, high-density integration, zero leakage and complementary metal oxide semiconductor (CMOS) compatibility are key features of NML. In fact, the energy dissipation of NML magnets during switching is in the low aJ-range, making NML one of the most promising low-power technologies (www.itrs.net). Two different implementations – in plane NML using permalloy films and perpendicular NML made of Co/Pt films are being developed at this time, though other more

exotic possibilities are possible, e.g., using multiferroics will potentially integrate electronic control into NML. For both implementations functional elementary circuits have been experimentally demonstrated, therefore current challenges first of all concern the applicability of NML circuitry, that is high area integration, speed signal routing, architecture and error rate. Optimizing all these aspects will be hugely aided by the enhanced magnetic imaging capabilities of DLSR (Figure III.3.4). One big issue of NML circuitry is the reliability of magnetic computation that may be impacted due to thermally induced variations. XPCS can ideally quantify thermal fluctuations in magnetic systems and contribute to the advancement of this technology.

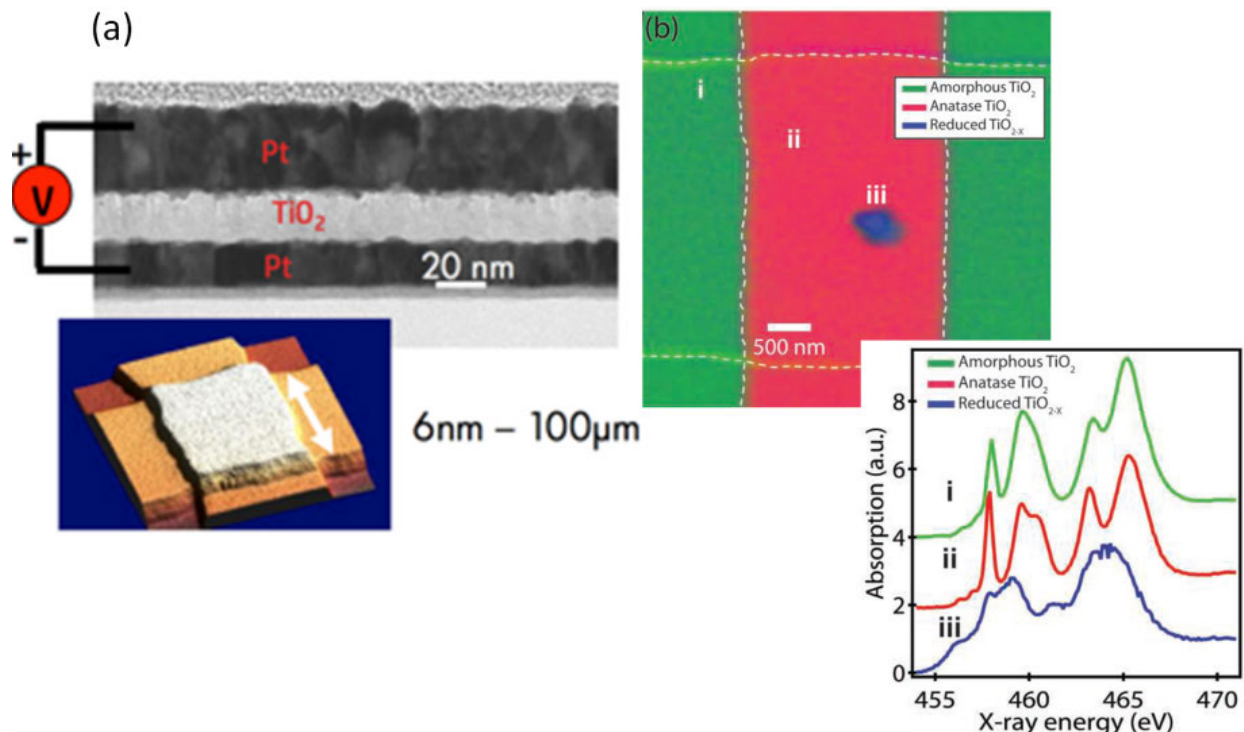


Figure III.3.5: Chemical and structural mapping of a functioning memristor by STXM following electroforming and ON/OFF cycling.⁴⁷ Memristors provide a platform for 3D high-density digital memory and low power information processing. The challenge is to probe the evolving 3D structure of memristor junctions with nanometer resolution and e.g. oxidation state contrast. The high sensitivity to oxidation state with low-nm resolution provided by diffraction limited light sources will provide the characterization tool essential for this development. (a) Cross section and lateral view of a memristor consisting of Pt top and bottom electrodes as well as a TiO_2 layer. (b) Chemical and structural mapping of the three observed phases of titanium oxide. Region i (green) is the as-grown amorphous TiO_2 , region ii is the anatase phase, and region iii shows a stoichiometrically reduced suboxide TiO_{2-x} , or equivalently a mixed-valence oxide with Ti^{+3} and Ti^{+4} ions.

Developing Memristors for Storage and Neuromorphological Processing

Memristors were originally envisioned in 1971 by circuit theorist Leon Chua as a missing non-linear passive two-terminal electrical component relating electric charge and magnetic flux linkage. A memristor's electrical resistance is not constant but depends on the history of current that had previously flowed through the device, i.e., its present resistance depends on how much electric charge was transmitted in a one direction through it in the past. The device remembers

its history, that is, when the electric power supply is turned off, the memristor stays in its most recent resistance until it is turned on again. Today memristors are considered a possible platform for 3D high density digital memory since they can be stacked and possibly integrated into a processor chip which has a large potential impact on power usage itself: Power efficiency results from not moving data far. HP utilizes the oxidation state of Ti, i.e. the $\text{TiO}_2 - \text{Ti}_2\text{O}_3$ cycle, to test for memristor functionality.⁴⁷ This and other approaches discussed today can ideally be probed coherent SXR techniques with the combination of nm spatial resolution element specificity, and magnetic and electronic contrast (see Figure III.0.1).

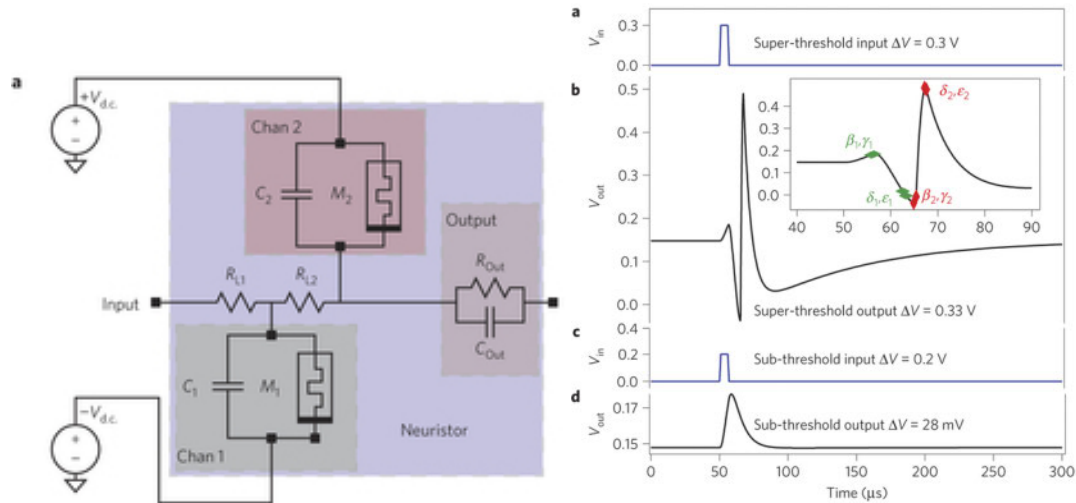


Figure 3: Left: circuit schematic of two coupled memristors that act as a neuristor that exhibits the thresholding, spiking, and gain of neural elements.⁴⁸

Memristors have also recently been proposed as candidates for low power neuromorphological processing (Figure III.3.6, left).⁴⁸ Two memristors appropriately coupled produce a so-called neuristor, which exhibits transient memory, negative differential resistance, and the important neural functions of all-or-nothing spiking with signal gain. At present the necessary materials characteristics for a neuristor are same as for a memristor, but a good goal is to produce artificially structured materials that will provide neuromorphological function directly and at ultralow power.

Imaging Spin Currents

Spin-transfer torque devices are widely studied as a candidate for the next generation of magnetic storage devices due to their high energy efficiency. They consist of a thick and magnetized ferromagnetic fixed layer and a thinner ferromagnetic free layer, magnetically decoupled by a nonmagnetic metallic spacer layer often made of Cu. The fixed layer partially spin polarizes an incoming electron current, which then passes through the spacer layer and exerts a torque on the spins in the free layer. There have been a few studies on spin-torque induced switching itself, using time-resolved scanning x-ray microscopy to image nanosecond domain and magnetization dynamics in the ferromagnetic layers. Only recently has it become possible to directly image the spin polarization of the current in the Cu layer by monitoring the

polarization dependent x ray absorption at the Cu L_{3,2} edges. The spin current can be detected as spin imbalance in the unoccupied density of states creating a magnetic moment of $8 \times 10^{-5} \mu_B$ per Cu atom. The higher brightness of DLSR will enable imaging these currents on the nanometer length scale and sub-nanosecond time scale and in that way will dramatically speed the development and optimization of spintronic devices.

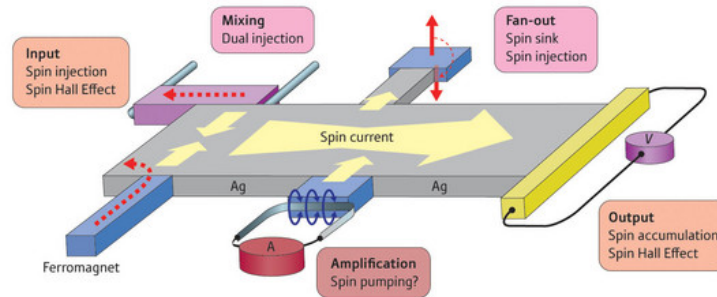


Figure III.3.7: Schematic of a device to inject, amplify, manipulate, and detect pure spin currents. Detecting spin currents with SXR has recently been achieved but remains a heroic experiment due to the very small net spin polarization. The high coherent flux of SXRs from a DLSR will facilitate detecting and mapping these subtle but very important currents in candidate structures with a resolution of a few nanometers. An intriguing idea that arose at the workshop was to develop highly sensitive interferometric detection techniques that would help detecting very low signals like this. (from <http://www.nanowerk.com/news/newsid=4446.php>)

Magnetoresistive Random Access Memory (MRAM)

One of the best solutions to limit power consumption and to fill the memory gap is the modification of the memory hierarchy by the integration of non-volatility at different levels (storage class memories, dynamic random-access memory main working memory, static random-access memory cache memory), which would minimize static power as well as paving the way towards normally off / instant-on computing (logic-in memory architectures). Besides computers, today's portable electronics have become intensively computational devices as the user interface has migrated to a fully multimedia experience. To provide the performance required for these applications, the actual portable electronics designer uses multiple types of memories: a medium-speed random access memory for continuously changing data, a high-speed memory for caching instructions to the central processing unit and a slower, non-volatile memory (NVM) for long-term information storage when the power is removed. Combining all of these memory types into a single memory has been a longstanding goal of the semiconductor industry, as computing devices would become much simpler and smaller, more reliable, faster and less energy consuming. Magnetoresistive random-access memory (MRAM) is one of a number of new technologies aiming to become a 'universal' memory device applicable to a wide variety of functions.

Unlike conventional RAM technologies, data in MRAM is not stored as electric charge or current flows, but in the non-volatile relative alignment of two ferromagnetic layers separated by a thin insulating layer confined to nanoscale lateral dimensions.

For phase separated materials like manganites, nanowires with widths in the 0.5 - 2 μm range have been shown to display discrete steps in the magnetotransport properties due to the lateral confinement. In the confined geometry of a nanowire, the formation of a single FM/M “filament” which spans the entire length of the nanowire determines the overall magnetotransport properties, while in an unpatterned film, the properties are determined by the network of a large number of filaments. These steps are triggered by changes in temperature or the application of ***H***, though joule heating from large currents were shown to destroy the filaments.⁴⁹ Because these resistance states differ in magnitude by several orders of magnitude, they may serve as the basis for new MRAM devices. To further understand and optimize the development of magnetic, electronic and orbital microphases and the impact of confinement, soft x ray based techniques with sensitivity to elemental, electronic, magnetic and orbital order will allow imaging the characteristics of these new devices with the required spatial and temporal resolution.

References: Section III

1. W. Xiaobin and C. Yiran, presented at the Design, Automation & Test in Europe Conference & Exhibition, 2010 (unpublished).
2. R. Suzuki, M. Sakano, Y. J. Zhang, R. Akashi, D. Morikawa, A. Harasawa, K. Yaji, K. Kuroda, K. Miyamoto, T. Okuda, K. Ishizaka, R. Arita and Y. Iwasa, *Nat Nano* **9** (8), 611-617 (2014).
3. X. Zhang, G. P. Zhao, H. Fangohr, J. P. Liu, W. X. Xia, J. Xia and F. J. Morvan, *Sci. Rep.* **5** (2015).
4. E. Irina, B. Stephan, Z. Grazvydas, C. György, P. Wolfgang and B. Markus, *Nanotechnology* **25** (33), 335202 (2014).
5. A. Ohtomo, D. A. Muller, J. L. Grazul and H. Y. Hwang, *Nature* **419** (6905), 378-380 (2002).
6. M. Imada, A. Fujimori and Y. Tokura, *Reviews of Modern Physics* **70** (4), 1039-1263 (1998).
7. E. Dagotto, *Science* **309** (5732), 257-262 (2005).
8. M. Bibes, J. E. Villegas and A. Barthélémy, *Advances in Physics* **60** (1), 5-84 (2011).
9. J. M. Rondinelli, S. J. May and J. W. Freeland, *MRS Bulletin* **37**, 261 (2012).
10. J. Chakhalian, J. W. Freeland, A. J. Millis, C. Panagopoulos and J. M. Rondinelli, *Reviews of Modern Physics* **86** (4), 1189-1202 (2014).
11. N. Reyren, S. Thiel, A. D. Caviglia, L. F. Kourkoutis, G. Hammerl, C. Richter, C. W. Schneider, T. Kopp, A. S. Rüetschi, D. Jaccard, M. Gabay, D. A. Muller, J. M. Triscone and J. Mannhart, *Science* **317** (5842), 1196-1199 (2007).
12. S. V. Kalinin, A. Borisevich and D. Fong, *ACS Nano* **6** (12), 10423-10437 (2012).
13. J. Zhang and R. D. Averitt, *Annual Review of Materials Research* **44** (1), 19-43 (2014).
14. C. H. Ahn, A. Bhattacharya, M. Di Ventra, J. N. Eckstein, C. D. Frisbie, M. E. Gershenson, A. M. Goldman, I. H. Inoue, J. Mannhart, A. J. Millis, A. F. Morpurgo, D. Natelson and J.-M. Triscone, *Reviews of Modern Physics* **78** (4), 1185-1212 (2006).
15. S. V. Kalinin and N. A. Spaldin, *Science* **341** (6148), 858-859 (2013).
16. J. Jeong, N. Aetukuri, T. Graf, T. D. Schladt, M. G. Samant and S. S. P. Parkin, *Science* **339** (6126), 1402-1405 (2013).
17. J. Shi, S. D. Ha, Y. Zhou, F. Schoofs and S. Ramanathan, *Nat Commun* **4** (2013).
18. J. Tao, D. Niebieskikwiat, M. Varela, W. Luo, M. A. Schofield, Y. Zhu, M. B. Salamon, J. M. Zuo, S. T. Pantelides and S. J. Pennycook, *Physical Review Letters* **103** (9), 097202 (2009).
19. C. V. Parker, P. Aynajian, E. H. da Silva Neto, A. Pushp, S. Ono, J. Wen, Z. Xu, G. Gu and A. Yazdani, *Nature* **468** (7324), 677-680 (2010).
20. C. L. Kane and E. J. Mele, *Physical Review Letters* **95** (22), 226801 (2005).
21. L. Fu, C. L. Kane and E. J. Mele, *Physical Review Letters* **98** (10), 106803 (2007).
22. M. Z. Hasan and C. L. Kane, *Reviews of Modern Physics* **82** (4), 3045-3067 (2010).
23. Y. Fan, P. Upadhyaya, X. Kou, M. Lang, S. Takei, Z. Wang, J. Tang, L. He, L.-T. Chang, M. Montazeri, G. Yu, W. Jiang, T. Nie, R. N. Schwartz, Y. Tserkovnyak and K. L. Wang, *Nat Mater* **13** (7), 699-704 (2014).
24. S. Mühlbauer, B. Binz, F. Jonietz, C. Pfleiderer, A. Rosch, A. Neubauer, R. Georgii and P. Böni, *Science* **323** (5916), 915-919 (2009).
25. X. Z. Yu, Y. Onose, N. Kanazawa, J. H. Park, J. H. Han, Y. Matsui, N. Nagaosa and Y. Tokura, *Nature* **465** (7300), 901-904 (2010).

26. U. K. Roessler, A. N. Bogdanov and C. Pfleiderer, *Nature* **442** (7104), 797-801 (2006).
27. S. Heinze, K. von Bergmann, M. Menzel, J. Brede, A. Kubetzka, R. Wiesendanger, G. Bihlmayer and S. Blugel, *Nat Phys* **7** (9), 713-718 (2011).
28. J. Li, A. Tan, K. W. Moon, A. Doran, M. A. Marcus, A. T. Young, E. Arenholz, S. Ma, R. F. Yang, C. Hwang and Z. Q. Qiu, *Nat Commun* **5** (2014).
29. N. Nagaosa and Y. Tokura, *Nat Nano* **8** (12), 899-911 (2013).
30. A. Fert, V. Cros and J. Sampaio, *Nat Nano* **8** (3), 152-156 (2013).
31. F. Jonietz, S. Mühlbauer, C. Pfleiderer, A. Neubauer, W. Münzer, A. Bauer, T. Adams, R. Georgii, P. Böni, R. A. Duine, K. Everschor, M. Garst and A. Rosch, *Science* **330** (6011), 1648-1651 (2010).
32. C. A. F. Vaz, *Journal of Physics: Condensed Matter* **24** (33), 333201 (2012).
33. J. T. Heron, J. L. Bosse, Q. He, Y. Gao, M. Trassin, L. Ye, J. D. Clarkson, C. Wang, J. Liu, S. Salahuddin, D. C. Ralph, D. G. Schlom, J. Iniguez, B. D. Huey and R. Ramesh, *Nature* **516** (7531), 370-373 (2014).
34. T. Zhao, A. Scholl, F. Zavaliche, K. Lee, M. Barry, A. Doran, M. P. Cruz, Y. H. Chu, C. Ederer, N. A. Spaldin, R. R. Das, D. M. Kim, S. H. Baek, C. B. Eom and R. Ramesh, *Nat Mater* **5** (10), 823-829 (2006).
35. A. Hoffmann, *Magnetics*, *IEEE Transactions on* **49** (10), 5172-5193 (2013).
36. K. Uchida, S. Takahashi, K. Harii, J. Ieda, W. Koshibae, K. Ando, S. Maekawa and E. Saitoh, *Nature* **455** (7214), 778-781 (2008).
37. R. Kukreja, Stanford University, 2014.
38. J. J. Lee, F. T. Schmitt, R. G. Moore, S. Johnston, Y. T. Cui, W. Li, M. Yi, Z. K. Liu, M. Hashimoto, Y. Zhang, D. H. Lu, T. P. Devereaux, D. H. Lee and Z. X. Shen, *Nature* **515** (7526), 245-248 (2014).
39. K. M. Lang, V. Madhavan, J. E. Hoffman, E. W. Hudson, H. Elsaki, S. Uchida and J. C. Davis, *Nature* **415**, 412 (2001).
40. F. Carey and R. Giuliano, *Organic Chemistry*, 8th ed. (McGraw-Hill, New York, 2010).
41. Y.-W. Son, M. L. Cohen and S. G. Louie, *Nature* **444** (7117), 347-349 (2006).
42. C. Jozwiak, J. Graf, G. Lebedev, N. Andresen, A. K. Schmid, A. V. Fedorov, F. El Gabaly, W. Wan, A. Lanzara and Z. Hussain, *Rev. Sci. Instr.* **81**, $\sqrt{\quad}$ (2014).
43. D. Vasilyev, C. Tusche, F. Giebels, H. Gollisch, R. Feder and J. Kirschner, *J. Elec. Spect.* **10**, 199 (2015).
44. M. Hayashi, L. Thomas, R. Moriya, C. Rettner and S. S. P. Parkin, *Science* **320** (5873), 209-211 (2008).
45. C. Donnelly, M. Guizar-Sicairos, V. Scagnoli, M. Holler, T. Huthwelker, A. Menzel, I. Vartiainen, E. Müller, E. Kirk, S. Gliga, J. Raabe and L. J. Heyderman, *Physical Review Letters* **114** (11), 115501 (2015).
46. Z. Gu, M. E. Nowakowski, D. B. Carlton, R. Storz, M.-Y. Im, J. Hong, W. Chao, B. Lambson, P. Bennett, M. T. Alam, M. A. Marcus, A. Doran, A. Young, A. Scholl, P. Fischer and J. Bokor, *Nat Commun* **6** (2015).
47. J. P. Strachan, M. D. Pickett, J. J. Yang, S. Aloni, A. L. David Kilcoyne, G. Medeiros-Ribeiro and R. Stanley Williams, *Advanced Materials* **22** (32), 3573-3577 (2010).
48. M. D. Pickett, G. Medeiros-Ribeiro and R. S. Williams, *Nat Mater* **12** (2), 114-117 (2013).
49. T. Wu and J. F. Mitchell, *Physical Review B* **74** (21), 214423 (2006).

IV. Understanding Soft Systems at their Natural Energy/Time Scale

By far the largest impact to date of synchrotron radiation in bioscience and soft condensed matter physics is structure determination. For example, there are now over 100,000 entries in the protein structure databank, and the vast majority was determined with macromolecular crystallography. Similarly, while spectroscopic and scattering studies of soft systems are common, they are most meaningful when the structural and chemical heterogeneity of natural systems can be resolved and correlated.

Emerging 4th generation storage ring facilities will certainly continue and significantly sharpen this focus on structure. For example, breakouts in these areas strongly supported continued development of SXR microscopy capabilities for tomographic chemical imaging to the radiation damage limit, which is expected to be ~10 nm for frozen soft and biological systems. Comparable imaging techniques on third generation facilities achieve typically 30-50 nm, and a 3- to 5-fold improvement in resolution will decrease the size of a resolution voxel by a factor of 30-100. Examples of the impact of this improvement will be discussed in the chapters in this section. Of course, structure relates to function, and measuring the crystal structure of a frozen, static enzyme-substrate complex has proven to be a key step in drug development, even though this configuration is clearly not functional in a biological context.

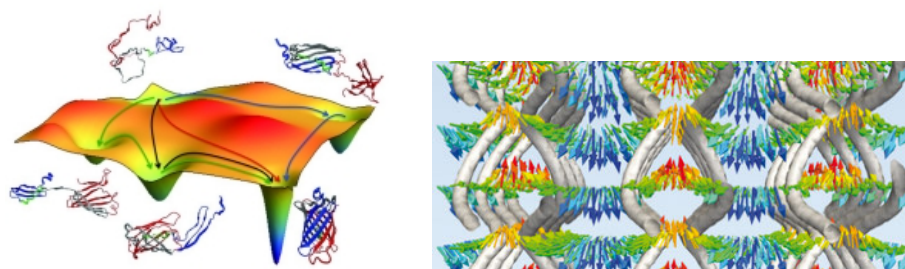


Figure IV.0.1: Exemplary soft systems where nanoscale structure and function rely on energies comparable to $k_B T$. Left: Protein folding offers a classic example of a system involving many low energy degrees of freedom. Despite thermal fluctuations at comparably low energy, the folding process occurs with astounding speed and efficiency to produce the biologically active folded configuration. Right: Simulated flow pattern in the liquid crystal ‘blue phase’.¹

But soft and biological systems are functional; their parts move around and interact on a very broad range of time and length scales (Figure IV.0.1). A defining feature of soft materials is that they have many degenerate microscopic modes at energy comparable to $k_B T$, which leads to small bulk moduli and interesting emergent behaviors. Modes with energy $< k_B T$ are important because they can be easily manipulated with little energy input, and thus are key to efficient function. They are also important because they are thermally excited and need to be understood and controlled so that function occurs with high fidelity. Biochemical function is built upon this concept: most enzymatic reactions are driven with an energy input of a few $k_B T$ per enzymatic turnover, yet these occur in a thermal environment so error correction, feedback, self-repair, and relatively low turnover rate are common ingredients.

The time range $\sim h/k_B T$ also represents a crossover between kinetic and dynamic regimes and therefore lies at the heart of many important chemical, biological, and material processes. Molecular dynamics is fast and occurs on a nm length scale; chemical kinetics is much slower and includes long-range diffusion, pattern formation, etc. Valuable pump-probe techniques have been developed to measure a diverse array of driven motion over very a broad time scale, yet these only probe motion averaged over many repeated cycles and cannot probe spontaneous thermally driven motion that is crucial to function in soft materials that are the focus of this section of the report.

Quasi-elastic neutron scattering probes excitations down to $\sim 1 \mu\text{eV}$ and has provided key information, for example, to understand polymer reptation. Beyond structure determination with SXR microscopy, quasi-elastic RIXS enabled by DLSR sources will probe similar soft modes with much higher signal, advantageous chemical and magnetic contrast, and tightly focused beams for straightforward application to thin films and nanostructures. The chemical contrast of SXRs, for example, can be combined with quasi-elastic RIXS to probe chemical and biochemical kinetic processes. How can we leverage the high brightness of DLSR sources to accomplish quasi-elastic SXR RIXS with nanoscale sensitivity and at an energy scale $< k_B T \sim 1 \text{ meV}$ or a time scale $> h/k_B T \sim 1 \text{ ps}$? This was discussed in Chapter I.3 and will be further illuminated in this section.

IV.1: Biosciences Using Diffraction Limited Soft X-ray Sources

Contributions from Paul Adams, Wayne Hendrickson, James Holton, Greg Hura, Jim Hurley, Cheryl Kerfeld, Howard Padmore, David Shapiro, John Tainer, Junko Yano, Peter Zwart

Introduction

The study of biological systems has benefitted greatly from the availability of better and better sources of X-rays and other electromagnetic radiation. As stated above, our current ability to determine macromolecular structures at atomic resolution is dependent on 3rd generation synchrotron sources, relying on the availability of bright X-ray beams. However, the impact extends beyond this single area. With 3rd generation sources it has been possible to develop methods that can image cells at sub-micron resolution using X-ray tomography, perform complex spectroscopic analyses across a broad range of the energy spectrum, and probe the chemistry of biological systems using infrared radiation. Finally, our ability to examine the conformations of molecules in solution has been transformed by the availability of powerful X-ray sources.

In contrast to inorganic or hard matter studies, biological samples usually suffer from rapid radiation damage. This presents challenges for many experiments that use probes such as X-rays, especially at longer wavelengths. However, novel approaches to sample delivery can help address this problem, as has been recently demonstrated at free electron laser X-ray sources. Traditional methods of analysis for biological systems typically provide information about structure or about chemistry, but not both simultaneously. Exploiting different regions of the X-ray spectrum can provide opportunities to address this issue. High brightness diffraction limited X-ray sources provide many opportunities for new research directions for biological samples, which make it possible to study systems in physiologically relevant conditions.

A. The Water Oxidation Reaction in Photosynthesis

The cycle of dioxygen metabolism that is essential to life on earth consists of the reduction of O₂ to H₂O by cytochrome c oxidase in the mitochondria during respiration and the oxidation of H₂O to O₂ in Photosystem II (PS II) by the oxygen-evolving complex (OEC) in the chloroplasts. It was the water-oxidation process that led to the formation of our oxygen atmosphere and its protective ozone layer, a step in our distant evolutionary history that was essential for the development of more complex forms of life. The conversion of light energy to chemical potential is accomplished efficiently by photosynthetic organisms, making use of water as an abundant raw material and oxidizing it to dioxygen, while producing reduced compounds that are a major source of our biological and fossil energy.

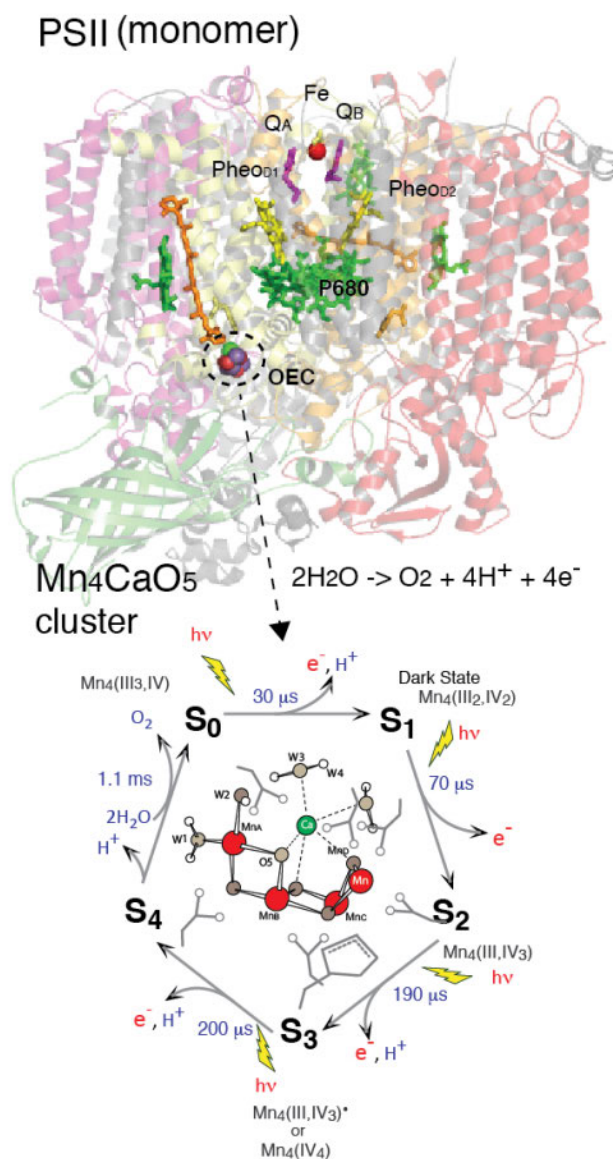


Figure IV.1.1: (top) PS II structure showing the location of the reaction center pigments, P₆₈₀, pheophytins (Pheo), the donor oxygen evolution complex (OEC), and acceptor side Fe and quinones Q_A and Q_B.

(bottom) The Kok clock with the S-state intermediates, proposed oxidation states, and kinetics. The inset shows the proposed structure of the Mn₄CaO₅ cluster from XRD, EXAFS, EPR and theoretical studies, with input from the XRD structure.²

The process of managing the light-induced, thermodynamically uphill, four electron, four proton redox chemistry of water-oxidation and O₂ evolution is accomplished by the OEC in PS II, a multi-subunit membrane protein in green plants, algae, and cyanobacteria. The OEC that catalyzes the reaction shown in (Figure IV.1.1) contains a Mn₄CaO₅ cluster² that couples the four-electron oxidation of water with the one-electron photochemistry occurring at the PS II reaction center by acting as the locus of charge accumulation. The OEC cycles through a series of five intermediate S-states (S₀ to S₄), representing the number of oxidizing equivalents stored on the OEC driven by the energy of four successive photons absorbed by the PS II reaction center.³ Once four oxidizing equivalents are accumulated in the OEC (S₄-state), release of O₂ results with the concomitant formation of the S₀-state. During the reaction, the Mn₄Ca cluster provides a high degree of redox and chemical flexibility, while the protein residues are critical for mediating the reaction by modulating the redox potentials and providing pathways for electrons, protons, substrate H₂O, and product O₂. Thus, PS II orchestrates the well-controlled catalytic reaction at close to the thermodynamic potential.⁴ Understanding the fundamental structural

and electronic parameters that control this complex photo-induced four-electron, four-proton reaction, and the mechanism of the water oxidation reaction will provide basic knowledge about the versatility of transition metal oxygen-chemistry in general.

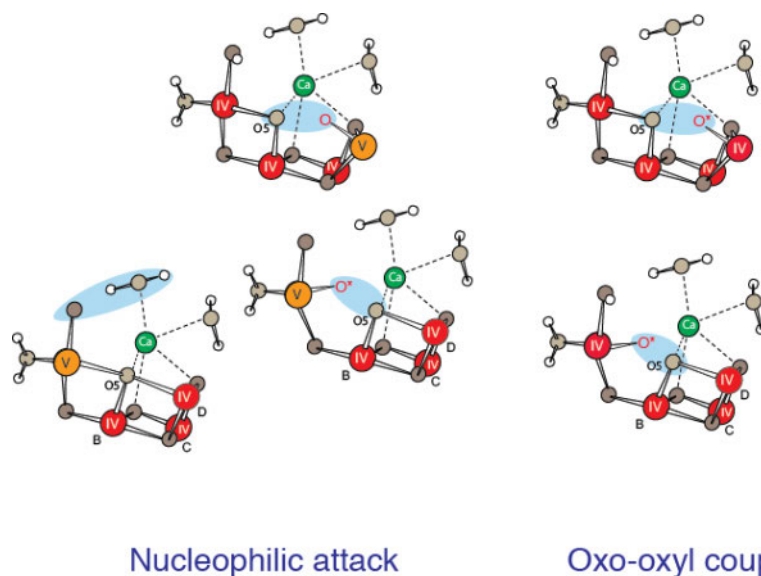


Fig. IV.1.2: Possible O-O bond formation mechanisms and sites from two of the many that have been proposed thus far.⁵

The detailed chemistry of the OEC has emerged slowly, but critical design aspects remain to be elucidated (Figure IV.1.2). X-ray diffraction and X-ray absorption methods have revealed insight about the protein scaffold and the overall geometry of the Mn_4Ca cluster. X-ray emission/absorption spectroscopy has also provided information about the electronic structure of the cryo-trapped stable intermediate states (S_0 to S_3). The Mn_4CaO_5 complex plays a key role owing to the versatile d -electron orbitals and their manipulation via ligand fields, from which emerge: charge-transfer states, a capability to change oxidation state at relatively small energy cost, and a high level of catalytic activity. How the OEC accumulates four oxidizing equivalents and stabilizes them for a sufficient period necessary for splitting water, therefore, remains as a central question. In addition, recent study shows the possible importance of spin-state transitions within one redox state (S-state), predicted to play an important role for substrate water exchange. The specific issues that can be anticipated to be addressed by Mn L-edge spectroscopy are:

1. Understand **the electronic structural changes** in the Mn_4CaO_5 cluster as PS II traverses the enzymatic cycle at room temperature.
2. Understand **the spin and the charge density delocalization**, beyond the notation of the formal oxidation state.
3. **Capture the transient states** between the S_3 and the S_0 with X-ray spectroscopy to identify **the sequential reaction** in the OEC, *i.e.* whether high-valent Mn^V is involved in the reaction, and if so, when it happens and at which Mn site (Figure IV.1.2)?

Technical Development: L-edge Spectroscopy at High Dilution

Many important **redox-active metalloenzymes** consist of 3d transition metals, such as Mn, Fe, Cu, Ni, Mo and others in their active sites. To probe the chemistry of these catalytic sites, metal K-edge spectroscopy (1s to np transition) in the hard X-ray energy range (>2 keV) has been widely used, providing element-specific information about the electronic structure and the local environment of metals. Thus, the metal K-edge spectroscopy has been a critical tool in the field of biological X-ray spectroscopy at synchrotron sources. On the contrary, metal L-edge spectroscopy has not been actively applied to the biological systems. This is in contrast to the field of **material sciences**, where metal L-edge XAS of 3d transition metals provides important electronic structure information through XAS and XES, as well as L-edge RIXS.

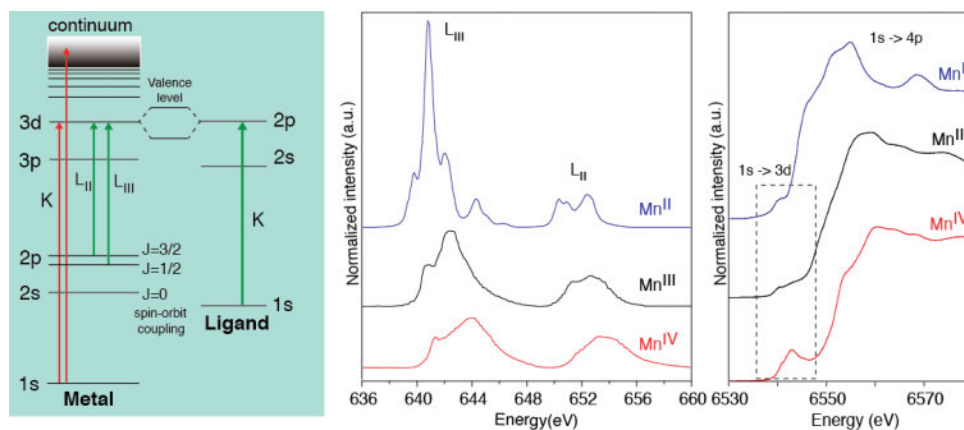


Figure IV.1.3: (left) L-edge energy level diagram. The L-edge 2p-3d transitions (middle) are dipole allowed and more intense compared to the 1s-3d K-edge transitions shown in a dotted line box (right), and are more resolved.

In general, examination of the L-edge region is more informative than the K-edge spectroscopy, as it can provide electronic structural information with significantly better resolution. The natural line widths at the L₂ and L₃ edges are about one-fourth of those at the K-edge (~0.3 eV for L-edge vs ~1.2 eV for K-edge), therefore more amenable to theoretical analysis (Figure IV.1.3). Furthermore, the SXR signal will be more intense since 2p → 3d transitions are allowed under dipole selection rules, while only s → p transitions are allowed at the K-edge. Greater sensitivity to the occupancy of the 3d orbitals should provide a better indication of the oxidation states and symmetry of the complex involved. The possibility of RIXS with sub-core-level-line width resolution is also a very attractive possibility as high-throughput RIXS spectrometers are further developed (Chapter I.3).

Difficulties of using L-edge spectroscopy for redox-active biological samples, however, arise from (i) severe radiation damage to the sample at SXR energies **even at cryogenic temperature**, (ii) detecting signals from very dilute samples (~1mM), as is the case for most biological samples, and (iii) the requirement of ultra high-vacuum for SXR spectroscopy, which dehydrates samples and prevents catalytic turnover. In addition, (iv) biological and bio-inspired samples often require energy discriminating detection using fluorescence signals, by separating out metal L_α from overwhelming ligand K_α background. The issues (i) and (iii) could be

addressed if samples are replaced faster than the rate of radiation damage **by isolated flow systems or injectors** combined with differential pumping to keep the sample environment close to ambient conditions. Issue (iv) becomes a problem if the system contains multiple elements, and the element of interest is a minority species. In case of PSII, for example, to investigate the electronic structural changes of Mn in the Mn_4CaO_5 catalytic center, discriminating the Mn L-fluorescence at ~640 eV from the dominant O K-fluorescence at 525 eV from is a significant challenge. While single crystal arrays or gratings spectrographs were often used for selecting characteristic photons from the sample, these generally are not suitable for dilute samples due to their small acceptance angle. One solution is to use a superconducting tunnel junction (STJ) detector with 20 eV resolution.⁶ A more robust way of detecting fluorescence signals have also been developed using a zone-plate spectrometer that can spatially discriminate metal $L\alpha$ signal from ligand $K\alpha$ (Figure IV.1.4).⁷ The solid angle of the zone-plate spectrometer can be several times higher than the current STJ detectors, which makes the data collection of the X-ray absorption spectra from dilute systems possible. This leaves item (ii) as the remaining challenge.

A DLSR with significantly improved brightness makes metal L-edge spectroscopy a method of choice for studying dilute biological samples, by combining an appropriate sample delivery system such as a liquid jet injector, which typically have a diameter of several micrometers. This makes the data collection of the fluorescence signal from metals of interest within a realistic time, while avoiding radiation damage by replacing the sample fast enough. Such a detection scheme also allows room temperature data collection at ambient temperature. We note that the shot-by shot experiment is possible with X-ray free electron lasers using a similar concept and the configuration. However, the high repetition rate of DLSRs provides an advantage for data collection (see Chapter II.1), in particular, with the highest coherent flux in the SXR regime.

B. Synthetic Biology for Microbial Engineering

While long-established for eukaryotes, in the past decade the importance of subcellular organization in the functioning of prokaryotic cells has become evident.^{8,9} Accordingly, the ability to visualize the mesoscale organization and dynamics of subcellular metabolism will play a transformative role in engineering microbial cell factories for biofuels and green chemicals. This will provide an entirely new means of phenotyping engineered biological systems.

DLSRs will enable high throughput tomographic diffractive imaging at the expected damage limited resolution of ~10 nm¹⁰ in just 10-20 seconds, thereby allowing subcellular positioning of macromolecular assemblies to be a design parameter in bioengineering. The importance of such spatial organization has recently been demonstrated for carboxysomes, which are microbial organelles for CO_2 fixation.(Figure IV.1.4).¹¹ This ensures that during cell division carboxysomes are equitably distributed to daughter cells. Moreover, given that inorganic carbon uptake by the carboxysome is a diffusion-based process, spatial distribution of the organelles is assumed to be important to the overall cellular efficiency of CO_2 fixation.

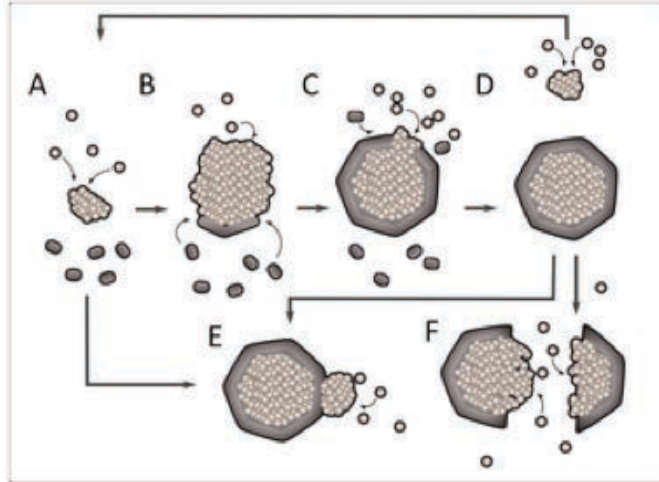


Figure IV.1.4: Model assembly pathway for carboxysomes.

The development of methods to label proteins with metals or other molecules detectable by SXR will enable x-ray based assays for sub-cellular biological self-assembly, catalysis and for the visualization of cellular responses to environmental perturbations.¹² Likewise imaging inclusions naturally containing sulfur or phosphorous may potentially serve as a sensitive readout of cellular metabolic status. For example, phosphate bodies associated with carboxysomes¹³ are presumed to reflect the energetic balance between the light and dark reactions of photosynthesis or serve as a marker for cell cycle position;¹⁴ visualization of the dynamics of these inclusions may become important markers for optimizing engineered cyanobacterial strains. More broadly, there are exciting new findings relating phosphate status and cellular homeostasis/stress responses that suggest a previously blacked out perspective on cellular metabolism could be visualized with SXR methodologies.¹⁵

Technical Development: Ptychographic Cellular Imaging with Chemical Contrast

SXRs have wavelengths from 5-50 Angstroms and typically have attenuation lengths of several microns in matter. This makes them well suited for studying biological structures on the mesoscale that have features that are inaccessible to optical microscopy and sample volumes too thick for electron microscopy.¹⁶⁻¹⁸ In addition, the interaction of SXRs with core shell electrons provides chemical contrast at the K-edges for light elements and the L-edges of the transition metals. SXR tomography has proved a very powerful technique that has been pioneered by the National Center for X-ray Tomography¹⁹ at the ALS. However, the resolution of x-ray microscopes is limited to the finest features that can be fabricated by electron-beam lithography in the diffractive x-ray optics. A complementary approach, discussed in Chapter I.3, is X-ray ptychography, which can achieve high resolution imaging without high resolution optics.²⁰ Novel X-ray optics, high coherent flux provided by a DLSR source, and advanced reconstruction algorithms will enable high throughput cryogenic microscopy with the goal of enabling damage limited spatial resolution of ~10 nm for cryogenic biological samples with full spectral contrast.¹⁰

C. Speeding Development of New Therapeutics

What if synchrotrons became the screening tool of choice for identifying new therapeutics? SXR sources of high brightness could play a new role in drug discovery and metabolomics with major contributions to human health and manipulation of microbial communities. The simplicity of solution scattering sample preparation (no crystals) and capability of collecting in nearly any solution environment make scattering a natural screening technique. The primary challenges of transforming X-ray scattering into a screening platform to identify important metabolites are three fold - sensitivity, quantity of material, and radiation damage. These challenges can only be overcome at a synchrotron using a high brightness SXR source.

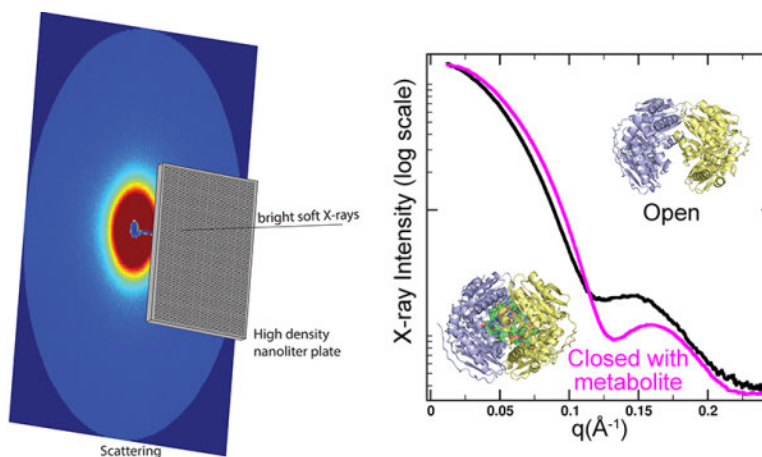


Figure IV.1.5: High density nanoliter screening of conformation to identify important drugs and metabolites with high brightness SXRs. Scattering from solutions of macromolecules is sensitive to conformation and can be used as an assay competitive with current fluorescence based screening techniques.

Using conformation as a screen, X-ray scattering senses conformation comprehensively from the sub-nanometer^{21, 22} to micrometer length scale²³. The structure of biological macromolecules often changes when small molecules bind to active sites. Macromolecules at the nanoscale are shaped by electrostatic interactions and subject to thermal fluctuations. In some cases a macromolecule's function within an organism is to bind and chemically modify metabolites for use in biological pathways. In other cases, binding changes activity by stabilizing a conformation that otherwise is transient due to thermal fluctuations. Binding events can shield a metabolite from solvent environments (Figure IV.1.5), avoiding wasteful side products and enabling remarkable chemistry. Solution X-ray scattering is sensitive to these changes (Figure IV.1.5). Typical drug screening paradigms use fluorescent labels and libraries of thousands of compounds on nanoliter-sized samples. They identify binding but not changes in conformation. Contrasting the conformation induced by members of these libraries as probed by X-ray scattering provides a thus far un-exploited alternative approach if nanoliter volumes of fluorescent screens can be probed.

To increase sensitivity and reduce the quantity of sample required, SXRs have a ten fold higher scattering cross-section relative to the hard X-rays in common use. Biological small angle X-ray

scattering or Bio-SAXS has relied on hard X-rays and is increasing in utilization for measuring macromolecular shape and shape variation. The preference for hard X-rays is in part historical: most new users are crystallographers with experience and access to hard X-ray sources. For screening with solution scattering, detecting conformational change is the primary goal rather than defining the structure. Sampling Bragg spacings of 0.1nm, only possible with hard X-rays, is rare. In fact hard X-rays add a challenge in that large length scale information of interest is close to the intense primary X-ray beam. By using SXR the information is conveniently further from the primary beam where background can be high plus the amount of sample required for equivalent signal is at least ten-fold smaller.

Maximizing brightness will be critical for several reasons. Small target samples are most desirable to increase the size of the screening library with limited quantities of macromolecules. With current hard X-rays at the ALS SIBYLS beamline, a sample of 4 microliters is required for optimal signal and to overcome unwanted signals from radiation damage. Reducing this by an order of magnitude, by using SXRs for an equivalent experiment implies the target will be less than 400 nanoLiters ($400 \mu\text{m}^3$). But further reduction can be gained by utilizing brightness. In Bio-SAXS, X-ray induced charging on the surface of a macromolecule often causes aggregation and is exhibited as radiation damage. During experiments with current sources and high quality measured signals, fewer than 2% of the macromolecules in solution interact with X-rays. Thus to beat this most common form of radiation damage on small sample volumes, sufficient signals must be generated before macromolecules diffuse and interact with one another. In analogy to the experiments conducted at free electron lasers where samples must diffract before they are destroyed, for scattering, the limiting factor is *scatter before they diffuse*. At ALS-U a single pulse is estimated to have 10^9 SXR photons in as small as a $1 \mu\text{m}$ spot, which should be sufficient for a complete experiment with currently used concentrations. To have adequate signal from small sample quantities (nl) at time scales of diffusion (microseconds) brighter SXR sources are required.

While experiments can be accomplished at free electron lasers, the capacity to tackle all macromolecules of interest cannot. The incredible diversity of targets, whether its proteins from Ebola²⁴ to proteins encouraging biofilm formation²⁵, is simply too large for limited capacity at free electron lasers. The value of the technique comes from comprehensive characterization of conformational changes induced by a large libraries of metabolites. New SXR sources are required to take advantage of the targets unveiled by increased genomic sequencing.

Technical Development: Fluctuation X-ray Scattering

X-ray solution scattering is a routine biophysical technique used to determine structure and dynamics of macromolecules in solution. When solution scattering data are interpreted, often with the aid of known atomic models, an improved understanding of the macromolecule's biological function and properties emerges. The main challenge associated with solution scattering data is the intrinsic low information that can be obtained from single solution scattering curves. By performing the solution scattering experiment with an ultra-bright source, probing small volumes of samples while using X-ray snapshots below rotational diffusion times, the information content of the data can be significantly enhanced (Figure IV.1.6).

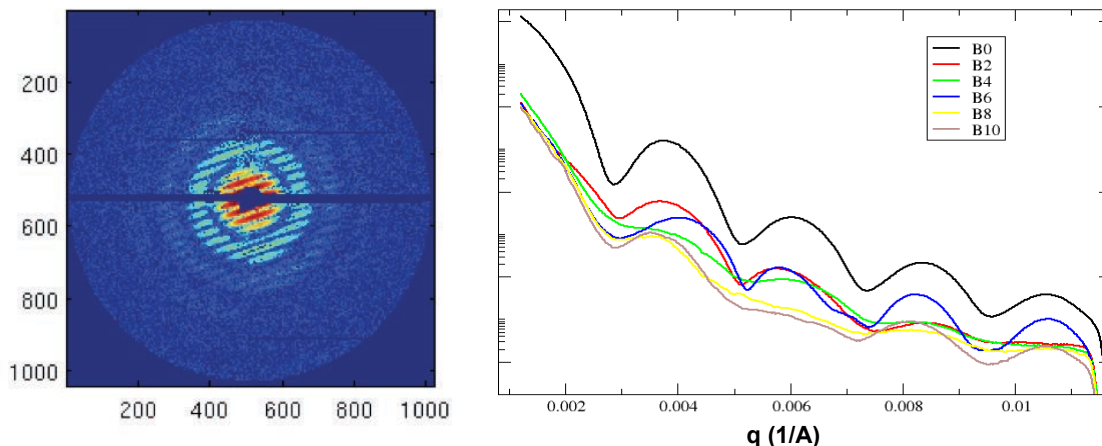


Figure IV.1.6: X-ray snapshot of macromolecules in solution below rotational diffusion times display speckle (left) from which FXS data can be extracted (right). FXS data consists of a large number of resolution dependent SAXS-like curves of which traditional SAXS data is a subset ($B_0(q)$).

The additional information leads to fewer ambiguities in derived structural models and a better understanding of the associated biology. This technique, called fluctuation X-ray scattering (FXS) is a natural extension of standard small angle x-ray scattering (SAXS). Whereas SAXS data provides only information on the mean scattered intensity as a function of scattering angle, FXS provides experimental access to the information describing the full variation of the scattered X-rays beyond the angular mean.²⁶ This additional information can be used to strengthen structure determination (Figure IV.1.7).

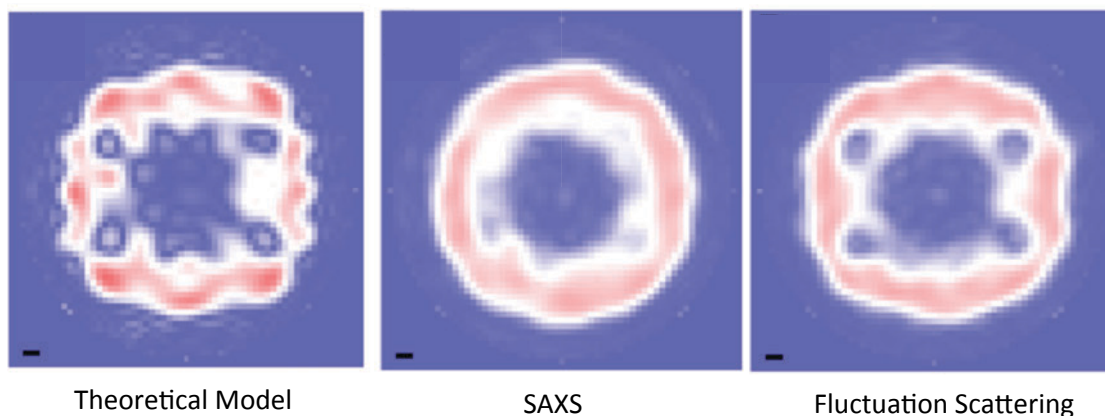


Figure IV.1.7: The added value of FXS data as compared to SAXS data is demonstrated on synthetic Satellite Tobacco Mosaic Virus (STMV) data. A density section of the STMV reference model is shown on the left. The scale bar is 10nm. *Ab initio* models generated from SAXS (middle) data show significantly fewer details as compared to those obtained from FXS data (right).

An FXS experiment on biological materials is performed either in solution, requiring exposures at the nanosecond time scale, or with particles frozen in ice, similar to a setup used in cryo electron microscopy. The ultra bright X-ray beams in the tender and SXR regime will allow rapid

acquisition of FXS data of biological systems. As shown in Figure IV.1.8, FXS data is more sensitive to small structural changes as compared to SAXS data alone. The effect of the additional data will result in structural models with tighter confidence intervals, thus allowing for an improved understanding of conformational changes in biology.

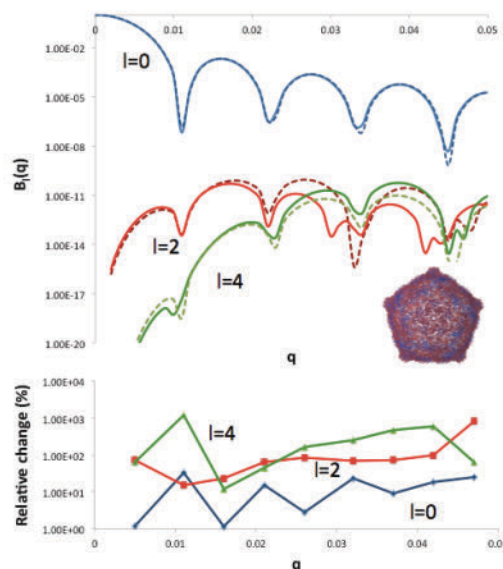


Figure IV.1.8: Synthetic data from a two viral capsid conformations show that SAXS data ($l=0$) is less sensitive to structural changes as compared to FXS data ($l>0$).

FXS experimental requirements dictate the use of ultra-bright beams as delivered by a DLSR light source. The total signal in an FXS experiment is mainly determined by the brilliance of the beam and the number of snapshots taken. By reducing the exposed area, it becomes easier to measure small intensity fluctuations that lie at the foundation of FXS. An increase in flux and an increase in scattering cross section by performing the experiment at soft and tender X-rays will strengthen the signal as well.

Technical Development: Tender Region X-ray Scattering

Biological solution scattering is traditionally performed at energies around 10 keV. In principle, small angle X-ray scattering experiments can be performed at lower energies, allowing one to utilize X-ray resonance effects to supplement standard SAXS data with chemical and elemental contrast. In biology, interesting emission and absorption K-edges lie within the so-called tender X-ray region, loosely defined by X-rays with energies between 1.2 and 8 keV. Elements such as phosphorus, sulphur and calcium have prominent absorption lines within this energy window. The regime requires special attention to due several technical challenges, but promises new and exciting insights in biology. Currently the number of dedicated tender resonant X-ray scattering (T-ReXS) beamlines in the world is limited and a dedicated development of this technique is currently being undertaken a few different facilities.

The use of T-ReXS will allow the determination of the structure and dynamics of biological membranes, membrane proteins, DNA and RNA/protein complexes at greater detail than can be accomplished with standard hard X-rays (Figure IV.1.9).²⁷ By performing the scattering experiment at different energies across the phosphorus adsorption edge, the contributions of the phosphorus atoms can be mathematically decoupled from the rest of the scattering mass, providing a competitive advantage over traditional hard X-ray scattering techniques. In particular, T-ReXS employed at grazing incidence geometry, will provide unique experimental information on the biology at a membrane interface.

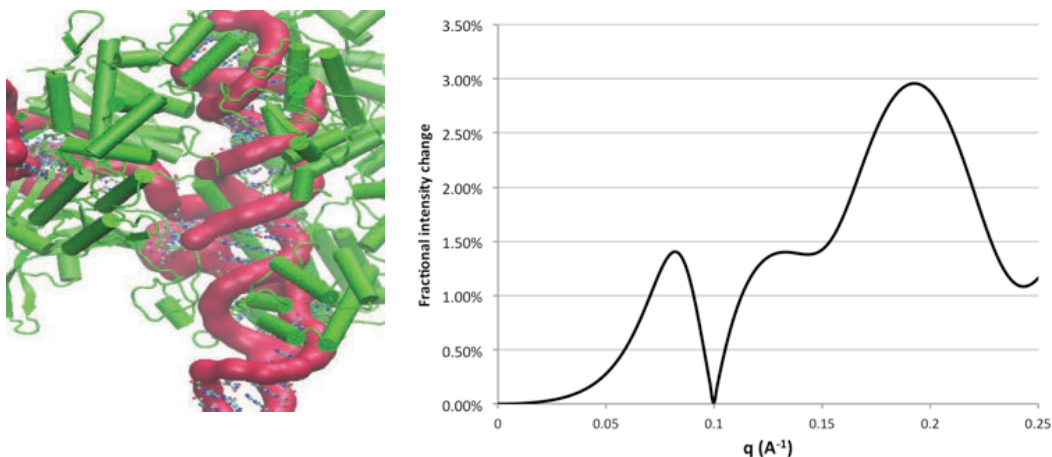


Figure IV.1.9: T-REXS data of a DNA/RNA complex collected around the P-edge is predicted to have up to 3% dispersive difference between datasets. The intensity difference obtained in this fashion can be used to better define the structural dynamics of the DNA/RNA with respect to the full complex.²⁷

T-ReXS will form an important pillar of a new soft and tender DLSR source, leveraging the high brightness and small-spot size. Although T-ReXS as described does not actively use the large coherence of the X-ray source, extending T-ReXS into the fluctuation scattering and/or XPCS regime will allow the more systematic study of complex, dynamic systems away from thermodynamic equilibrium.

D. Barriers and Challenges

DLSRs will provide new opportunities for biosciences research. However, there are other developments that will be required to make this possible. At the cellular level it is important to be able to probe the location of molecules within the cell. To do this it will be necessary to label macromolecules with protein tags that bind specific chemical elements that can be probed using the X-ray beam. Improved instrumentation will also be needed to deliver the full potential of DLSR sources. For homogenous samples, radiation damage can be mitigated by the analysis of many samples, each of which only receives a small dose. To make these kinds of experiments practical it will be necessary to develop and adapt current systems, such as liquid jet technologies, for optimal use at DLSR sources.

Ultimately, our ability to extract information from biological samples using small, high brightness beams will be limited by our detectors. These will need to be improved by reducing noise, increasing detection efficiency, expanding dynamic range, and increasing repetition rates. The later will be particularly important for experiments where damage is overcome by continuous sample replacement. Finally, for many of the experimental approaches described above, successful analysis of results will be critically dependent on new computational approaches. Novel algorithms are required for the analysis of data from new experiments, such as fluctuation scattering. In addition, faster algorithms are needed to enable real time data processing, allowing researchers to make decisions during their experiments.

IV.2 Spatiotemporal Scales in Soft Condensed Matter

Contributions from Chinedum Osuji, Michael Chabynic, Karina Thånell, Harry Westfahl, Tom Russell, Alex Hexemer, Cheng Wang

Fully coherent, diffraction limited, soft-x-ray beams offer unique opportunities to make fundamental advances in our understanding of the complicated relationship between structure and dynamics in soft condensed matter. These span a broad range of areas, from the spatial, compositional and temporal heterogeneities in glassy materials, membranes and nanoscopic objects to transport phenomena in thermoelectric and organic photovoltaic materials. While the time structure and coherence of the incident x-rays offer unique opportunities to probe the dynamic behavior, ptychographic methods will open opportunities to obtain real space images with unprecedented spatial and chemical detail. In addition, the characteristics of the x-rays enable the development of new scattering methods to probe how relaxation phenomena on very short length and time scales are coupled to slower diffusive processes on a longer length scale, an area in soft matter that has not been considered up to now.

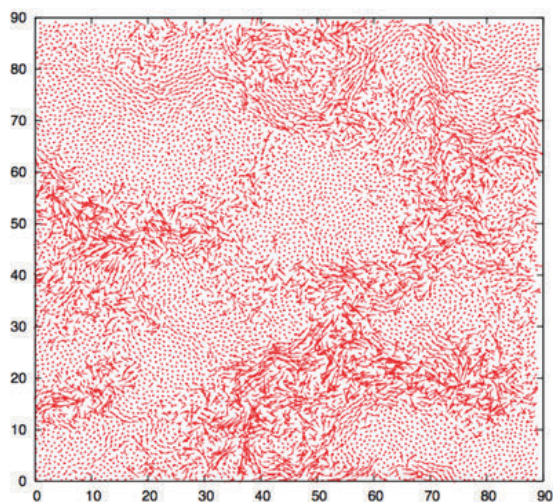


Figure IV.2.1: Spatial map of single particle displacements in the simulation of a Lennard-Jones model of a supercooled liquid in two spatial dimensions, revealing that particles with different mobilities are spatially correlated.²⁸ Dynamic heterogeneity is observed in virtually all disordered systems with glassy dynamics.²⁹

A common feature of many soft condensed matter systems, and also soft manifolds in nominally hard condensed matter systems (see Chapters III.1 and III.2), is dynamic heterogeneity. Dynamic heterogeneity is the existence of transient spatial fluctuations in the local dynamical behavior and/or structure (see Figure IV.2.1). We can think of dynamic heterogeneity as a kind of emergent behavior in which a collection of finite sized-subregions interact and exhibit properties that are different from what the subsystems would exhibit in the thermodynamic limit. It is in the thermodynamic limit that size independence of intensive thermodynamic quantities and additivity of extensive parameters is properly justified. The singular behavior of the free energy or its derivatives associated with phase transitions can only occur in this limit. The

domains in a system exhibiting dynamic heterogeneity are not in the thermodynamic limit, but the whole material is and can exhibit renormalized emergent properties. As noted above, similar words can be applied to magnetic domains, to the microphase separated regions in colossal magnetoresistance manganites or the high temperature superconducting cuprates, to ferrofluids, and many others. It is the existence of many degenerate microscopic modes at energy comparable to $k_B T$ that produces, and to a degree unifies, the behavior of these divergent systems.

Canonical examples of finite-size effects include the modification of transition temperatures and melting enthalpies in confined liquid crystals^{30, 31} as well as changes to the specific heat and thermal conductivity of ^4He at the superfluid transition.^{32, 33} The suppression of melting temperature in nanoparticles due to surface energy as captured by the Gibbs-Thompson equation and the paramagnetic behavior of nanoparticles of bulk ferromagnetic materials, i.e. superparamagnetism, are also manifestations of the impact of finite-sizes on thermodynamics. Clearly, finite size effects are abundant in condensed matter physics and emergence of nanotechnological applications of hard and soft condensed matter alike has heightened the need to effectively survey and understand such effects.

Given the obvious correlation between spatial and temporal variables in systems exhibiting dynamic heterogeneity, DLSR sources provide a unique opportunity to advance the study of finite-size effects in soft condensed matter physics. The chemical specificity of resonant SXR scattering and combined with the structural and dynamical studies enabled by high SXR coherent flux enable studies linked to chemical, compositional, and density heterogeneities in systems due to their nm-scale dimensions. Moreover, CDI and ptychography will permit unparalleled 3-dimensional (3D) imaging of nanostructures with chemical specificity. In all cases the studies will benefit significantly from the high brilliance provided by SXR DLSR sources, and the ability to make statistically meaningful measurements over large ensembles of finite-sized systems or heterogeneous regions of a large system. The discussion below is advanced in the context of compositional heterogeneity, but similar considerations can be made for phase behavior in terms of density fluctuations arising from finite size. A sampling of major challenges pertaining to finite size effects in soft matter that can be addressed with a DLSR includes

- What are the critical length scales at which compositional heterogeneity arises in macromolecular systems?
- What is the functional relationship between the magnitude of the heterogeneity and the system size?
- How does compositional heterogeneity manifest itself in the structure and dynamics of ensembles of nano or mesoscopic objects, and thus in developing useful function?
- How are the ensemble average properties of finite size structured soft matter systems correlated with the corresponding bulk behavior?
- How do we achieve a mechanistic understanding of the structure-transport interplay in chemically heterogeneous structures, e.g., to allow design of ionomer membranes and thin films with enhanced transport functionalities for energy and environmental applications?

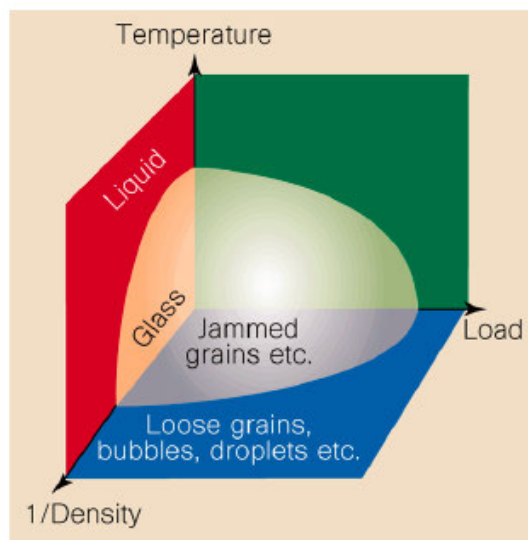


Figure IV.2.2: Schematic jamming phase diagram.³⁴

A. Bulk Glasses and Jamming

Perhaps one of the most challenging, long-standing problems in materials science is to understand the nature of glasses. When a material is cooled from the liquid state the thermal expansion coefficient of the liquid dictates the volume change. However, when the volume contraction can no longer follow the reduction in the temperature, the system is trapped in a highly non-equilibrium state as a glassy material, where short range relaxations can still occur, but long range motions are significantly retarded. Even before the glass transition temperature is reached, long-range motions can be arrested or jammed where the units comprising the liquid form a load bearing percolated pathway through the material, i.e. the liquid will jam. These are schematically described in the “phase map” put forth by Liu and Nagel shown in Figure IV.2.2. Jamming is ubiquitous, seen, for example, in polymers, small molecule glass forming materials and granular flow. The fundamental principles underlying jamming for this wide range of systems are essentially the same. While glass can, with time, relax, relaxation of a jammed system can occur only by breaking the percolated pathway to relieve the load placed on the system.

Both the glassy and jammed states represent structures far removed from equilibrium, one of the Grand Science Challenges (2007 BESAC report “*The New Era of Science: Directing Matter and Energy: Five Challenges for Science and the Imagination*”) and are long outstanding problems in materials science. Quantifying the dynamics and inhomogenities in glassy and jammed systems is essential to understand their properties. Furthermore, if we can obtain a fundamental understanding insights into the mechanisms and pathways by which jamming and glass formation occur, the possibility arises to control non-equilibrium structures from the nanoscopic to mesoscopic to macroscopic length scales. While these materials are certainly

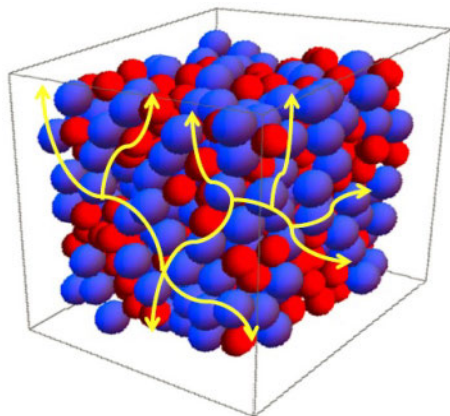


Figure IV.2.3: Continuous pathways of jammed nanoparticles in mixed nanoparticle systems.

not ordered, controlling these disordered assemblies may produce materials with a well-defined property or functionality arising from a cooperative behavior of the constituents, i.e. mesoscale ordering with emergent properties. For example, consider the assembly of a mixture of nanoparticles where one is a metal and the second is an insulating material, the optical or electronic properties of the materials will change due to the pathway established by the jammed metal particles. This is schematically shown in Figure IV.2.3. If control over the jamming is possible, novel routes for device fabrication are opened. Such challenges to control assemblies on the mesoscale were set forth in the 2012 report for the Basic Energy Sciences Advisory Committee entitled “*From Quanta to the Continuum: Opportunities for Mesoscale Sciences*”.

With existing x-ray sources, using XPCS and other techniques like melt rheology, the fast and slow relaxation processes in amorphous materials can be accessed. However, a large range of times scales are simply not accessible with current methodologies. These will be opened and combined with chemical and structural contrast when fully coherent DLSR SXR sources become available. Accessing the entire frequency range of the relaxation spectrum over a broad range of length scale, from nanometers to several microns, is essential to determine the mechanism by which materials are frozen into the glassy state or lock into jammed states. Quantitatively characterizing two point correlations and higher order correlations can only be done with fully coherent sources with high brightness. While some theories make prediction, it is impossible to differentiate between fact and fiction and, as such, predictability and, therefore, control over these non-equilibrium processes remains out of reach at this point.

B. Rare Events

Consider a material undergoing crystallization. The material is rapidly brought from the molten state to a temperature where crystallization can occur. If one remains close to the equilibrium melting point, the system will thermally equilibrate and remain in a quenched liquid state until nucleation occurs. Nucleation phenomena have been well described theoretically by assuming the existence of a critical nucleus, given by a balance between surface energies and internal energies holding the polymer chain segments or molecules in registry. Once nucleation occurs,

crystals grow with theoretical arguments defining, yet again, a critical nucleus for the addition of more crystalline material to the growth front. But these classical nucleation theories are not well validated by experiment since we lack to requisite tools to measure rare events on fast time scales and with nanoscale precision. Prior to crystallization, the liquid is thermally equilibrated, with density fluctuations rampant in the system; there is evidence, for example, that pre-nucleation clusters or dynamic heterogeneity play a significant role, and both of these models deviate significantly from classical nucleation theory.³⁵⁻³⁷ In any of these cases, the system must wait until there is a fluctuation in the density of sufficient size and strength (amplitude), a rare event, to allow crystallization.

Other systems that show similar characteristics are mixture undergoing phase separation (whether this be by a nucleation and growth process or by a spinodal mechanism). In diffusion processes, diffusants show local Brownian motion locally and then suddenly move to another site in the samples. Many biological processes depend on the system fluctuating, sampling energy and configuration space, rapidly assuming an intermediate high-energy state, then changing rapidly to a lower energy state. But we do not understand the nature of the fluctuations just prior to the spontaneous change. Are there correlations in the density fluctuations in the material so that one fluctuation feeds off another to generate a fluctuation of sufficient size and amplitude to bring about a change?

A fully coherent, DLSR SXR source will be able to address this question and provide important insight into the mechanism of nucleation. While we cannot provide the best experimental design to address this question, there is no question that this is an important phenomenon that is found in many different systems and underpins some of the most basic processes found in materials and biological sciences.

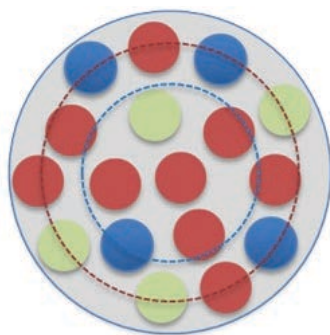


Figure IV.2.4: Compositional heterogeneity in a system of finite size. As the system size is decreased, the ability to maintain the overall stoichiometry $A_9B_4C_4$ is compromised by the non-negligible size of the atomic (or molecular) constituents relative to the system size.

C. Compositional Heterogeneity in Systems of Finite Size

The presence of boundaries drives deviations of properties from their bulk values. The average coordination number of atoms in a nanoparticle is lowered due to the reduced coordination of atoms at the interface of the particle. As the relative abundance of these atoms increases, the deviation of the average coordination number from the bulk increases. Likewise, in a heterogeneous system, deviations from the bulk stoichiometry or composition must occur as the

size of the system is reduced below a characteristic length scale. This is illustrated schematically Figure IV.2.4. Such changes in composition as a function of system size can have dramatic consequences on the thermophysical properties of the system. For example in a multi-component alloy that forms a bulk metallic glass, the glass forming ability is a very sensitive function of the precise composition of the system. One may expect for example that in quaternary systems containing less than ~ 1000 atoms that the stochastic fluctuations in composition from one finite volume to another would significantly alter the glassy dynamics and thermophysical properties of the material. The dynamics of the systems can be studied with chemical sensitivity using X-ray photon correlation spectroscopy (XPCS) and quasielastic RIXS, while ptychography can be used to provide high-resolution information on the intrinsic compositional heterogeneity resulting from finite size effects. A groundbreaking experiment would pursue direct measurements of dynamics related to intermittent relaxation in shear transformation zones using XPCS at ns time scales. Amorphous metals are an emerging class of materials with engineering applications that take advantage of their high specific strength, fracture toughness and low damping behavior.³⁸

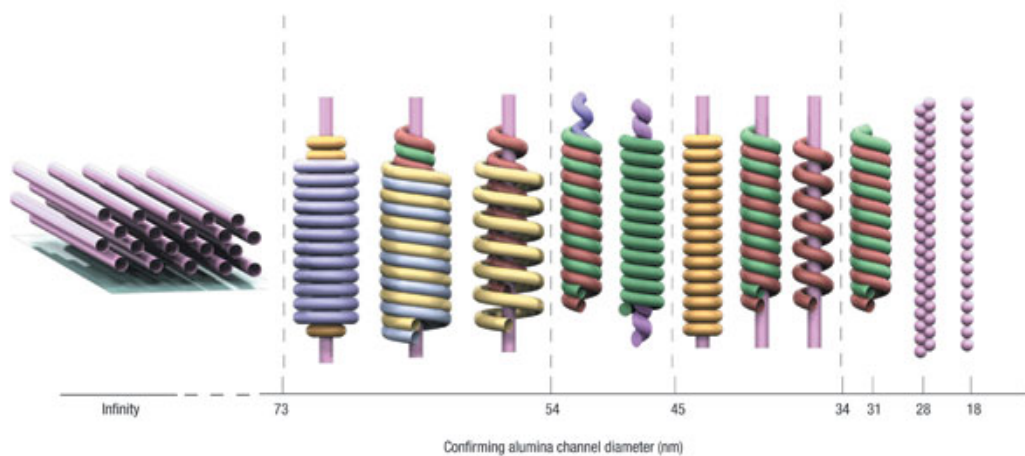


Figure IV.2.5: Simulation results for the morphology of a cylinder-forming diblock copolymer confined to cylindrical nanopores.

In homopolymer blends deviations from the bulk stoichiometry can drive changes in the dynamics of the system and the aging behavior, where the systems are glassy polymers. In block copolymers, the stochastic variations in composition and molecular weight can have profound effects on the self-assembly process in systems of finite size. As Figure IV.2.5 shows, the morphology in confined block copolymer melts is a very sensitive function of system size and interfacial wetting, under assumptions of perfectly monodisperse chains. In a real system, the dispersity of molecular weight and composition will lead to changes in morphology that occur simply as a result of these finite sizes. The importance of these considerations is underscored by the intense interest in leveraging block copolymer self-assembly for pattern transfer in fabrication of high-density storage devices.

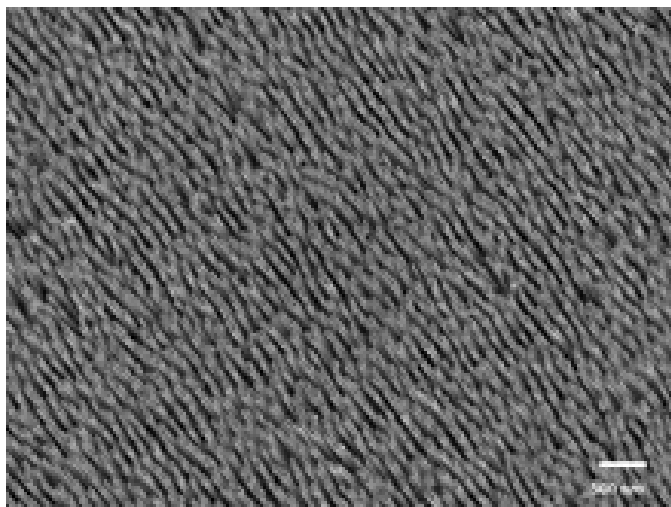


Figure IV.2.6: 50nm diameter nanorods produced by melt press extrusion of $\text{Pt}_{57.5}\text{Cu}_{14.7}\text{Ni}_{5.3}\text{P}_{22.5}$ bulk metallic glass through an anodic aluminum oxide template.³⁹

Both polymer systems and amorphous metals can be studied as ensembles of large numbers of small-scale systems. Such objects can be produced using simple extrusion through ceramic templates as shown in Figure IV.2.6, where 50 nm nanorods of a $\text{Pt}_{57.5}\text{Cu}_{14.7}\text{Ni}_{5.3}\text{P}_{22.5}$ bulk metallic glass have been produced by this method at elevated temperature. It is similarly feasible to generate 2D (films) and 0D (nanoparticles) objects using known deposition and sacrificial templating techniques.

D. Structure/Transport Relationship of Ionomers

Ionomers are ion-containing polymers that facilitate ion transport through the ion-rich phase in their morphology and are commonly used as the solid-electrolyte separator between the electrodes in many electrochemical-energy devices. These materials must conduct the ions in a mechanically robust matrix that also inhibits the crossover of reactants and products of the electrochemical reaction. A class of ionomers well suited for this role is perfluorosulfonic acid (PFSA), which has been widely used as the proton-exchange membrane (PEM) for fuel-cells since the introduction of Nafion® in 1960s. PFSAs owe their remarkable conductivity in the hydrated state to the nano-phase separation of their structure into hydrophilic acid and hydrophobic fluoropolymer mesoscale connected domains that enable facile proton and water transport (see Figure IV.2.7)⁴⁰.

Hard X-ray SAXS/WAXS, and more recently by Small Angle Neutron Scattering (SANS) have historically been a useful tools to study the average morphology of dry and hydrated PFSA and similar random copolymers. However, the information from the PFSA scattering is typically a single, broad so-called ionomer peak in the corresponding to the spacing of water domains on the order of nanometers. Interpretation of the SAXS data to understand the correlated role of domains in selective ion transport continues remains a challenge with important technological manifestations.⁴¹⁻⁴⁴

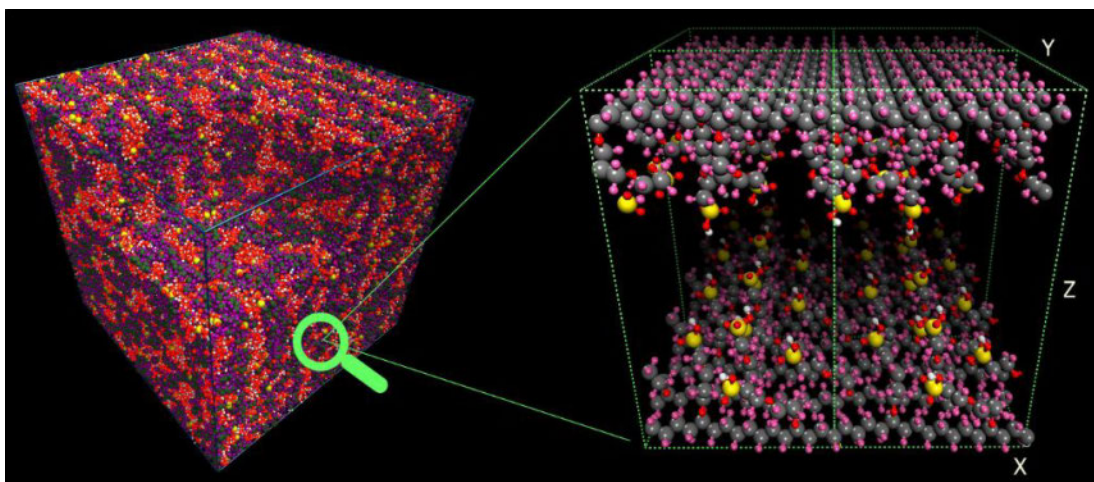


Figure IV.2.7: Atomistic simulation of the pore structure a hydrated Nafion membrane.⁴⁰

Quasi-elastic neutron scattering (QENS) has been demonstrated to be useful for probing the picosecond dynamic behavior of water in the polymers to explore confinement, characteristic residence time, and diffusion of water in clusters or ion-channels,^{45, 46} which can provide dynamical information complementary to structural information obtained by elastic x-ray neutron scattering techniques. Similarly, XPCS and quasielastic RIXS on SXR DLSR sources will probe the distribution, connectivity and behavior of sulfonic-acid moieties, and their dynamic interactions with the other species (counter-ions, solvents, etc.). The techniques have the potential to probe across critical time and length scales to (i) probe the water behavior around the ionic moieties and their mobility, (ii) measure the confinement and relaxation time of solvents, and, most importantly, (iii) observe the mesoscale transport pathways and responsive interfaces as well as their sub-second response to environmental excitations. With such knowledge base, one can elucidate the structure-transport-function relationship of ion-conductive polymers and lead the way for designing new materials by exploiting the solvent-polymer interactions, manipulating non-covalent interactions, and tuning mesoscale connectivity of domains, all of which can improve ionomer conductivity and performance in devices.

Of course, there are many applications where chemically selective transport in nanoporous media is a technology of key importance, e.g., water purification, providing a landscape for selective catalysis (Chapter II.2), regulating chemical transport and sensors, etc. In all of these applications, the goal is to tailor the selectivity and efficiency of transport by controlling the chemical structure of the pores. Coherent SXR beams on DLSR sources will provide the necessary spatial and temporal sensitivity and chemical contrast to help optimize these structures.

References: Section IV

1. O. Henrich, K. Stratford, P. V. Coveney, M. E. Cates and D. Marenduzzo, *Soft Matter* **9** (43), 10243-10256 (2013).
2. Y. Umena, K. Kawakami, J.-R. Shen and N. Kamiya, *Nature* **473**, 55-60 (2011).
3. B. Kok, B. Forbush and M. McGloin, *Photochem. Photobiol.* **11**, 457-475 (1970).
4. A. W. Rutherford, A. Osyczka and F. Rappaport, *Febs Letts.* **586**, 603-616 (2012).
5. J. Messinger, T. Noguchi and J. Yano, in *Molecular Solar Fuels* (2011), pp. 163-207.
6. S. Friedrich, *J. Low Temp. Phys.* **151**, 277-286 (2008).
7. R. Mitzner, J. Rehanek, J. Kern, S. Gul, J. Hattne, T. Taguchi, R. Alonso-Mori, R. Tran, C. Weniger, H. Schröder, W. Quevedo, H. Laksmono, R. G. Sierra, G. Han, Lassalle-Kaiser, K. B., S., K. Kubicek, S. Schreck, K. Kunnus, M. Brzhezinskaya, A. Firsov, M. P. Minitti, J. J. Turner, S. Moeller, N. K. Sauter, M. J. Bogan, D. Nordlund, W. F. Schlotter, J. Messinger, A. Borovik, S. Techert, F. M. F. de Groot, A. Föhlisch, A. Erko, U. Bergmann, V. K. Yachandra, P. Wernet and J. Yano, *J. Phys. Chem. Letts.* **4**, 3641-3647 (2013).
8. K. Nevo-Dinur, S. Govindarajan and A.-C. O, *Trends Genet.* **28**, 314-322 (2012).
9. M. Wilson and G. Z, *Curr. Opin. Microbiol.* **16**, 177-183 (2013).
10. M. R. Howells, T. Beetz, H. N. Chapman, C. Cui, J. M. Holton, C. J. Jacobsen, J. Kirz, E. Lima, S. Marchesini, H. Miao, D. Sayre, D. A. Shapiro, J. C. H. Spence and D. Starodub, *Journal of Electron Spectroscopy and Related Phenomena* **170** (1-3), 4-12 (2009).
11. D. Savage, B. Afonso, A. Chen and P. Silver, *Science* **327**, 1258-1261 (2010).
12. M. Foss, Y. Eun and D. Weibel, *50* (7719-34) (2011).
13. C. Iancu, D. Morris, Z. Dou, S. Heinhorst, G. Cannon and G. Jensen, *J. Mol Biol.* **396**, 105-117 (2010).
14. Y. Seki, K. Nitta and Y. Kaneko, *Plant Biol.* **16**, 258-263 (2014).
15. M. Gray, W. Wholey, N. Wagner, C. Cremers, A. Mueller-Schickert, N. Hock, A. Krieger, E. Smith, R. Bender, J. Bardwell and U. Jakob, *Mol Cell.* **53**, 689-699 (2014).
16. C. Jacobsen, J. Kirz and S. S. Williams, *Ultramicroscopy* **47**, 55-79 (1992).
17. C. J. Jacobsen, M. R. Howells and J. Kirz, *Rev. Biophys.* **28**, 33-130 (1995).
18. R. Falcone, J. Kirz, C. J. Jacobsen, J. C. H. Spence, S. Marchesini and D. A. Shapiro, *Contemporary Physics* **52**, 293-318 (2011).
19. M. Le Gros, G. McDermott and C. Larabell, *Current Opinion in Structural Biology* **15**, 593-600 (2005).
20. O. Bunk, M. Dierolf, S. Kynde, I. Johnson, O. Marti and F. Pfeiffer, *Ultramicroscopy* **108**, 481-487 (2008).
21. H. S. Cho, F. Schotte, N. Dashdorj, J. Kyndt and P. A. Anfinrud, *Journal of Physical Chemistry B* **117** (49), 15825-15832 (2013).
22. K. H. Kim, S. Muniyappan, K. Y. Oang, J. G. Kim, S. Nozawa, T. Sato, S. Y. Koshihara, R. Henning, I. Kosheleva, H. Ki, Y. Kim, T. W. Kim, J. Kim, S. Adachi and H. Ihee, *Journal of the American Chemical Society* **134** (16), 7001-7008 (2012).
23. C. D. Putnam, M. Hammel, G. L. Hura and J. A. Tainer, *Quarterly reviews of biophysics* **40** (3), 191-285 (2007).
24. T. Hashiguchi, M. L. Fusco, Z. A. Bornholdt, J. E. Lee, A. I. Flyak, R. Matsuoka, D. Kohda, Y. Yanagi, M. Hammel, J. E. Crowe and E. O. Saphire, *Cell* **160** (5) (2015).
25. A. Ghosh, S. Hartung, C. van der Does, J. A. Tainer and S. V. Albers, *Biochem J* **437**, 43-52 (2011).
26. E. Malmerberg, C. A. Kerfeld and P. H. Zwart, *IUCrJ* **2**, 309 (2015).
27. S. H. Sternberg, S. Redding, M. Jinek, E. C. Greene and J. A. Doudna, *Nature* **507** (7490), 62-67 (2014).
28. L. Berthier, *Physics* **4**, 42 (2011).

29. L. Berthier, G. Biroli, J.-P. Bouchaud, L. Cipeletti and W. van Saarloos, (Oxford University Press, Oxford, 2011).
30. G. S. Iannacchione and D. Finotello, *Physical Review Letters* **69** (14), 2094-2097 (1992).
31. Z. Kutnjak, S. Kralj, G. Lahajnar and S. Žumer, *Physical Review E* **68** (2), 021705 (2003).
32. R. Garcia and M. H. W. Chan, *Physical Review Letters* **83** (6), 1187-1190 (1999).
33. F. M. Gasparini, M. O. Kimball, K. P. Mooney and M. Diaz-Avila, *Reviews of Modern Physics* **80** (3), 1009-1059 (2008).
34. A. J. Liu and S. R. Nagel, *Nature* **396** (6706), 21-22 (1998).
35. D. Gebauer, A. Völkel and H. Cölfen, *Science* **322** (5909), 1819-1822 (2008).
36. E. M. Pouget, P. H. H. Bomans, J. A. C. M. Goos, P. M. Frederik, G. de With and N. A. J. M. Sommerdijk, *Science* **323** (5920), 1455-1458 (2009).
37. A. F. Wallace, L. O. Hedges, A. Fernandez-Martinez, P. Raiteri, J. D. Gale, G. A. Waychunas, S. Whitelam, J. F. Banfield and J. J. De Yoreo, *Science* **341** (6148), 885-889 (2013).
38. M. Telford, *Materials Today* **7** (3), 36-43 (2004).
39. M. Gopinadhan, Z. Shao, Y. Liu, S. Mukherjee, R. C. Sekol, G. Kumar, A. D. Taylor, J. Schroers and C. O. Osuji, *Appl. Phys. Lett.* **103**, 111912 (2013).
40. P. V. Komarov, P. G. Khalatur and A. R. Khokhlov, *Beilstein Journal of Nanotechnology* **4**, 567-587 (2013).
41. G. Gebel and O. Diat, *Fuel Cells* **5** (2), 261-276 (2005).
42. K. A. Mauritz and R. B. Moore, *Chemical Reviews* **104** (10), 4535-4586 (2004).
43. M.-H. Kim, C. J. Glinka, S. A. Grot and W. G. Grot, *Macromolecules* **39** (14), 4775-4787 (2006).
44. A. Kusoglu, S. Savagatrup, K. T. Clark and A. Z. Weber, *Macromolecules* **45** (18), 7467-7476 (2012).
45. J.-C. Perrin, S. Lyonnard and F. Volino, *The Journal of Physical Chemistry C* **111** (8), 3393-3404 (2007).
46. A. M. Pivovar and B. S. Pivovar, *The Journal of Physical Chemistry B* **109** (2), 785-793 (2005).

Appendix 1: Workshop Charge, Organization, and Agenda

Charge

- 1) What transformational research opportunities will be enabled by storage-ring-based ultrahigh brightness soft and intermediate x-ray beams?
- 2) What are the primary challenges to accomplish this science?

Organization

With targeted participation from the soft x-ray synchrotron radiation community worldwide, this workshop will outline the future of soft x-ray science on high brightness storage rings over the next decade and beyond. This project will begin with advance planning to start developing a workshop report, which will be further developed with an interactive workshop. The workshop itself will entail one morning of plenary talks, followed by 1.5 days of science-oriented breakout sessions focused on the above charges. Two leaders with the relevant expertise, facilitated by an ALS or LBNL scientific staff member, will organize each breakout. The final morning will be used for final discussion and work on a rough draft of a 100-150 page report in the style of a DOE/BES workshop report (see <http://science.energy.gov/bes/news-and-resources/reports/>).

**Workshop on Soft X-ray Science using Diffraction Limited Storage Rings
Advanced Light Source, Lawrence Berkeley National Laboratory
October 1- 3, 2014**

AGENDA

Wednesday, October 1

Plenary Session (8:00 AM – 1:00 PM) in Building 15 Room 253

7:45	Continental breakfast	
8:15	Welcome and Introduction	
8:25	Materials with ultrabright soft x-ray beams	Wolfgang Eberhardt
9:00	Bioscience with ultrabright soft x-ray beams	Wayne Hendrikson
9:35	Storage Rings: near and far future	Mikael Eriksson
10:10	Break	
10:30	Diffraction imaging	David Shapiro
10:45	Soft x-ray nano-spectroscopy	Andrea Goldoni
11:00	Magnetic microscopy	Bastian Pfau
11:15	Photon correlation spectroscopy	Stuart Wilkins
11:30	Chemical dynamics/fluctuations	Oliver Gessner
11:45	Fluctuation SAXS	Peter Zwart
12:00	nanoARPES	Eli Rotenberg
12:15	(nano-)RIXS	Thorsten Schmitt
12:30	nano-APXPS	Hendrik Bluhm
1:00	Lunch	
2:00	Breakout session 1:	

Location	Breakout	Session Leaders
6-2202	Magnetism and spin structures	Hermann Duerr, Ives Idzerda, Elke Arenholz
15-253	Catalysis	Lou Terminello, Miquel Salmeron, Jinghua Guo
2-400F	Material fluctuations, excitations & dynamics	Brian Stephenson, Oleg Shpyrko, Yi-De Chuang, Sujoy Roy
80-234	Bioscience beyond structure	John Tainer, Paul Adams, Peter Zwart, Greg Hura
15-300	Earth and environmental science	Gordon Brown, Peter Nico, Ben Gilbert

Reconvene in 15-253

5:00 Panel discussion: feedback from breakout session 1

Transfer to Perseverance Hall (Building 54 Room 130)

6:00 Workshop Dinner

Thursday, October 2

8:00 Continental breakfast in 15-253

8:30 Breakout session 2:

Location	Breakout	Session Leaders
6-2202	Quantum materials	Peter Johnson, Peter Abbamonte, Eli Rotenberg
15-253	Energy Materials	Wolfgang Eberhardt, Harald Ade, Wanli Yang
2-400F	Chemical fluctuations, kinetics & dynamics	Nora Berrah, Alex Foehlich, Oliver Gessner
80-234	Bioscience beyond structure	John Tainer, Paul Adams, Peter Zwart, Greg Hura
15-300	Earth and environmental science	Gordon Brown, Peter Nico, Ben Gilbert
6-1105	Soft condensed matter	Tom Russell, Alex Hexemer

Reconvene in 15-253

11:30 Panel discussion: feedback from breakout session 2

12:30 Lunch

1:30 Breakout Session 3:

Location	Breakout	Session Leaders
6-2202	Ultralow power information processing	Jeff Bokor, Elke Arenholz
2-400F	Catalytic networks	Lou Terminello, Hendrik Bluhm
15-253	Energy conversion and storage devices	Wolfgang Eberhardt, Harald Ade, Wanli Yang
80-234	Bioscience beyond structure	John Tainer, Paul Adams, Peter Zwart, Greg Hura
15-300	Earth and environmental science	Gordon Brown, Peter Nico, Ben Gilbert
6-1105	Soft condensed matter	Tom Russell, Alex Hexemer

Reconvene in 15-253

4:30 Panel discussion: feedback from breakout session 3

5:30 Workshop summary/discussion

6:00 Dinner on own

Friday, October 3

Writing Session (8:00 AM – 12 Noon) in 15-253

8:00 Continental breakfast

8:30 Drafting workshop report

Breakout leads & facilitators

12:00 Adjourn

Appendix 2: Soft X-ray tools that benefit from high brightness

Acronym	Technique	Benefit of high brightness
ARPES	Angle-resolved photoelectron spectroscopy	ARPES: no inherent benefit; nanoARPES benefits in proportion to source brightness
APXPS	Ambient pressure x-ray photoelectron spectroscopy	APXPS: no inherent benefit; nanoAPXPS benefits in proportion to source brightness
CDI	Coherent diffraction imaging	Benefits in direct proportion to source brightness
EXAFS	Extended x-ray absorption fine structure	EXAFS: no inherent benefit; nanoEXAFS benefits in proportion to source brightness
FXS	Fluctuation x-ray scattering	Depending on sample delivery can benefit in direct proportion to source brightness
PEEM	Photoelectron microscopy	Generally no inherent benefit from source brightness since illumination is incoherent $\sim 10 \mu\text{m}$ spot
(none)	Ptychography	Benefits in direct proportion to source brightness
RIXS	Resonant inelastic x-ray scattering	RIXS: no inherent benefit; nanoRIXS benefits in proportion to source brightness; double dispersion RIXS can benefit by 5-10x from circular beam; FT-RIXS can benefit in direct proportion to brightness, depending on implementation
SAXS	Small angle x-ray scattering	SAXS: no inherent benefit; coherent SAXS is a generalization of XPCS, CDI, etc, which do benefit from brightness
STXM	Scanning transmission x-ray microscopy	Benefits in direct proportion to source brightness
TXM	Transmission x-ray microscopy	Generally no inherent benefit from source brightness since illumination is incoherent $\sim 10 \mu\text{m}$ spot
XAS	X-ray absorption spectroscopy	XAS: no inherent benefit; nanoXAS is a generalization of STX, CDI, and ptychography and benefits in proportion to source brightness
XES	X-ray emission spectroscopy	XES: no inherent benefit; nanoXES benefits in proportion to source brightness
XMCD	X-ray magnetic circular dichroism	XMCD: no inherent benefit; nanoXMCD benefits in proportion to source brightness
XMLD	X-ray magnetic linear dichroism	XMLD: no inherent benefit; nanoXMLD benefits in proportion to source brightness
XPCS	X-ray photon correlation spectroscopy	Accessible time resolution scales inversely with the square of source brightness
XRD	X-ray diffraction	XRD: no inherent benefit; nanoXRD benefits in proportion to source brightness
XT/XRT	X-ray tomography	No inherent benefit when using incoherent illumination; nanoXT can benefit in direct proportion to source brightness

Appendix 3: Workshop Registration List

Abbamonte	Peter	University of Illinois	abbamont@illinois.edu
Adams	Paul	LBNL	PDAdams@lbl.gov
Ade	Harald	North Carolina State University (NCSU)	harald_ade@ncsu.edu
Alayoglu	Selim	LBNL	salayoglu@lbl.gov
Allaire	Marc	ALS/LBNL	mallaire@lbl.gov
Andersen	Jesper	MAX IV Laboratory	Jesper.andersen@maxlab.lu.se
Arenholz	Elke	ALS/LBNL	earenholz@lbl.gov
Banda	Michael	ALS/LBNL	mjbanda@lbl.gov
Berrah	Nora	University of Connecticut	nora.berrah@uconn.edu
Bluhm	Hendrik	ALS/LBNL	hbluhm@lbl.gov
Bokor	Jeffrey	EECS Department	jbokor@eecs.berkeley.edu
Brown	Gordon	Stanford University	gordon.brown@stanford.edu
Byrd	John	LBNL	JMByrd@lbl.gov
Catalano	Jeffrey	Washington University	catalano@eps.wustl.edu
Chabinyc	Michael	University of California Santa Barbara	mchabinyc@engineering.ucsb.edu
Chiang	Tai	U. of Illinois	tcchiang@illinois.edu
Chuang	Yi-De	ALS/LBNL	ychuang@lbl.gov
Chueh	William	Stanford University	wchueh@stanford.edu
Crabtree	George	ANL	Crabtree@anl.gov
Crommie	Mike	UCB Physics Dept. / LBNL	crommie@berkeley.edu
Devereaux	Thomas	SLAC	tpd@stanford.edu
Ding	Hong	Institute of Physics, Chinese Acad. Sciences	dingh@iphy.ac.cn
Durr	Hermann	SLAC National Accelerator Laboratory	hdurr@slac.stanford.edu
Eberhardt	Wolfgang	DESY-CFEL	wolfgang.eberhardt@desy.de
Eriksson	Mikael	MAX IV Laboratory	Mikael.Eriksson@maxlab.lu.se
Falcone	Roger	LBNL	RWFalcone@lbl.gov
Fischer	Peter	CXRO/LBNL	PJFischer@lbl.gov
Foehlich	Alexander	Helmholtz-Zentrum Berlin	jeannette.bonge@helmholtz-berlin.de
Freeland	John	Argonne National Laboratory	freeland@anl.gov
Frei	Heinz	Lawrence Berkeley National Laboratory	HMFrei@lbl.gov
Gessner	Oliver	ALS/LBNL	ogessner@lbl.gov
Gilbert	Benjamin	LBNL	bgilbert@lbl.gov
Gilles	Mary	Chemical Sciences, LBNL	mkgilles@lbl.gov
Glover	Ernie	Gordon & Betty Moore Foundation	Ernie.Glover@moore.org
Goldoni	Andrea	Elettra-Sincrotrone Trieste	goldonia@elettra.eu
Guehr	Markus	SLAC	mguehr@stanford.edu
Guo	Jinghua	ALS/LBNL	jguo@lbl.gov
Hendrickson	Wayne	Columbia University	wayne@xtl.cumc.columbia.edu
Hexemer	Alexander	ALS/LBNL	alexander_hexemer@mac.com
Horn	Karsten	Fritz Haber Institute	horn@fhi-berlin.mpg.de
Huang	Di-Jing	NSRRC, Taiwan	chiang.cathy@nsrrc.org.tw

Hura	Greg	PBD/LBNL	glhura@lbl.gov
Hurley	James	UC Berkeley	jimhurley@berkeley.edu
Hussain	Zahid	ALS/LBNL	ZHussain@lbl.gov
Idzerda	Yves	Montana State University	Idzerda@montana.edu
Johnson	Peter	Brookhaven National Laboratory	pdj@bnl.gov
Kerfeld	Cheryl	LBNL, MSU, UCB	ckerfeld@lbl.gov
Kevan	Steve	ALS/LBNL	SDKevan@lbl.gov
Kiskinova	Maya	Elettra-Sincrotrone Trieste	maya.kiskinova@elettra.eu
Kostko	Oleg	LBNL	okostko@lbl.gov
Kusoglu	Ahmet	Berkeley Lab (LBNL)	akusoglu@lbl.gov
Lanzara	Alessandra	UC Berkeley	alanzara@lbl.gov
Markovic	Nenad	Argonne National Lab	nmarkovic@anl.gov
Myneni	Satish	Princeton University	smyneni@princeton.edu
N'Diaye	Alpha	ALS/LBNL	atndiaye@lbl.gov
Nico	Peter	ESD/LBNL	psnico@lbl.gov
Nix	Jay	Molecular Biology Consortium	jcnix@lbl.gov
Osuji	Chinedum	Yale University	chinedum.osuji@yale.edu
Padmore	Howard	ALS/LBNL	hapadmore@lbl.gov
Pejakovic	Dusan	Gordon and Betty Moore Foundation	dusan.pejakovic@moore.org
Petroff	Yves	LNLS	yves.petroff@gmail.com
Pfau	Bastian	Lund University	bastian.pfau@sljus.lu.se
Preobrajenski	Alexei	MAX IV laboratory	alexeip@maxlab.lu.se
Qiu	Z. Q.	UC Berkeley	qiu@berkeley.edu
Robin	David	LBNL	dsrobin@lbl.gov
Rolles	Daniel	DESY	Daniel.Rolles@desy.de
Rotenberg	Eli	LBNL	erotenberg@lbl.gov
Roy	Sujoy	ALS/LBNL	sroy@lbl.gov
Rumbles	Garry	NREL	garry.rumbles@nrel.gov
Russell	Thomas	University of Massachusetts Amherst	tom.p.russell@gmail.com
Salahuddin	Sayeef	UC Berkeley	sayeef@berkeley.edu
Salmeron	Miquel	LBNL	mbsalmeron@lbl.gov
Sannibale	Fernando	LBNL	fsannibale@lbl.gov
Schmitt	Thorsten	Paul Scherrer Institut	thorsten.schmitt@psi.ch
Scholl	Andreas	ALS/LBNL	a_scholl@lbl.gov
Senanayake	Sanjaya	Brookhaven National Laboratory	ssenanay@bnl.gov
Shapiro	David	ALS/LBNL	dashapiro@lbl.gov
Shpyrko	Oleg	University of California, San Diego	oshpyrko@ucsd.edu
Sinha	Sunil	UCSD	ssinha@physics.ucsd.edu
Staub	Urs	Paul Scherrer Institut	Urs.Staub@psi.ch
Steier	Christoph	LBNL	CSteier@lbl.gov
Stephenson	Brian	Argonne National Laboratory	stephenson@anl.gov
Strachan	John Paul	HP Labs	john-paul.strachan@hp.com
Tainer	John	The Scripps Research Institute	jat@scripps.edu

Terminello	Lou	PNNL	louis.terminello@pnnl.gov
ThCEnell	Karina	MAX IV Laboratory	karina.schulte@maxlab.lu.se
van Buuren	Tony	LLNL	vanbuuren1@llnl.gov
Weber	Adam	LBNL	azweber@lbl.gov
Westfahl	Harry	Brazilian Synchrotron Light Laboratory	westfahl@lnls.br
Wilkins	Stuart	Brookhaven National Laboratory	swilkins@bnl.gov
Yang	Peidong	University of California, Berkeley	p_yang@berkeley.edu
Yang	Wanli	Lawrence Berkeley National Laboratory	WLYang@lbl.gov
Yano	Junko	LBNL	JYano@lbl.gov
Zwart	Peter	PBD/LBNL	phzwart@lbl.gov